GENETIC AND MOLECULAR CHARACTERIZATION OF GENES INVOLVED IN BARLEY-*COCHLIOBOLUS SATIVUS* INTERACTION

A Dissertation
Submitted to the Graduate Faculty
of the
North Dakota State University
of Agriculture and Applied Science

By

Rui Wang

In Partial Fulfillment of the Requirements
for the Degree of
DOCTOR OF PHILOSOPHY

Major Department:
Plant Pathology

October 2015

Fargo, North Dakota

North Dakota State University
Graduate School

Title

GENETIC AND MOLECULAR CHARACTERIZATION OF GENES INVOLVED IN BARLEY-*COCHLIOBOLUS SATIVUS* INTERACTION

By

Rui Wang

The Supervisory Committee certifies that this ***disquisition*** complies with North Dakota State University's regulations and meets the accepted standards for the degree of

DOCTOR OF PHILOSOPHY

SUPERVISORY COMMITTEE:

Shaobin Zhong
Chair

Robert S. Brueggeman

Zhaohui Liu

Wenhao (David) Dai

Approved:

Nov. 3, 2015
Date

Jack Rasmussen
Department Chair

ABSTRACT

Spot blotch caused by ascomycete fungus *Cochliobolus sativus* (Ito & Kurib.) Drechs. ex Dastur. [anamorph: *Bipolaris sorokiniana* (Sacc.) Shoem.] is one of the most common and economically important diseases on barley. To better understand the molecular interaction between the different pathotypes of this pathogen and barley differential lines, fungal genes involved in virulence and barley genes for spot blotch resistance were characterized in this study. Previous studies have revealed that the virulence factor in the pathotype 2 isolate ND90Pr making cv. Bowman susceptible is a secondary metabolite peptide synthesized by two non-ribosomal peptide synthesdases (NRPSs). However, the global regulation of biosynthesis of this secondary metabolite is not well understood in this fungus. Recently, the *velvet*-complex proteins containing LaeA and *velvet* proteins (VeA, VelB, VelC and VosA) have been shown to be involved in global regulation of secondary metabolism and fungal development in many fungal pathogens. To characterize the functions of the orthologous of *velvet*-complex proteins in *C. sativus*, single and double gene knockout mutants were generated. The results indicated that the *velvet*-complex factors affect virulence of the fungus by regulating expression of the NRPSs involved in virulence. In addition, *velvet*-complex proteins were found to coordinately and distinctly regulate fungal development, such as conidiogenesis and conidia germination. To identify and characterize genes for resistance to the new pathotype, 2,062 barley accessions from a USDA barley core collection were screened for spot blotch resistance to this pathotype and 24.5% of them showed resistance or moderate resistance at the seedling stage. Genome-wide association analysis identified four QTLs associated with the seedling resistance, which were located on chromosome 1H, 2H, 3H, and 6H, respectively. A genetic analysis of the cross between a highly resistant line (PI 235186) and a highly susceptible accession (PI 356741)

suggested a single dominant gene confers the resistance in PI 235186. The resistance gene was further mapped to the short arm of chromosome 6H based on bulk segregant analysis using 194 SSR markers and genotyping-by-sequencing using 20 SNP markers in a F_2 population. Additional markers were developed to fine map the resistance gene to a ~6.5 cM genomic region.

ACKNOWLEDGEMENTS

Throughout my graduate studies at North Dakota State University, I have been fortunate to be surrounded by some of the best people in world, who have provided a vast amount of support. It is great pleasure to express my sincere gratitude to all of them.

First of all, I am deeply grateful to my supervisor, Dr. Shaobin Zhong, for all his continuous guidance and patience throughout my graduate studies. He has been a mentor and a friend throughout not only my research but also my life. He has guided me in the exploration of fungal genetics as well as plant disease resistance, and provided encouragement whenever needed. He also taught me a lot on writing and presentation. I am also grateful to my other committee members: Dr. Robert Brueggeman, Dr. Zhaohui Liu, and Dr. Wenhao (David) Dai, who have been invaluable in providing advice, discussion, and support in my research.

I would like to thank Dr. Justin D. Faris and Dr. Timothy F. Friesen for supplying equipment and facilities for the Southern blot analysis and pathogenicity tests. Thank Dr. Xiwen Cai for providing guidance and help in the fungal structures observation. Thank Dr. Steven S Xu for providing equipment, software and important guidance on genome-wide association analysis. I also want to thank Dr. Shiaoman Chao for providing the primers for barley SSR markers and other help in barley genotyping. I also want to give my thanks to Dr. María Muñoz-Amatriaín for her precious suggestions on the association analysis and for her time on the revision of my manuscripts.

I would like to thank Dr. Yueqiang Leng and his family as well as Dr. Gongjun Shi for guiding in my research and sharing of research experience. They also provided me a lot of help in my life living in Fargo.

I would like to thank Dr. Shaukat Ali and Mr. Joseph Mullins for assistance in the greenhouse work. I also like to thank the help from all other lab members (Mingxia Zhao, Subidhya Shrestha, and Bikash Poudel) and the part time helpers (Zhongxing Sun and Qiang Li) in the greenhouse work and many other things.

I would like to thank Dr. Jack B. Rasmussen, the head of the Department of Plant Pathology, and all others in the department for providing such a good working environment.

I want to give my great thanks to my friends Dr. Qun Sun, Dr. Xianwen Zhu, Prabin Tamang, Jonathan Richards, and Steven A. Carlsen for providing many suggestions and helps in my research. Thank them all.

I would like to give the deepest gratitude to my grandparents, my parents for their love and support throughout my life.

Lastly, and most importantly, I want to give a heartfelt thanks to my wife Xiqian Yan for her love, encouragement and understanding in my journey of graduate study. I love you very much!

TABLE OF CONTENTS

LIST OF TABLES

LIST OF FIGURES

LITERATURE REVIEW

The host: barley

Introduction

Barley (*Hordeum vulgare* L.) is one of the earliest cultivated crops in the world and ranks fourth among the cereals in worldwide production. More than half of the world's barley production is used as feed supplement for domestic animals, while the rest is used for human diet, brewing malts, seed production and starch production (Fischbech, 2002; Sreenivasulu et al. 2008). There are two sub-populations of barley based on spike morphology: two-row and six-row barley. Barley spikes have three spikelets at each node of the rachis: one central and two lateral spikelets. The lateral spikelets in two-row barley bear sterile florets that do not produce any seed, whereas all three spikelets in six-row barley are fertile. Based on archeological remains of barley, it was suggested that two-row barley is older than six-row barley (Helbaek, 1959 ; Zohary, 1973). The growth habits further differentiates cultivated barley into spring, winter and facultative types (Poehlman, 1994). The spring barley is planted in the spring and harvested in the same summer, whereas the winter barley is planted in late fall and harvested in the following summer. The facultative barley is cold tolerant, so it can be planted either in the spring or the fall and is harvested in the same or following summer. Winter barley requires vernalization to initiate flowering and produce grain, whereas the other two types don't need vernalization.

Origin and dissemination of barley

Like many other crops, lots of many studies have suggested controversies regarding the exact center of origin of barley. However, most of the researchers identified the Fertile Crescent

as the origin of barley because most of the archaeological remains of domesticated barley was discovered in the Fertile Crescent area (Harlan 1966; Wilcox 2005; Zohary and Hopf 2000) which spans the present Syria, Iraq, Palestine, Israel , Lebanon and Jordan. Badr et al. (2000) demonstrated the monophyletic nature of barley domestication based on allelic frequencies using 400 AFLP markers studied in 317 wild and 57 cultivated lines and found that wild populations from Israel-Jordan are molecularly more similar than any others to the cultivated gene pool, suggesting that Israel-Jordan is the main point of Fertile Crescent where the barley was first domesticated.

However, according to the new genetic evidence came from genotyping of chloroplast microsatellite markers and re-sequencing of a region linked to the tough rachis locus (Molina-Cano et al. 2005), it is suggested that barley was domesticated more than once and falls into at least two genetically distinct clusters, each with a different geographical origin. More extensive re-sequencing of 18 loci containing 684 single-nucleotide polymorphisms (SNP) gave greater clarity (Morrell et al. 2007), describing that barley was domesticated not only in the Israel-Jordan region but also in a region to the east of the Fertile Crescent, possibly in the western foothills of the Zagros mountains, where early farming sites exist at Ali Kosh and Jarmo. This eastern domestication appears to have given rise to many of the landraces subsequently grown in central and East Asia (Saisho and Purugganan 2007). Furthermore, some other scientists also considered Ethiopia, Himalayas and Morocco as the center of barley domestication (Aberg 1938; Bekelle 1983; Molina-cano et al. 1987), though sufficient strong evidence is not found.

It is believed that with the spread of ancient agriculture, barley was spread in three directions: 1) Southwards to Egypt and ultimately into Africa; 2) Northwards and westwards through Asia Minor to Europe and 3) Eastwards to the Valley of Indus (Clarlk 1967). At least

three ways of migration of barley cultivation in Europe were found: 1) Through southern Asia Minor to Greece; 2) Through the Balkans to the valley of Danube; 3) Through Southern Russia. Time frame of this migration is from 4200 BC to 2500 BC (Clarlk 1967). Barley was introduced in English Islands around 3000 BC and in Scandinavian countries in around 2000 BC (Newman and Newman 2006).

Barley production in the U.S.

Barley was first brought to the American Continent in 1494 by Columbus during his second voyage though the actual site is not clearly identified (Wiebe 1968). However, barley was introduced more successfully by the English in the Eastern Colonies in 17th Century and by the Spanish in the southern colonies during Spanish Mission Movement (Wiebe 1968).

United States now produces barley in four major regions: East, Upper Midwest, West, and Southwest (Horsley and Harvey 2011). Most barley sown under dry-land conditions in the Upper Midwest region is six-row malting barley cultivars because of the original barley improvement efforts in the early 1900s. In the West region, two-row barley for malting is typically grown under irrigation. These barley accessions mainly came from central Europe and formed the germplasm pool. In the East and Southwest region, non-malting winter barley and non-malting spring barley cultivars are typically grown, respectively (Horsley and Harvey 2011). Nationwide estimated barley plantings in 2015 totaled 2.92 million acres, with North Dakota at 0.83 million hectares, the second largest barley planting state in the U.S. The total production of harvested barley in the U.S. increased from 2.44 million bushels in 2014 to 2.92 million bushels in 2015, as reported by the USDA National Agricultural Statistical Service (NASS, Jun 30, 2015).

Barley germplasm in the U.S.

The National Small Grains Collection (NSGC) in Aberdeen, Idaho is the part of the USDA-ARS's National Plant Germplasm System that has a large collection of cultivated and wild barley accessions and their relatives. NSGC Barley Collection is one of the largest barley germplasm in the world (Knüpffe 2009; Valkoun 2008), which is comprised of 33,176 barley accessions that have been acquired and maintained over the past 100 years. This germplasm includes barley cultivars, breeding lines, landraces, and genetic stocks from more than 100 countries (Bockelman 2011; Bonman et al. 2011). This germplasm can serve as great sources of genotypes that are tolerant or resistant to most economically important biotic and abiotic stresses. By randomly selecting accessions based on the source origin, with a minimum of one accession each country (Bockelman 2011), a subset representing approximately 10% of the entire accessions was established in 1995 and with final additions in 2006. This subset germplasm was named 'NSGC Barley Core' by Munoz-Amatriain et al. (2014).

The pathogen: *Cochliobolus sativus*

Introduction

Cochliobolus sativus (Ito & Kurib.) Drechs. ex Dastur. [anamorph: *Bipolaris sorokiniana* (Sacc.) Shoem.] is a filamentous fungus belonging to the family Pleosporaceae in the order Pleosporales of Dothideomycetes. It can cause serious diseases on root (known as common root rot), leaf and stem (known as spot blotch), and head tissue (known as black point and glume blight) on a wide variety of cereals (Mathre 1997; Wiese 1987). *C*. *sativus* also attacks many grasses, including *Panicum virgatum* L. (switch grass) that is currently being developed as a

source of biomass for biofuel and bioproduct production as well as *Brachypodium distachyon* that is being used as a new model system for functional genomics in grasses.

Taxonomy

The anamorph of *Cochliobolus sativus* (Ito & Kurib.) Drechs. ex Dastur. is *Bipolaris sorokiniana* (Sacc.) Shoem.], which belongs to the Pleosporaceae family in the order Pleosporales of Dothideomycetes class. Dothideomycetes is the largest and most diverse class of ascomycete fungi, which comprises 11 orders, 90 families, 1,300 genera and more than 19,000 known species (Kirk 2008). It contains the majority of the fungal species with ascolocular development and bitunicate asci (Luttrell 1951).

There are three main orders in Dothideomycetes: Dothideales, Pleosporales and Myriangiales (Luttrell 1951; Luttrell 1955). The presence of pseudoparaphyses (sterile cells extending down from the upper portion of the sexual structures, initially attached at both ends, although the upper part may become free) is a notable character for the classification of these three orders. Pleosporales has the pseudoparaphyses together with mainly ostiolate flask shaped sexual structures. In contrast, Dothideales and Myriangiales don't have pseudoparaphyses. In addition, Dothideales develop groups of asci and Myriangiales produce single ascus in multiple locules (Luttrell 1951; Luttrell 1955).

Bipolaris, together with *Drechslera, Curvularia* and *Exserohilum* formed the family of Pleosporaceae that belongs to the order of Pleosporales. The four genera are closely related based on the traditional morphology method. The differentiation between them relies upon a combination of characters including conidial shape, the presence or absence of a protruding

hilum, the contour of the basal portion of the conidium and its hilum, the point at which the germ tube originates from, as well as the sequence and location of the first three conidial septa. *Bipolaris* species are common, and are most closely related to *Drechslera* and *Exserohilum*. The only morphological difference between *Bipolaris* and *Drechslera* is that *Drechslera* spores germinate from any cell of the spore while *Bipolaris* germinates only from polar cells. *Exserohilum* spores have an inner cup-like structure that is visible in the basal cell, whereas *Bipolaris* doesn't have (Domsch et al. 1980).

Morphological characteristics

Colonies of *Bipolaris sorokiniana* are moderately fast growing, effuse, and grey to blackish brown, suede-like to floccose with a black reverse. The mycelium is usually deep olive-brown. New cultures produce abundant simple conidiophores, which may be single or clustered and measure 6-10 x 110-220 μm with septations. Conidia develop laterally from pores beneath each conidiophore setpum. The conidiogenesis pattern follows a sympodial fashion in which conidia are normally produced by an expansion and swelling of the apex of the conidiophore, and after the formation of the first conidium, the active apical tip moves to the side to produce the next conidium. Multiple rounds of conidiation result in three to five spores borne sympodially on a conidiophore. The produced conidia are olive-brown and ovate to oblong, with rounded ends and a prominent basal scar. They are measured at 15-28 x 40-120 μm and have 3 to 10 septate. The cell wall is smooth and noticeably thickened at the septa. Conidia germinate only from the two end cells of the conidium (bipolar) (Shoemaker 1955; Sivanesan 1987).

The sexual state of *B*. *sorokiniana* (*Cochliobolus*. *sativus*) is rarely found in nature (Tinline, 1988). However, it can be induced in the lab using Such's agar media containing sterilized barley grains (Tinline, 1951). When *C*. *sativus* formed in culture, it is in the form of black, globose pseudothecia that are 300-400 μm in diameter, with erect beaks 50-200 μm long. Asci are clavate and measured 20-35 x 150-250 μm. Ascospores are hyaline, uniformly filamentous, and spirally flexed within asci. They are measured at 5-10 x 200-250 μm and have 4 to 10 septate (Wiese 1987).

Pathotypes

In the Upper Midwest region of the U.S., three pathotypes (0, 1 and 2) of the pathogen have been identified based on their virulence patterns on three barley differential lines (ND 5883, Bowman and ND B112) (Valjavec-Gratian and Steffenson 1997a). Pathotype 0 isolates (represented by ND93-1) have low virulence on all three barley differential lines. Pathotype 1 isolates (represented by ND85F) exhibit high virulence on ND 5883 but low virulence on Bowman and ND B112 while pathotype 2 isolates (represented by ND90Pr) show high virulence on Bowman, but low virulence on ND 5883 and ND B112 (Valjavec-Gratian and Steffenson 1997a). Zhong and Steffenson (2001) evaluated 22 isolates of *B*. *sorokiniana* collected from three U.S. states, Canada, Poland, Brazil, New Zealand, and Uruguay and classified them into the three pathotypes (0, 1 and 2). Ghazvini and Tekauz (2007) tested the virulence of 127 isolates from Canada, Australia, Uruguay, Poland, Brazil, the United States, and Mexico on 12 barley genotypes and divided them into 7 virulence groups based on 12 barley genotypes. Some isolates originated in Manitoba of Canada were designated as virulence groups 7.7.7.5, 7.7.5.1 and 6.3.5.0 possess

unique virulence on ND 5883, ND B112 and Bowman (Ghazvini and Tekauz 2007). More recently, *C*. *sativus* isolates with high virulence on the three barley differential lines were also identified in North Dakota of U.S. (Gyawali 2010), and were classified as pathotype 3 (Zhong et al. 2015).

Different pathotypes of *C*. *sativus* have been identified in other countries or regions. In Australia, Meldrum et al. (2004) identified six pathotypes among the tested 34 isolates using 20 differential lines; In Syria, Arabi and Jawhar (2004) classified 11 *C*. *sativus* isolates into three virulence groups using 10 differential barley genotypes; In Uruguay, three virulence groups of *C*. *sativus* were classified based on their infection responses (IRs) on 20 Uruguayan barley genotypes (Gamba and Estramill 2002).

Molecular basis of virulence

One unique feature of *Cochliobolus* species is that they produce host selective toxins as the virulence factors to infect the hosts. Three common examples are: HC-toxin produced by *Cochliobolus carbonum*, the causal agent of corn northern leaf spot (Liesch et al. 1982); T-toxin produced by *Cochliobolus heterostrophus*, the southern corn leaf blight pathogen (Kono and Daly 1979); and Victorin produced by *Cochliobolus victoria*, the causal agent of victoria blight of oat, (Wolpert et al. 1985).

The symptoms of necrosis and chlorosis produced by *Cochliobolus sativus* on leaves of susceptible barley hosts suggest that host-selective toxins (HSTs) are also involved in the pathogenecity of this pathogen (Pringle 1979). Three forms of predominant toxins produced by *C*. *sativus* are prehelminthosporol (PHL), helminthosporol, and sorokinianin (Gayad 1961; Ludwig

1957; Nakajima et al. 1994). Although the toxicity of these toxins had been revealed, none of them produced the typical necrotic or chlorotic symptoms of spot blotch when infiltrated into detached barley leaves, suggesting they are not HSTs (Pringle 1979; Nakajima et al. 1998).

In the Upper Midwest region of the U.S., the pathotype 2 (ND90Pr) of *C*. *sativus* was first found to be highly virulent on barley cv. Bowman (Fetch and Steffenson 1994). It produces the typical symptoms with necrosis surrounded by chlorosis, indicative of HSTs involved in the disease development. Although no HSTs have been identified and purified from culture filtrates of this pathotype by now, intracellular wash fluids from ND90Pr-infected Bowman leaves induced specific necrotic symptoms when infiltrated on barley genotype susceptible to ND90Pr (Leng and Zhong, unpublished data), suggesting that HSTs are likely produced during host infection. Valjavec-Gratian and Steffenson (1997b) and Zhong et al. (2002) indicated a single locus (*VHv1*) controls the high virulence of ND90Pr on Bowman based on the genetic analysis and molecular mapping of a population derived from the cross between pathotype 0 (ND93-1, avirulent on Bowman) and pathotype 2 (ND90Pr, highly virulent on Bowman). Recent comparative genome sequence analyses revealed that the *VHv1* locus contains two genes (protein IDs 115356 and 140513 in http://genome.jgi-psf.org/ Cocsa1/Cocsa. home.html) for nonribosomal peptide synthetases *(NRPSs)* unique to the *C*. *sativus* isolate ND90Pr (Condon et al. 2013). Deletion of either of these two NRPS encoding genes led to significant reduction in virulence on the barley cv. Bowman (Condon et al. 2013; Leng and Zhong, unpublished data). This result suggests that the virulence factor or HST in ND90Pr is a secondary metabolite peptide synthesized by NRPSs. However, global regulation on biosynthesis of secondary metabolites in this fungus has not been investigated.

The fungal global regulators: *velvet*-complex factors

Introduction

Fungal morphological development and secondary metabolism can be regulated by many genes or gene families. Recent studies revealed that LaeA and *velvet* proteins (VeA, VelB, VelC and VosA) act as global regulators of fungal development and secondary metabolism through their formation of multimeric complexes, such as LaeA/VeA/VelB, VelB/VosA, VelB/VelB (Bayram et al. 2008; Bayram et al. 2010b; Park et al. 2012b), VelC/VosA (Park et al. 2014), and VelC/VeA (Lan et al. 2014). LaeA was first identified as a putative methyltransferase in *A*. *nidulans* (Bok and Keller 2004), whereas the *velvet* superfamily proteins have been shown to be regulators in several fungal species by acting as transcription factors (Ahmed et al. 2013). LaeA, VeA, VelB, and VelC are highly conserved in many fungal species, especially in ascomycetes (Lan et al. 2014). However, not like other four *velvet*-complex proteins, VosA was less conserved in ascomycetes and was not found in the genus *Fusarium* (*F. graminearum*, *F. verticillioides*, *F. solani*, and *F*. *oxysporum*) (Lan et al. 2014; Lopez-Berges et al. 2013). Studies indicated that although *velvet*-complex proteins are conserved among filamentous fungi, their functions on regulating fungal development and biosynthesis of secondary metabolites might be similar or unique depending on the fungal species involved.

Regulations on fungal development

Although LaeA was first reported to positively regulate the asexual development of *A*. *nidulans*, *Penicillium chrysogenum*, and *F*. *fujikuroi* (Bayram et al. 2010b; Kosalkova et al. 2009; Wiemann et al. 2010), deletion of ChLae1 in *C*. *heterostrophus* increases asexual

sporulation and female sterility, reduces tolerance to oxidative stress and aerial hyphal growth (Wu et al. 2012). VeA was first identified as a positive regulator of sexual sporulation and negative regulator of asexual development in *A*. *nidulans* (Kafer 1965). Similarly, in *C*. *heterostrophus*, ChVel1 positively regulates oxidative stress responses, sexual development, and aerial hyphal growth, but negatively controls asexual differentiation (Wu et al. 2012). Furthermore, in *F*. *verticillioides*, deletion of FvVE1 suppresses aerial hyphal growth, reduced colony surface hydrophobicity, and activates conidiation with an increased ratio of macroconidia to microconidia (Li et al. 2006). In contrast, the VeA homologs in *A*. *flavus*, *P*. *chrysogenum* and *F*. *graminearum* positively regulate asexual reproduction (Amaike and Keller 2009; Hoff et al. 2010; Merhej et al. 2012).

The VelB and VosA forms VelB/VosA and VelB/VelB dimers, positively controlling trehalose biosynthesis, spore viability and conidial germination but negatively controlling conidial production in *A*. *nidulans* (Ni and Yu 2007; Park et al. 2012a). In the southern corn leaf blight pathogen *Cochliobolus heterostrophus*, Vel2 (a homolog of VelB) and Vos1 (a homolog of VosA) positively regulates trehalose biosynthesis, conidial morphology, such as the size, septum number, germination rate, as well as tolerance to oxidative and thermal stresses. They also play positive regulatory roles in sexual reproduction, but negatively regulate production of asexual spores (Wang et al. 2014). In the rice blast fungus *M*. *oryzae*, *MoVLEB* positively regulates the conidial germination and conidia production, whereas *MoVOSA* appears dispensable for the fungal development (Kim et al. 2014). In the dimorphic human pathogen *Histoplasma capsulatum*, Ryp2 (a homolog of VosA) and Ryp3 (a homolog of VelB) are essential for the temperature-dependent transition from the saprophytic filamentous phase to the single-cell pathogenic yeast form (Webster and Sil 2008). Similar to the functions of the *A*. *nidulans VosA* and *VelB*, the *ryp2*

mutants and *ryp3* mutants in *H*. *capsulatum* were reduced in spore viability (Webster and Sil 2008). *In A*. *fumigatus*, VosA exerts negative feedback control of conidiation by down-regulating *brlA* expression as found in *A*. *nidulans* (Ni and Yu 2007; Park et al. 2012b). In *Penicillium chrysogenum*, the *PcVelB* and *PcVosA* knockout strains showed a severe conidiation defect with a reduced sporulation of about 60% and 70%, respectively, compared to the reference strain, indicating that *PcVelB* and *PcVosA* positively regulates conidiation (Kopke et al. 2013). It was also found that viability (germination rate) of the Δ*PcVosA* mutant spores was approximately 20% of that of the reference strain after 4 days of culture, but gradually increased as the culture time elongated (7, 10, and 13 days) and finally was close or identical to that of the reference strain (Kopke et al. 2013). In *Ustilago maydis*, the Δ*umv2* (a ortholog of *VelB*) mutants were able to induce galls and teliospores in maize, but in slower manner and thus reduced in virulence, whereas the knockout mutants of *umv1* (a ortholog of *VosA*) failed to induce galls or teliospores in maize. Chlorazol black E staining of leaves infected with Δ*umv1* dikaryons revealed that the Δ*umv1* hyphae did not proliferate normally and were its development stopped before teliospore formation (Karakkat et al. 2013).

Functions of VelC were only studied in a few fungal species. Deletion of VelC in *A*. *nidulans* increases conidiation but significantly reduces the number of sexual fruiting bodies (Park et al. 2014). Similarly, deletion of PcVelC in *P*. *chrysogenum* also increases conidiation (Kopke et al. 2013). In contrast, deletion of *MoVELC* in *M*. *oryzae* affects the cell wall integrity of appressoria, significantly decreases the conidia production, and reduces the conidial size (Kim et al. 2014).

Regulations on secondary metabolism

The *velvet*-complex factors play important roles on regulation of secondary metabolism. Deletion of LaeA in *A*. *nidulans* blocks the expression of metabolic gene clusters, leading to reduced production of sterigmatocystin, penicillin, and lovastatin (Bok and Keller 2004). Similarly, deletion of LaeA in *Fusarium verticillioides* down regulated the expression of gene clusters encoding biosynthesis of bikaverin, fumonisin, fusaric acid, fusarin and two unknown secondary metabolites (Butchko et al. 2012). Transcriptional profiling of the LaeA mutant of the human pathogen *A. fumigatus* revealed that LaeA controls expression of 13 out of 22 secondary metabolite gene clusters, including those involved in biosynthesis of siderophores and mycotoxins (Perrin et al. 2007)

The VeA orthologs had been reported to control biosynthesis of various secondary metabolites such as aflatoxin, cyclopiazonic acid, and aflatrem in *A*. *flavus* (Duran et al. 2009), trichothecenes in *F*. *graminearum* (Merhej et al. 2012), and melanin in *M*. *graminicola* (Choi and Goodwin 2011). In *C*. *heterostrophus*, ChLae1 and ChVel1 positively regulate T-toxin biosynthesis but negatively control melanin biosynthesis in mycelia (Wu et al. 2012).

In *F*. *verticillioides,* Fvve1 *and* FvvelB positively regulate fumonisin production (Lan et al. 2014). In *P*. *chrysogenum*, the PcLaeA and PcVelA activate penicillin biosynthesis, whereas PcVelB represses this process (Kopke et al. 2013). In *Fusarium oxysporum*, the LaeA, VeA, and VelB proteins play light-dependent roles in biosynthesis of three secondary metabolites, ferricrocin, triacetylfusarinine C and beauvericin (BEA), which are synthesized by non-ribosomal peptide synthetase (NRPS) genes (Lopez-Berges et al. 2013).

For the roles of VelC on secondary metabolism, it is reported that the PcVelC activate penicillin biosynthesis (Kopke et al. 2013). However, the role of VosA on regulation of secondary metabolism has not been reported.

The disease: spot blotch on barley

Introduction

Spot blotch, caused by *Cochliobolus sativus*, is one of the most common and economically important foliar diseases of barley found in nearly every region of the world where the crop is grown (Mathre, 1982). It has been reported in many regions of the world, including the Upper Midwest region of the U.S., Prairie Provinces of Canada, Australia and Uruguay.

Distribution and importance

In the U.S., spot blotch of barley was first recorded at Ames, Iowa in 1890 (Pammel et al. 1910). However, the disease is more severe in the Upper Midwest region (Mathre 1997). Under favorable conditions, it can cause up to 30% yield losses and more commonly impact the malting quality (Wilcoxson et al. 1990).

In Canada, spot blotch mainly occurs in the Prairie Provinces. In 2002, this disease was predominant in barley and affected every field sampled in Manitoba (Tekauz et al. 2003). Under experimental conditions using artificial inoculation, yield losses up to 30% have been reported for susceptible barley cultivars in Canada (Clark 1979; Ghazvini and Tekauz 2004).

In Australia, spot blotch mainly occurs in sub-tropical areas of northern New South Wales and Queensland. It causes greater than 30% of localized barley yield losses with an average

annual loss of $1 million and potential annual losses of $2 million under highly favorable conditions (Murray and Brennan 2010).

In Uruguay, spot blotch is one of the most important barley diseases. Estimated grain yield losses in epidemic years varied from 7% to 30%. The incidence of spot blotch has increased in the last 15 years due to wide adoption of no-till practice (Pereyra et al. 2003).

Symptoms and disease cycle

The most common characteristic of the spot blotch symptoms is the brown necrotic lesions with or without chlorosis, depends on the barley genotypes and the pathotypes of the pathogen (Fetch and Steffenson 1994; Fetch and Steffenson 1999; Mathre 1997). Based on the lesion type (presence of necrosis and chlorosis) and relative size of lesions observed on barley lines, a 1-9 rating scale was developed to assess infection responses (IRs) of barley lines at the seedling stage (Fetch and Steffenson 1999). IRs at the adult stage were assessed based on four classes: resistant (R), moderately resistant (MR), moderately susceptible (MS), and susceptible (S), which were distinguished based on the type (presence of necrosis and chlorosis) and relative size of lesions according to the descriptions of Fetch and Steffenson (1999).

C. *sativus* is a polycyclic plant pathogen and the disease cycle begins when conidia (asexual spores) are attached on the leaf surfaces of barley (Braun and Howard 2015). Subsequently, the conidium germinates and develops an appressorium, a specialized infection structure to assist penetration into the leaves (Kumar et al. 2002). After successful penetration, the fungus produces infection hyphae to invade the mesophyll leaf tissues and cause cell death of the host (Santen et al. 2005). Then, necrosis and/or chlorosis forms. After the successful infection, the pathogen will live

on the dead tissue and produce asexual spores to start the next infection cycle. *C*. *sativus* overwinters as mycelia or conidia on barley or other crop residues, or on infected seeds. These can serve as the primary inoculum for the infection in next growing season (Duczek 1984).

Disease management

Spot blotch can be controlled by several management strategies: cultural practices such as destruction of crop residues and crop rotation to reduce or eliminate the inoculum sources; application of fungicides such as chemical seed treatment and foliar fungicide sprays; and breeding of resistance cultivars (Bailey et al. 2003; Kiesling 1985; Mathre 1997). Other management strategies such as biological control and induced resistance have also been studied (Kumar et a1., 2002) and may be promising alternative method to control spot blotch in the future.

Cultural practices

C. *sativus* can survive on plant debris as mycelia or conidia, which serve as the important inoculum source for primary infection of plants (Duczek et al. 1999). So the destruction of crop residues by cultural practices such as burying, burning or removal, is an important practice to control spot blotch. Primary inoculum in crop residue can also be reduced by crop rotation with non-susceptible crops, or with a fallow, resting period between crop plantings (Mathre 1997). Conner et al. (1996) indicated that rotations of two or more years to flax (*Linum usitatissimum* L.) as a break crop in the barley planting field reduced the amount of viable inoculum of *C*. *sativus* in the soil.

Fungicides

Another inoculum source of *C*. *sativus* is the infected seed and therefore using fungicide treated seed may reduce the infection level (Mathre 1997). Systemic fungicide such as captan, mancozeb, maneb, thiram, carboxin, gaazatine as well as iprodione and triadimefon are commonly used to destroy seed-borne pathogens in cereals (Sharma-Poudyal et al. 2005; Stack and McMullen 1991). Richardson (1972) found that *C*. *sativus* could not grow on barley seed treated with carboxin. In addition, seed dressings with systemic fungicides Narimol and fenapanil have also been reported as effective to control seed-borne infection of barley seedling caused by *C*. *sativus* (Luz and Vieira 1982).

Foliar spray of fungicides can significantly reduce the level of infection caused by *C*. *sativus* in barley and increase yields (Mathre, 1997). It was reported that application of foliar fungicides mancozeb, RH-2161, chlorothalonil, fentin hydroxide, triadimefon and anilazine significantly reduced the spot blotch severity by 63,68, 68, 77, 82 and 88% respectively, in barley (Couture and Sutton 1978b). Couture and Sutton (1978a) found Triadimefon could markedly suppress the progress of spot blotch and delay leaf senescence in barley.

Genetic resistance

Although application of fungicides is effective in controlling spot blotch, deployment of resistant cultivars is the most economic and environmentally sound approach for management of the disease. In the Upper Midwest region of the U.S., great efforts have been made to identify sources of resistance to spot blotch caused by pathotype 1 (isolate ND85F) of *C*. *sativus* since it is the predominant pathogen in this region (Ghazvini and Tekauz 2007). In six-row barley cultivars, the resistance identified from the barley line ND B112 has been effective for over 50

years (Steffenson et al. 1996). ND B112 was selected from the cross CI 7117-77 x Kindred at North Dakota State University (Wilcoxson et al. 1990a) and is widely applied in barley breeding programs, leading to the development of resistant barley cultivar Morex and most of the six-rowed barley varieties currently used in this region. Fetch et al. (2008) screened over 5,000 spring barley accessions from the USDA National Small Grains Collection for resistance to spot blotch at the adult plant stage in the field and found that only 5.8% (373 accessions) was resistant. Most of these resistant lines were from North America and possibly carry the resistance from ND B112 due to its broad use in barley breeding programs in the Upper Midwest region (Bonman et al. 2005; Fetch et al. 2008). Sources of spot blotch resistance have also been identified in wild barley *Hordeum vulgare* subsp. *spontaneum* (C. Koch) Thell (Fetch et al. 2003; Roy et al. 2010), which possesses a high level of genetic diversity and carry novel alleles for many economically important traits including resistance to diseases (Ellis et al. 2000; Fetch et al. 2003; Shakhatreh et al. 2010; Steffenson et al. 2007).

The resistance identification: molecular mapping

Introduction

Identification of genomic loci governing complex traits is important for their effective application in breeding programs and can be accomplished by the quantitative trait locus (QTL) mapping approach. Traditionally, QTL mapping is performed using segregating biparental populations, such as F_2 population, Recombinant Inbred Lines (RILs) population, and Double Haploid (DH) population. Nowadays, genome-wide association studies (GWAS) have been commonly used in the identification of candidate loci associated with numerous traits in many

plant species (Appels et al. 2013; Korte and Farlow 2013). Both methods have their advantages and disadvantages. To obtain the best mapping resolution and understanding of the genetics of the resistance, QTL mapping and GWAS are needed to perform together to mitigate each other's limitations (Brachi et al. 2010; Sonah et al. 2015; Zhao et al. 2007).

Bi-parental linkage mapping

In the past years, great efforts have been made to characterize genetic loci conferring the resistance to spot blotch using the bi-parental linkage mapping method. Wilcoxson et al. (1990) first studied genetics of spot blotch resistance in populations developed from crosses of five spot blotch resistant barley lines (Minn 33, Minn 65-241, Minn 65-243, Minn 65-244, and Minn 7) with the susceptible cultivar Larker, and revealed that spot blotch resistance is conditioned by one or two major genes. Using the doubled haploid (DH) populations derived from the crosses of the resistant cultivar Morex and three susceptible cultivars (Steptoe, Dicktoo, and Harrington), respectively, Bilgic et al. (2005), Steffenson et al. (1996), and Bilgic et al. (2005) mapped QTLs for resistance to the pathotype 1 (represented by isolate ND85F) on chromosomes 1H, 3H and 7H, respectively. Using a doubled haploid population derived from the Calicuchima-sib / Bowman-BC cross, Bilgic et al. (2006) mapped the genetic loci conferring resistance to pathotype 1 and 2 on chromosome 4H and 1H, respectively. Several other research groups also conducted QTL analysis for spot blotch resistance at the seedling stage. Bovill et al. (2010) identified two QTL for resistance to the isolate SB61 on chromosome 5HL and 7HS using four populations [VB9524/ ND11231-12 (VB/ND-12), ND11231-11/WI2875-17 (ND-11/WI), TR251/Gairdner (TR/GA) and WPG84 12-9-2-1/Lindwall (WP/LI)]. In addition, Grewal et al.

(2012) mapped three QTL (*QRcss1, QTcss3, and QRcss5*) on chromosome 1H, 3H, and 5H for resistance to three different isolates (WRS1909, WRS1908, and SK1-1) using a DH population from the cross between CDC Bold and TR251.

Although the traditional bi-parental mapping approach is effective for identification of QTL for resistance to diseases, the main disadvantage of this method is that only a very limited genetic diversity of the species is captured since only two genotypes are used as parents in the population. Furthermore, the genetic resolution of bi-parental mapping is often at a range of 10 cM to 30 cM because of the restricted number of meiotic events that are captured in the bi-parental mapping population (Bilgic et al. 2006; Laido et al. 2014).

Association mapping

Association mapping (AM), which is based on linkage disequilibrium (LD) in a large population of unrelated individuals (Risch 2000), provides an alternative method for identifying QTL. With AM, one can utilize diverse germplasm panels, including worldwide collections, and therefore the genetic diversity of the mapping population is greatly increased. Besides, in AM populations, recombination events occurred throughout their evolutionary history, contributing to the breakage of LD blocks within the genome. Thus, LD decays much faster in AM populations than in bi-parental mapping populations (Rafalski 2002), greatly increasing the map resolution. Considering all of these advantages, AM has been successfully used in various plant species to identify markers associated with many different traits, including resistance to spot blotch. AM has been conducted with a collection of 318 wild barley lines (Roy et al. 2010), US barley breeding germplasm (Zhou and Steffenson 2013) and Virginia Tech winter barley lines (Berger

et al. 2013) and QTL for spot blotch resistance to pathotype 1 (ND85F) were detected on barley chromosome 1H, 3H, and 7H, respectively. More recently, a total of 2,417 barley accessions selected from the USDA National Small Grains Collection (NSGC) were genotyped using the Infinium iSelect SNP assay through the Triticeae Coordinated Agricultural Project (http://www.triticeaecap.org/). Munoz-Amatriain et al. (2014) analyzed the LD pattern and population structure of these barley accessions and demonstrated the utility of this barley core collection for locating genetic alleles affecting phenotypes by genome-wide association mapping. Using this same barley core collection, Tamang et al. (2015) detected 21 putative novel loci significantly associated with resistance or susceptibility to the spot form net blotch disease caused by four different isolates of *Pyrenophora teres* f. *maculata*.

In the GWAS approach, however, the fact that very low limited linkage disequilibrium between pairs of neighboring markers exhibited in many of the association mapping panels of unrelated genotypes requires a much larger number of markers to provide adequate coverage of the entire genome (Hyten et al. 2007). For example, it has been estimated that tens of thousands of markers are needed to provide exhaustive coverage of the soya bean genome (Bastien et al. 2014; Hyten et al. 2007).

References

Aberg, E. 1938. *Hordeum agriocrithon* nova sp., a wild six-rowed barley. Ann. R. Agric. Col. Swed. 6:159–216.

Ahmed, Y. L., Gerke, J., Park, H. S., Bayram, Ö., Neumann, P., Ni, M., Dickmanns, A., Kim, S. C., Yu, J. H., Braus, G. H., and Ficner, R. 2013. The velvet family of fungal regulators contains a DNA-binding domain structurally similar to NF-κB. PLoS Biol. 11:e1001750.

Amaike, S., and Keller, N. P. 2009. Distinct roles for VeA and LaeA in development and pathogenesis of *Aspergillus flavus*. Eukaryot. Cell 8:1051-1060.

Appels, R., Barrero, R. and Bellgard, M. 2013. Advances in biotechnology and informatics to link variation in the genome to phenotypes in plants and animals. Funct. Integr. Genomic. 13:1–9.

Arabi, M. I. E., and Jawhar, M. 2004. Identification of *Cochliobolus sativus* spot blotch isolates expressing differential virulence on barley genotypes in Syria. J. Phytopathol. 152:461-464.

Baba, S., Kinoshita, H., and Nihira, T. 2012. Identification and characterization of *Penicillium citrinum* VeA and LaeA as global regulators for ML-236B production. Curr. Genet. 58:1-11.

Badr, A., Muller, K., Schafer-Pregl, R., EI, R. H., Effgen, S., Ibrahim, H. H., Pozzi, C., Rohde, W., Salamini, F. 2000. On the origin and domestication history of barley *Hordeum vulgare*. Mol. Biol. Evol. 17:499–510.

Bailey, K. L., Gossen, B. D., Gugel, R. K. and Morrall, R. A. A. 2003. Diseases of field crops in Canada. 3rd ed. The Canadian Phytopathological Society. Ontario, Canada. pp. 304.

Bastien, M., Sonah, H. and Belzile, F. 2014. Genome wide association mapping of *Sclerotinia sclerotiorum* resistance in soybean with a genotyping by sequencing approach. Plant Genome. 7:1–13.

Bayram, O., and Braus, G. 2012. Coordination of secondary metabolism and development in fungi: the velvet family of regulatory proteins. FEMS Microbiol. Rev. 36:1-24.

Bayram, O., Valerius, O., Park, H. S., Irniger, S., Gerke, J., Ni, M., Han, K. H., Yu, J. H., and Braus, G. H. 2010. LaeA control of velvet family regulatory proteins for light-dependent development and fungal cell-type specificity. PLoS Genet. 6:e1001226.

Bayram, O., Krappmann, S., Ni, M., Bok, J., Helmstaedt, K., Valerius, O., Braus-Stromeyer, S., Kwon, N., Keller, N., Yu, J., and Braus, G. 2008. VelB/VeA/LaeA complex coordinates light signal with fungal development and secondary metabolism. Science 320:1504-1506.

Bekelle, E. 1983. A differential rate of regional distribution of barley flavonoid patterns in Ethiopia, and a view on the center of origin of barley. Hereditas. 98:269–280.

Berger, G. L., Liu, S., Hall, M. D., Brooks, W. S., Chao, S., Muehlbauer, G. J., Baik, B. K., Steffenson, B., and Griffey, C. A. 2013. Marker-trait associations in Virginia Tech winter barley identified using genome-wide mapping. Theor. Appl. Genet. 126:693-710.

Bilgic, H., Steffenson, B. J., and Hayes, P. 2005. Comprehensive genetic analyses reveal differential expression of spot blotch resistance in four populations of barley. Theor. Appl. Genet. 111:1238-1250.

Bilgic, H., Steffenson, B. J., and Hayes, P. M. 2006. Molecular mapping of loci conferring resistance to different pathotypes of the spot blotch pathogen in barley. Phytopathology 96:699-708.

Bockelman, H. E., Valkoun, J. 2011. Barley germplasm conservation and resources. In: Ullrich S. E., editor. Barley: production, improvement, and uses. Wiley-Blackwel. 144–159.

Bok, J. W., and Keller, N. P. 2004. LaeA, a regulator of secondary metabolism in *Aspergillus* spp. Eukaryot. Cell 3:527-535.

Bonman, J. M., Bockelman, H. E., Jackson, L. F., and Steffenson, B. J. 2005. Disease and insect resistance in cultivated barley accessions from the USDA national small grains collection. Crop Sci. 45:1271-1280.

Bonman, J. M., Gu, Y., Coleman-Derr, D., Jackson, E. W., Bockelman, H. E. 2011. Inferring geographic origin of barley *Hordeum vulgare* L. subsp. *vulgare* accessions using molecular markers. Genetic Resour. Crop. Evol. 58:291–298.

Bovill, J., Lehmensiek, A., Sutherland, M. W., Platz, G. J., Usher, T., Franckowiak, J., and Mace, E. 2010. Mapping spot blotch resistance genes in four barley populations. Mol. Breed. 26:653-666.

Brachi, B., Faure, N., Horton, M., Flahauw, E., Vazquez, A., Nordborg, M., Bergelson, J., Cuguen, J. and Roux, F. 2010. Linkage and association mapping of *Arabidopsis thaliana* flowering time in nature. PLoS Genet. 6:e1000940.

Braun, E. J., and Howard, R. J. 2015. Adhesion of fungal spores and germlings to host plant surfaces. Protoplasma 181:202-212

Butchko, R. A., Brown, D. W., Busman, M., Tudzynski, B., and Wiemann, P. 2012. Lae1 regulates expression of multiple secondary metabolite gene clusters in *Fusarium verticillioides*. Fungal Genet Biol 49:602–612.

Chang, P. K., Scharfenstein, L. L., Li, P., and Ehrlich, K. C. 2013. *Aspergillus flavus* VelB acts distinctly from VeA in conidiation and may coordinate with FluG to modulate sclerotial production. Fungal Genet. Biol. 58-59:71-79.

Choi, Y. E., and Goodwin, S. B. 2011. *MVE1*, encoding the velvet gene product homolog in *Mycosphaerella graminicola*, is associated with aerial mycelium formation, melanin biosynthesis, hyphal swelling, and light signaling. Appl. Environ. Microb. 77:942-953.

Clarlk, H.H. 1967. The origin and early history of the cultivated barleys. Agric. Hist. Rev. 15:1

Condon, B., Leng, Y. Q., Wu, D., Bushley, K., Ohm, R., Otillar, R., Martin, J., Schackwitz, W., Grimwood, J., MohdZainudin, N., Xue, C., Wang, R., Manning, V., Dhillon, B., Tu, Z., Steffenson, B., Salamov, A., Sun, H., Lowry, S., LaButti, K., Han, J., Copeland, A.,

Lindquist, E., Barry, K., Schmutz, J., Baker, S., Ciuffetti, L., Grigoriev, I., Zhong, S. B., and Turgeon, B. 2013. Comparative genome structure, secondary metabolite, and effector coding capacity across *Cochliobolus* pathogens. PLoS Genet. 9:e1003233.

Conner, R. L., Duczek, L. J., Kozub, G. C. and Kuzyk, A. D. 1996. Influence of crop rotation on common root rot of wheat and barley. Can. J. Plant Pathol. 18:247-254.

Couture, L. and Sutton, J. C. 1978a. Control of spot blotch in barley by fungicide applications timed according to weather factors. Phytoprotection. 59:65-75.

Couture, L. and Sutton, J. C. 1978b. Efficacies of fungicides in controlling spot blotch of barley. Can. J. Plant Sci. 58:311-317.

Domsch, K. H., Gams, W. and Anderson, T. H. 1980. Compendium of soil fungi. Volume 1. Academic Press.

Duczek, L. J. 1984. Comparision of common root rot reaction of barley lines and cultivars in northwestern Alberta and central Saskatchewan. Can. J. Plant Pathol. 6:81-89.

Duczek, L. J., Sutherland, K. A., Reed, S. L., Bailey, K. L. and Lafond, G. P. 1999. Survival of leaf spot pathogens on crop residues of wheat and barley in Saskatchewan. Can. J. Plant Pathol. 2l:165-173.

Duran, R. M., Cary, J. W., and Calvo, A. M. 2009. The role of VeA in *Aspergillus flavus* infection of peanut, corn and cotton. Open Mycol. J. 3:27-36.

Ellis, R. P., Forster, B. P., Robinson, D., Handley, L. L., Gordon, D. C., Russell, J. R., and Powell, W. 2000. Wild barley: a source of genes for crop improvement in the 21st century? J. Exp. Bot. 51:9-17.

Wiley, E. O., Siegel-Causey, D., Brooks, D. R., and Funk, V.A. 1991. The compleat cladist: A primer of phylogenetic procedures. Univ. Kansas Mus. Nat. Hist. Lawrence, KS, Spec. Publ. No. 19 online at Internet Archive.

Fetch, T. G., and Steffenson, B. J. 1994. Identification of *Cochliobolus sativus* isolates expressing differential virulence on 2-row barley genotypes from North Dakota. Can. J. Plant Pathol. 16:202-206.

Fetch, T. G., and Steffenson, B. J. 1999. Rating scales for assessing infection responses of barley infected with *Cochliobolus sativus*. Plant Dis. 83:213-217.

Fetch, T. G. Jr., Steffenson, B. J., Bockelman, H. E., and Wesenberg, D. M. 2008. Spring barley accessions with dual spot blotch and net blotch resistance. Can. J. Plant Pathol. 30:534-542.

Fetch, T. G., Steffenson, B. J., Nevok, E. 2003. Diversity and sources of multiple disease resistance in *Hordeum spontaneum*. Plant Dis. 87:1439-1448.

Fischbech, G. 2002. Contribution of barley to agriculture: A brief overview. In: Barley science, recent advances from molecular biology to agronomy of yield and quality. Slafer, G. A., Molina-Cano, J. L., Savin, R., Araus, L. and Romagosa, I. eds. Food Product Press, New York. pp. 1-14.

Gamba, F., and Estramill, E. 2002. Variation in virulence within Uruguayan population of *Cochliobolus sativus*. In: Proc. 2nd Int. Workshop Barley Leaf Blights. ICARDA, Aleppo, Syria. pp. 59-62

Gayad, S. K. 1961. Production of symptoms of barley leaf spot disease by cultural filtrates of *Helminthosporium sativum*. Nature 191:725–726.

Grewal, T. S., Rossnagel, B. G., and Scoles, G. J. 2012. Mapping quantitative trait loci associated with spot blotch and net blotch resistance in a doubled-haploid barley population. Mol. Breed. 30:267-279.

Harlan, J. R. and Zohary, D. 1966. Distribution of wild wheat and barley. Science 153:1074-1079

Helbaek, H. 1959. Domestication of food plants in the old world. Science 130:365-372.

Hoff, B., Kamerewerd, J., Sigl, C., Mitterbauer, R., Zadra, I., Kurnsteiner, H., and Kuck, U. 2010. Two components of a velvet-like complex control hyphal morphogenesis, conidiophore development, and penicillin biosynthesis in *Penicillium chrysogenum*. Eukaryot. Cell 9:1236-1250.

Horsley, R. D., and B. L. Harvey. 2011. Barley breeding, history, progress, objectives, and technology: North America p.171-186. In S.E. Ullrich ed. Barley. John Wiley & Sons, West Sussex, UK.

Hyten, D. L., Choi, I. Y., Song, Q., Shoemaker, R. C., Nelson, R. L., Costa, J. M., Specht, J. E. and Cregan, P. B. 2007. Highly variable patterns of linkage disequilibrium in multiple soybean populations. Genetics 175:1937–1944.

Jiang, J., Yun, Y., Liu, Y., and Ma, Z. 2012. *FgVELB* is associated with vegetative differentiation, secondary metabolism and virulence in *Fusarium graminearum*. Fungal Genet. Biol. 49:653-662.

Kafer, E. 1965. Origins of Translocations in *Aspergillus nidulans*. Genetics 52:217-232.

Karakkat, B. B., Gold, S. E., and Covert, S. F. 2013. Two members of the *Ustilago maydis* velvet family influence teliospore development and virulence on maize seedlings. Fungal Genet. Biol. 61:111-119.

Kiesling, R. L. 1985. The diseases of barley. In: Barley. Rasmusson, D. C. ed. Agronomy Monograph No. 26, ASA. Madison WI. pp. 269-312.

Kim, H. J., Han, J. H., Kim, K. S., and Lee, Y. H. 2014. Comparative functional analysis of the velvet gene family reveals unique roles in fungal development and pathogenicity in *Magnaporthe oryzae*. Fungal Genet. Biol. 66:33-43.

Kim, H. K., Lee, S., Jo, S. M., McCormick, S. P., Butchko, R. A. E., Proctor, R. H., and Yun, S. H. 2013. Functional roles of FgLaeA in controlling secondary metabolism, sexual development, and virulence in *Fusarium graminearum*. PLoS One 8:15.

Kirk, P. M., Cannon, P. F., Minter, D. W., Stalpers, J. A. 2008. Dictionary of the Fungi. 10th ed.. Wallingford: CABI. pp. 221.

Knüpffe, H. 2009. Triticeae genetic resources in ex situ genebank collections. In: Springer science business media. Feuillet C, Muehlbauer G. J., editors. Genetics and Genomics of the Triticeae. LLC: 31–79.

Kono, Y., and Daly, J. M. 1979. Characterization of the host-specific pathotoxin produced by *Helminthosporium maydis* lace T affecting corn with Texas male sterile cytoplasm. Bioorg. Chem. 8:391-397.

Kopke, K., Hoff, B., Bloemendal, S., Katschorowski, A., Kamerewerd, J., and Kuck, U. 2013. Members of the *Penicillium chrysogenum* velvet complex play functionally opposing roles in the regulation of penicillin biosynthesis and conidiation. Eukaryot. Cell 12:299-310.

Korte, A. and Farlow, A. 2013. The advantages and limitations of trait analysis with GWAS: a review. Plant Methods 9:29.

Kosalkova, K., Garcia-Estrada, C., Ullan, R. V., Godio, R. P., Feltrer, R., Teijeira, F., Mauriz, E., and Francisco Martin, J. 2009. The global regulator LaeA controls penicillin biosynthesis, pigmentation and sporulation, but not roquefortine C synthesis in *Penicillium chrysogenum*. Biochimie 91:214-225.

Kumar, J., Schafer, P., Huckelhoven, R., Langen, G., Baltruschat, H., Stein, E., Nagarajan, S., and Kogel, K. H. 2002. *Bipolaris sorokiniana*, a cereal pathogen of global concern: cytological and molecular approaches towards better control. Mol. Plant Pathol. 3:185-195.

Laido, G., Marone, D., Russo, M. A., Colecchia, S. A., Mastrangelo, A. M., De Vita, P., and Papa, R. 2014. Linkage disequilibrium and genome-wide association mapping in tetraploid wheat (Triticum Turgidum L.). PLoS One 9:e95211.

Lan, N., Zhang, H., Hu, C., Wang, W., Calvo, A. M., Harris, S. D., Chen, S., and Li, S. 2014. Coordinated and distinct functions of velvet proteins in *Fusarium verticillioides*. Eukaryot. Cell 13:909-918.

Liesch, J. M. C, Sweeley, C. C, Staffeld, G. D., Anderson, M. S., Weber, D. J., and Scheffer, R. P. 1982. Structure of HC-toxin, a cyclic tetrapeptide from *Helminthosporium carbonum*. Tetrahedron 38:45-48.

Li, S. J., Myung, K., Guse, D., Donkin, B., Proctor, R. H., Grayburn, W. S., and Calvo, A. M. 2006. FvVE1 regulates filamentous growth, the ratio of microconidia to macroconidia and cell wall formation in *Fusarium verticillioides*. Mol. Microbiol. 62:1418-1432.

Lopez-Berges, M. S., Hera, C., Sulyok, M., Schafer, K., Capilla, J., Guarro, J., and Di Pietro, A. 2013. The velvet complex governs mycotoxin production and virulence of *Fusarium oxysporum* on plant and mammalian hosts. Mol. Microbiol. 87:49-65.

Luttrell, E. S. 1951. Taxonomy of Pyrenomycetes. University of Missouri Studies in Sciences. 24.

Luttrell, E. S. 1955. The ascostromatic Ascomycetes. Mycologia 47:511-532.

Ludwig, R. A. 1957. Toxin production by *Helminthosporium sativum* P.K. & B. and its significance in disease development. Can. J. Bot. 35:291–303.

Luz, W. C., and Vieira, J. C. 1982. Seed treatment with systemic fungicides to control *Cochliobolus sativus* on barley. Plant Dis. 66:135-136.

Mathre, D. E. 1982. Compendium of barley disease. Proc. Am. Phytopathol. Soc. pp. 32-34

Mathre, D. E. 1997. Compendium of barley diseases, 2nd Edition. American Phytopathological Society Press, St Paul, MN.

Meldrum, S. I., Ogle, H. J., and Platz, G. J. 2004. Pathotypes of *Cochliobolus sativus* on barley in Australia. Aust. Plant Pathol. 33:109-114.

Merhej, J., Urban, M., Dufresne, M., Hammond-Kosack, K. E., Richard-Forget, F., and Barreau, C. 2012. The velvet gene, *FgVe1*, affects fungal development and positively regulates trichothecene biosynthesis and pathogenicity in *Fusarium graminearum*. Mol. Plant Pathol. 13:363-374.

Molina-Cano, J. L. et al. 2005. Chloroplast DNA microsatellite analysis supports a polyphyletic origin for barley. Theor. Appl. Genet. 110:613–619

Molina-cano, J. L., Fra-Mon, P., Salcedo, G., Aragoncillo, C., De-Togores, F. R., and Garcia-Olmedo, F. 1987. Morocco as a possible domestication center for barley: biochemical and agromorphological evidence. Theor.Appl. Genet. 73:531–536.

Morrell, P. L. and Clegg, M. T. 2007. Evidence for a second domestication of barley *Hordeum vulgare* east of the Fertile Crescent. Proc. Natl. Acad. Sci. U. S. A. 104, 3289–3294

Munoz-Amatriain, M., Cuesta-Marcos, A., Endelman, J. B., Comadran, J., Bonman, J. M., Bockelman, H. E., Chao, S., Russell, J., Waugh, R., Hayes, P. M., and Muehlbauer, G. J. 2014. The USDA barley core collection: genetic diversity, population structure, and potential for genome-wide association studies. PLoS One 94:e94688.

Murray, G. M., and Brennan, J. P. 2010. Estimating disease losses to the Australian barley industry. Australas. Plant Pathol. 39:85–96

Nakajima, H., Isomi, K., Hamasaki, T. and Ichinoe, M. 1994. Sorokinianin: a novel phytotoxin produced by the phytopathogenic fungus *Bipolaris sorokiniana*. Tetrahedron Lett. 35:9597–9600.

Nakajima, H., Toratsu, Y., Fujii, Y., Ichinoe, M. and Hamasaki, T. 1998 Biosynthesis of sorokinianin, a phytotoxin of *Bipolaris sorokiniana*: evidence of mixed origin from the sesquiterpene and TCA pathways. Tetrahedron Lett. 39:1013–1016.

Newman, C. W., Newman, R. K. 2006. A brief history of barley foods. Cereal Foods World 51:1–5

Ni, M., and Yu, J. H. 2007. A novel regulator couples sporogenesis and trehalose biogenesis in *Aspergillus nidulans*. PLoS One 2:e970.

Pammel, L. H., King, C. M., and Bakke, A. L. 1910. Two barley blights, with comparison of species of *Helminthosporium* upon cereals. Iowa Agric. Exp. Stn. Res. Bull. 116:178-188.

Park, H. S., Bayram, O., Braus, G. H., Kim, S. C., and Yu, J. H. 2012a. Characterization of the velvet regulators in *Aspergillus fumigatus*. Mol. Microbiol. 86:937-953.

Park, H. S., Nam, T. Y., Han, K. H., Kim, S. C., and Yu, J. H. 2014. VelC positively controls sexual development in *Aspergillus nidulans*. PLoS One 9:e89883.

Park, H. S., Ni, M., Jeong, K. C., Kim, Y. H., and Yu, J. H. 2012b. The role, interaction and regulation of the velvet regulator VelB in *Aspergillus nidulans*. PLoS One 7:e45935.

Perrin, R. M., Fedorova, N. D., Bok, J. W., Cramer, R. A., Wortman, J. R., Kim, H. S., Nierman, W. C., and Keller, N. P. 2007. Transcriptional regulation of chemical diversity in *Aspergillus fumigatus* by LaeA. PLoS Pathog. 3: e50.

Pringle, R. B. 1979. Role of toxins in etiology of spot blotch disease of barley. Can. Plant Dis. Surv. 59:74-79.

Poehlman, J. M. 1994. Breeding barley and oats, In Poehlman, J. M. ed. Breeding field crops 3rd ed, Iowa State University Press, Ames, Iowa. pp. 378-420.

Rafalski, A. 2002. Applications of single nucleotide polymorphisms in crop genetics. Curr. Opin. Plant Biol. 5:94-100.

Richardson, L.T., 1972. Effectiveness of systemic fungicide seed dressings as protectants of barley seedlings against *Cochliobolus sativus*. Can. J. Plant Sci. 52:949-953.

Risch, N. J. 2000. Searching for genetic determinants in the new millennium. Nature 405:847-856.

Roy, J., Smith, K., Muehlbauer, G., Chao, S., Close, T., and Steffenson, B. J. 2010. Association mapping of spot blotch resistance in wild barley. Mol. Breed. 26:243-256.

Saisho, D. and Purugganan, M. D. 2007. Molecular phylogeography of domesticated barley traces expansion of agriculture in the Old World. Genetics 177:1765–1776

Santen, K., Marttila, S., Liljeroth, E., and Bryngelsson, T. 2005. Immunocytochemical localization of the pathogenesis-related PR-1 protein in barley leaves after infection by *Bipolaris sorokiniana*. Physiological and Mol. Plant Pathol. 66:45-54.

Shakhatreh, Y., Haddad, N., Alrababah, M., Grando, S., and Ceccarelli, S. 2010. Phenotypic diversity in wild barley *Hordeum vulgare* L. ssp *spontaneum* C. Koch Thell. accessions collected in Jordan. Genet. Resour. Crop Ev. 57:131-146.

Sharma-Poudyal, D., Duveiller, E. and Sharma, R. C. 2005. Effects of seed treatment and foliar fungicides on Helminthosporium leaf blight and on performance of wheat in warmer growing conditions. J. Phytopathol. 153 :401-408.

Shoemaker, R. A. 1955. Biology, cytology, and taxonomy of *Cochliobolus sativus*. Can. J. Bot. 33:562-576.

Sivanesan, A. 1987. Graminicolous species of *Bipolaris*, *Culvularia*, *Drechslera*, *Exorhilum* and their teleomorphs. Mycological papers, 158. CAB International Mycological Institute, Surrey, England.

Sivanesan, A., and Holliday, P. 1981. *Cochliobolus sativus*. C.M.I. Descr. Pathog. Fungi Bact. 701:1-2

Sonah, H., O'Donoughue, L., Cober, E., Rajcan, I. and Belzile, F. 2015. Identification of loci governing eight agronomic traits using a GBS-GWAS approach and validation by QTL mapping in soya bean. Plant Biotechnol. J. 13:211-221

Sreenivasulu, N., Graner, A., and Wobus, U. 2008. Barley genomics: an overview. Int. J. Plant Genomics 2008:486258.

Stack, R.W., and McMullen, M.P. 1991. Effect of fungicidal seed treatments on corrunon root rot of spring wheat and barley. North Dakota Farm Res. 49:13-16.

Steffenson, B. J., Hayes, P. M., and Kleinhofs, A. 1996. Genetics of seedling and adult plant resistance to net blotch *Pyrenophora teres* f *teres* and spot blotch *Cochliobolus sativus* in barley. Theor. Appl. Genet. 92:552-558.

Steffenson, B. J., Olivera, P., Roy, J. K., Jin, Y., Smith, K. P., and Muehlbauer, G. J. 2007. A walk on the wild side: mining wild wheat and barley collections for rust resistance genes. Aust. J. Agr. Res. 58:532-544.

Tamang, P., Neupane, A., Mamidi, S., Friesen, T., and Brueggeman, R. 2015. Association mapping of seedling resistance to spot form net blotch in a worldwide collection of barley. Phytopathology 105:500-508.

Tekauz, A. 2003. Spot blotch caused by *Bipolaris sorokiniana*: an emerging problem in barley in western Canada. In: Proc. of 8th International Congress of Plant Pathology. Vol. II. Christchurch, New Zealand. pp. 103.

Tinline, R. D. 1951. Studies of the perfect stage of *Helminthosporium sativum*. Can. J. Bot. 29:467-478.

Tinline, R. D. 1988. *Cochliobolus sativus*, a pathogen of wide host range. In: Advances in plant pathology, Vol. 6. Ingram, D. S. and Williams, P. H. eds. Academic Press, London, England. pp. 113-122.

Valjavec-Gratian, M., and Steffenson, B. J. 1997a. Pathotypes of *Cochliobolus sativus* on barley in North Dakota. Plant Dis. 81:1275-1278.

Valjavec-Gratian, M., and Steffenson, B. J. 1997b. Genetics of virulence in *Cochliobolus sativus* and resistance in barley. Phytopathology 87:1140-1143.

Valkoun, J. 2008. Global strategy for the ex situ conservation and use of barley germplasm. Available at http://www.croptrust.org/documents/cropstrategies/ barley.pdf.

Wang, W., Wu, D., Pan, H., and Turgeon, B. G. 2014. Vel2 and Vos1 hold essential roles in ascospore and asexual spore development of the heterothallic maize pathogen *Cochliobolus heterostrophus*. Fungal Genet. Biol. 70:113-124.

Webster, R. H., and Sil, A. 2008. Conserved factors Ryp2 and Ryp3 control cell morphology and infectious spore formation in the fungal pathogen *Histoplasma capsulatum*. Proc. Natl. Acad. Sci. U.S. 105:14573-14578.

Wiebe, G. A. 1968. Introduction of barley into the new world. In: Barley: origin, botany, culture, winter hardiness, genetics, utilization, pests, agricultural handbook No. 38 U.S.

Department of Agriculture, Agricultural Research Service, Washington, D.C., 1968, pp. 2-8.

Wiemann, P., Brown, D. W., Kleigrewe, K., Bok, J. W., Keller, N. P., Humpf, H. U., and Tudzynski, B. 2010. FfVel1 and FfLae1, components of a velvet-like complex in *Fusarium fujikuroi*, affect differentiation, secondary metabolism and virulence. Mol. Microbiol. 77:972-994.

Wiese, M. V. 1987. Compendium of wheat diseases. 2nd Ed. American Phytopathological Society Press, St. Paul, Minn.:112.

Willcox, G. 2005. The distribution, natural habitats and availability of wild cereals in relation to their domestication in the Near East: multiple events, multiple centers. Veget. Hist. Archaeobot 14:534–541.

Wilcoxson, R. D., Rasmusson, D. C., and Miles, M. R. 1990. Development of barley resistant to spot blotch and genetics of resistance. Plant Dis. 74:207-210.

Wolpert, T. J., Macko, V., Acklin, W., Jaun, B., Seibl, J., Meili, J., and Arigoni, D. 1985. Structure of victorin C, the major host-selective toxin from *Cochliobolus victoriae*. Experientia 41:1524-1529.

Wu, D. L., Oide, S., Zhang, N., Choi, M. Y., and Turgeon, B. G. 2012. ChLae1 and ChVel1 regulate T-toxin production, virulence, oxidative stress response, and development of the maize pathogen *Cochliobolus heterostrophus* PLoS Pathog. 8:e1002542.

Zhao, K., Aranzana, M.J., Kim, S., Lister, C., Shindo, C., Tang, C., Toomajian, C., Zheng, H., Dean, C. and Marjoram, P. 2007 An Arabidopsis example of association mapping in structured samples. PLoS Genet. 3:e4.

Zhong, S. B., Steffenson, B., Martinez, J., and Ciuffetti, L. 2002. A molecular genetic map and electrophoretic karyotype of the plant pathogenic fungus *Cochliobolus sativus*. Mol. Plant Microbe In. 15:481-492.

Zhong, S. B., and Steffenson, B. J. 2001. Virulence and molecular diversity in *Cochliobolus sativus*. Phytopathology 91:469-476.

Zhou, H., and Steffenson, B. J. 2013. Genome-wide association mapping reveals genetic architecture of durable spot blotch resistance in US barley breeding germplasm. Mol. Breed. 32:139-154.

Zohary, D. 1973. The origin of cultivated cereals and pulses in the Near East. Curr. Anthropol. 52:S221–S235.

Zohary, D., and Hopf, M. 2000. Domestication of plants in the old world: the origin and spread of cultivated plants in west Asia, Europe, and the Nile valley. Oxford Univ Press, Oxford.

CHAPTER 1: THE REGULATORY GENE *VOSA* AFFECTS CONIDIOGENESIS AND IS INVOLVED IN VIRULENCE OF THE FUNGAL CEREAL PATHOGEN *COCHLIOBOLUS SATIVUS*

Abstract

VosA is one of the four components in the *velvet* complex shown to be involved in regulation of fungal development and secondary metabolism in filamentous fungi. However, the function of VosA has only been studied in few plant pathogenic fungi. In this study, we identified the ortholog (*CsVosA*) of *VosA* in the cereal spot blotch pathogen *Cochliobolus sativus* and generated gene knockout mutants for functional characterization of the gene. Conidia of the *CsVosA* knockout mutants (Δ*CsVosA*) lacked trehalose, were significantly reduced in viability, had less pigmentation, and showed a dramatic reduction in tolerance to heat, oxidative and ion stresses. However, Δ*CsVosA* produced more conidia than the wild type under both constant dark and constant light conditions, suggesting that *CsVosA* is a negative-feedback regulator in conidiation. Interestingly, the Δ*CsVosA* mutants exhibited a hypermorphic conidiation phenotype with indeterminate growth of the conidial tip cells resulting in head-to-tail (acropetal) arrays of conidiogenesis, indicating that some genes involved in conidiation are also regulated by *CsVosA*. The Δ*CsVosA* mutants showed significantly reduction in virulence on susceptible barley plants and the two genes for *nonribosomal peptide synthetases* (NRPSs) involved in virulence during host infection were down-regulated in Δ*CsVosA*, suggesting that *CsVosA* may affect virulence of the fungus by regulating the expression of the genes for NRPSs as well as other genes directly or indirectly involved in virulence.

Introduction

Cochliobolus sativus (Ito & Kurib.) Drechs. ex Dastur. [anamorph: *Bipolaris sorokiniana* (Sacc.) Shoem.] is a filamentous fungus belonging to the family Pleosporaceae in the order Pleosporales of Dothideomycetes. It causes several important diseases, including common root rot, spot blotch, and black point in barley and wheat (Mathre 1997; Wiese 1987). Three pathotypes (0, 1 and 2) of the pathogen have been identified based on virulence patterns on three barley differential lines (ND 5883, Bowman and ND B112) (Valjavec-Gratian and Steffenson 1997b). Pathotype 0 isolates (represented by ND93-1) have low virulence on all three barley differential lines. Pathotype 1 isolates (represented by ND85F) exhibit high virulence on ND 5883 but low virulence on Bowman and ND B112 while pathotype 2 isolates (represented by ND90Pr) show high virulence on Bowman, but low virulence on ND 5883 and ND B112 (Valjavec-Gratian and Steffenson 1997b). Genetic analysis and molecular mapping indicated that a single locus (*VHv1*) controls the high virulence of ND90Pr on Bowman (Valjavec-Gratian and Steffenson 1997a; Zhong et al. 2002). Recent comparative genome sequence analyses revealed that the *VHv1* locus contains two genes (protein IDs 115356 and 140513 in http://genome.jgi-psf.org/ Cocsa1/Cocsa. home.html) for nonribosomal peptide synthetases (*NRPSs)* unique to the *C*. *sativus* isolate ND90Pr (Condon et al. 2013). Deletion of either of these two NRPS encoding genes led to mutants with significantly reduced virulence on the barley cultivar Bowman (Condon et al. 2013). This result demonstrated that the virulence factor in ND90Pr is a secondary metabolite peptide synthesized by NRPSs. However, global regulation of the secondary metabolite biosynthesis in this fungus remains to be investigated.

Fungal morphological development and secondary metabolism can be regulated by many genes or gene families. The four components (VeA, VelB, VelC and VosA) of *velvet* complex

have been shown to be regulators for these processes in several fungal species (Bayram and Braus 2012; Bayram et al. 2008; Jiang et al. 2012; Kim et al. 2013). Among them, VeA, VelB, and VelC are highly conserved in many fungal species, especially in ascomycetes (Lan et al. 2014). VeA and VelB have been extensively studied in a number of fungi (Baba et al. 2012; Chang et al. 2013; Choi and Goodwin 2011; Jiang et al. 2012; Kim et al. 2013; Lan et al. 2014; Li et al. 2006; Lopez-Berges et al. 2013; Wiemann et al. 2010). However, not like other three *velvet* proteins, VosA was less conserved in ascomycetes and was not found in genus *Fusarium* (*F. graminearum*, *F. verticillioides, F. solani*, and *F*. *oxysporum*) (Lan et al. 2014; Lopez-Berges et al. 2013). Its functions have been studied in some fungi but not been well understood, especially in Ascomycota plant pathogens. The gene *VosA (for **v**iability **o**f **s**pores)* was first identified in *Aspergillus nidulans*, which is essential for the long-term viability of spores (Bayram et al. 2010; Ni and Yu 2007) and for the regulation of conidial maturation and conidiogenesis (Ahmed et al. 2013). The deletion of *VosA* in *A*. *nidulans* results in mutant spores lacking trehalose, losing cytoplasm and organelles, and dramatically reducing viability, and being more sensitive to heat and oxidative stresses (Ni and Yu 2007). VosA also exerts negative feedback control of conidiation by down-regulating *brlA* expression in *A*. *nidulans* (Ni and Yu 2007). In the dimorphic human pathogen *Histoplasma capsulatum*, Ryp2 (a homolog of VosA) is essential for the temperature-dependent transition from the saprophytic filamentous phase to the single-cell pathogenic yeast form (Webster and Sil 2008). Similar to the functions of the *A*. *nidulans VosA*, the *ryp2* mutants were reduced in spore viability in *H*. *capsulatum* (Webster and Sil 2008). *In A*. *fumigatus*, VosA exerts negative feedback control of conidiation by down-regulating *brlA* expression as found in *A*. *nidulans* (Ni and Yu 2007; Park et al. 2012). In *Penicillium chrysogenum*, the *PcVosA* knockout strain showed a severe conidiation defect with a

reduced sporulation of about 70% compared to the reference strain, indicating that *PcVosA* positively regulates conidiation (Kopke et al. 2013). It was also found that viability (germination rate) of the Δ*PcVosA* mutant spores was approximately 20% of that of the reference strain after 4 days of culture, but gradually increased as the culture time elongated (7, 10, and 13 days) and finally was close or identical to that of the reference strain (Kopke et al. 2013). In *Ustilago maydis*, the knockout mutants of *umv1* (ortholog of *VosA*) failed to induce galls or teliospores in maize. Chlorazol black E staining of leaves infected with Δ*umv1* dikaryons revealed that the Δ*umv1* hyphae did not proliferate normally and were blocked developmentally before teliospore formation (Karakkat et al. 2013). More recently, Kim et al. (2014) showed that the *VosA* ortholog (*MoVOSA*) in the rice blast pathogen *Magnaporthe oryzae* was dispensable for the fungal development and pathogenicity. However, in the Southern corn leaf blight pathogen *Cochliobolus heterostrophus*, Vos1 plays a positive regulatory role in sexual reproduction, but negatively regulates production of asexual spores (Wang et al. 2014). It also positively regulates conidial morphology, such as the size, septum number, germination rate, as well as tolerance to oxidative and thermal stresses in *C*. *heterostrophus* (Wang et al. 2014). All these studies indicate that although *VosA* is conserved among filamentous fungi, its function on regulating fungal development and biosynthesis of secondary metabolites may be similar or unique depending on the fungal species involved. In this study, we explored the role of the *VosA* ortholog, *CsVosA*, in regulating morphological development, secondary metabolism and pathogenicity in *C*. *sativus*.

Materials and methods

Fungal isolates, media and general growth conditions

The *C*. *sativus* isolate ND90Pr (ATCC 201652) was used as the wild type (WT) in this study. Unless mentioned otherwise, all isolates were grown on V8 potato dextrose agar (V8 PDA) under 14 hour fluorescent light at approximately 23 °C as described by Leng et al. (2011). Potato dextrose agar (PDA), minimal medium (MM) (Tinline et al. 1960), and water agar plates were also used for fungal growth in specific experiments.

Identification of the VosA ortholog in *C. sativus*

The *A*. *nidulans* VosA (accession number: DQ856465.1) protein sequence was used to query the genome sequence of the *C*. *sativus* isolate ND90Pr (http://genome.jgi-psf.org/Cocsa1 /Cocsa1.home.html) using the BLASTP algorithm. Pfam (http://pfam.xfam.org/search) was used to predict conserved domains of proteins. The nucleotide and protein sequences of *CsVosA* and CsVosA were deposited in GenBank under accession number XM_007697459.1 and EMD67942.1, respectively.

Phylogenetic analyses

The *velvet* protein sequences (VeA, VelB, VelC and VosA) in different fungi were downloaded from the GenBank database and used for phylogenetic analysis. Alignment of the protein sequences was made with ClustalX 1.8. Phylogenetic tree was constructed using the

neighbor-joining method in MEGA 6.0 (Tamura et al. 2013). Bootstrap values were expressed as a percentage of 1000 replicates.

Gene replacement and complementation

CsVosA was deleted and replaced with a 2.6-kb fragment carrying the *Escherichia coli* hygromycin phosphotransferase gene (*hph*) using the split-marker system (Catlett et al. 2003). The transformation protocol was the same as previously described by Leng and Zhong (2012). Complementation was conducted using a co-transformation method. The plasmid pII99 carrying the *NPT II* gene for G418 resistance (Beck et al. 1982) was linearized with *Eco*RV and then used to co-transform with the coding and flanking sequences of *CsVosA* into the *CsVosA* knockout mutant (Δ*CsVosA5*). The primers used for gene deletion and complementation are listed in Table 1.1. The procedure for Southern blot and PCR confirmation was the same as previously described by Leng and Zhong (2012). The deletion of *CsVosA* in Δ*CsVosA5* was further confirmed by Southern blot of the *Eco*RI-digested genomic DNA from the wild type and mutants using a probe amplified from the gene encoding sequence of *CsVosA* using primer pair SP-*CsVosA*-F and SP-*CsVosA*-R (Table 1.1). The 9.6 kb fragment in the wild type strain (ND90Pr) was presented and no band was detected in the Δ*CsVosA* strain (Δ*CsVosA5*). Specially, the genomic DNA from the wild type strain and the deletion mutants were digested with *Eco*RI and then transferred to Hybond N+ membrane (Amersham Biosciences, Piscataway, NJ, USA). The probes used to detect the deletion of *CsVosA* gene is indicated in Fig. 1.2A. Sequences of primers for hybridization probe and PCR confirmation are listed in Table 1.1.

Table 1.1. Primers used in this study

Primer	Sequence 5' to 3' *	Purpose
SP-*CsVosA*-F	ACGACAAGGACGAACCAATC	**Southern confirmation**
SP-*CsVosA*-R	TGGTAGCGCTCGAGATCTTT	
CP-*CsVosA*-F-2	CGGCACTTTACCTCTCTTCG	**Generation of complimentary mutant**
CP-*CsVosA*-R	GTGTGCTCCGTTTTCCTCAT	
Cs-brlA-L	TCCCGAAGCTATGGTGGATC	**Expression of conidiation-related genes**
Cs-brlA-R	CTGGCTGGAGGTTGATGGTA	
Cs-wetA-L	TACGCCCCTTCAACAACTCT	
Cs-wetA-R	GAAGCTCTGGTCACACTCCT	
Cs-medA-L	TGGTGGGAAGAAAAGGACGA	
Cs-medA-R	TCGCTGTCTTGCTTTGCTTT	
Cs-stuA-L	ACCCAAAGACAGAGATGGCA	
Cs-stuA-R	ACTCATTGCCGTGATCATGC	
TpsA-F-2	TCATGCACAAGTCCGTCTCT	**Expression of trehalose-related genes**
TpsA-R-2	AATGAGACTGCCGTTCAAGC	
TpsB-F-1	ACTACCTTGAGCGTGTCGAA	
TpsB-R-1	TGGCTCAATGACGACTGAGT	
CsOrlA-F-1	ATGAGCGCCCCTACAGATAC	
CsOrlA-R-1	TCGTCAAAGTAGGCGGTCTT	
Cs-treA-L	TTCGTCTCAAGCCTGGATGT	
Cs-treA-R	AGCCTGACTACTGCCTTGTT	
TreB-F-1	TCTCCAACTTGCTCCAGGAG	
TreB-R-1	GCAATGTTGGAGCCATCGAT	
CsNPS1-F1	GTCGACTGCCATCTGGAAAC	**Expression of NRPS-related genes**
CAN1-F2-2	TGCGGGGTCATCTTAAAAAC	
CsNPS4-RT-F3	ACAGGATCATTGGCCAGTTC	
CsNPS4-RT-R3	AAGGAGGACTTTGGCCATTT	
08856-F	GTGGTGTCATGGCATACGAG	**Expression of PKS-related gene**
PKS18F4-KO	AGTGAGGAAGGAGCCATGAA	
RT-Actin-F	GTATGGGCCAAAAGGACTCA	**Control for gene expression**
RT-Actin-R	CACGCAGCTCGTTGTAGAAG	

Table 1.1. Primers used in this study (continued)

Primer	Sequence 5' to 3' *	Purpose
M13F	GACGTTGTAAAACGACGGCCAGTG	**Generation of knockout mutant**
M13R	CACAGGAAACAGCTATGACCATGA	
HY	GGATGCCTCCGCTCGAAGTA	
YG	CGTTGCAAGACCTGCCTGAA	
CsVosA-F1	TATAGGTCGCCATTGCCTTC	

* Italic sequences are complementary to M13F and M13R sequences, respectively.

Spore viability test on MM

To test spore viability on MM, the wild type (ND90Pr), Δ*CsVosA* and complemented strains were plated on V8 PDA. After growth at 25 ºC for 6, 10, 14, 18, 29 and 33 days, conidia were harvested and spread inoculated on MM. After incubation at 25 ºC for 12 hours, and conidia were examined for viability under a microscope. The spore viability was calculated as the percentage of viable conidia in the total number of conidia examined. Only those conidia producing hyphae at least 5 times longer than the conidia after 12 hours of incubation on MM were considered viable since some of the mutant conidia germinated when they were attached to the conidiophores but they failed to grow on MM. Three replicates (MM plates) were used for each fungal strain and 100 conidia were examined for each replicate.

Trehalose assay

The trehalose amounts in conidia and mycelia were measured according to the protocol described in Ni and Yu (2007) and Al-Bader et al. (2010), respectively. Briefly, conidia (10^5) and mycelia (30 mg) of each fungal strain were harvested from V8 PDA and PDB, respectively, and dried in a freeze dryer. The fungal samples were re-suspended in 200 ul of ddH_2O and

incubated in boiled water for 20 minutes. Then, the supernatants were collected by centrifugation, mixed with equal volume of 0.2 M sodium citrate (pH 5.5) and incubated at 37 °C overnight after adding 6 mU of trehalase (Sigma). The amount of glucose generated by trehalase was assayed with the glucose assay kit (Sigma) following manufacturer's instruction, and used to calculate the amount of trehalose. The sample without trehalase treatment was served as a negative control. For each sample, three replicates were conducted.

Assays of thermal, oxidative, and ion stresses

To test sensitivity of spores to thermal stress, conidia of wild type, knockout mutants and complemented strain were harvested from cultures grown at 25 °C for 6 days on V8 PDA plates, plated on MM and incubated at 40 °C for 0, 1, 2, 3 hours, respectively, and then returned to 25 °C for 12, 11, 10, and 9 hours before viability of conidia was examined. Furthermore, the conidia were also incubated in water bath at 50 °C for 0, 1.5, 3.5 minutes, respectively, and then plated on MM and incubated at 25 °C for 12 hours before viability of conidia was examined. To test the response to oxidative stress, conidia of each fungal strain grown on V8 PDA for 6 days were harvested and plated on MM plates supplemented with different concentrations (0, 1.3 and 2.6 mM) of H2O2, and then incubated at 25 °C for 12 hours before the conidial viability rate was calculated. To test the response to ion (NaCl) stress, conidia of each fungal strain were harvested from cultures grown at 25 °C for 6 days on V8 PDA plates, plated on MM plates containing different NaCl concentrations (0, 0.6 and 1.0 M) and incubated at 25 °C for 12 hours before viability of conidia was examined.

Examination of conidial size and melanin production

To examine the size and pigmentation of conidia, wild type and mutants were grown on V8 PDA under constant dark and constant light conditions for 7 days. Conidia of each strain were harvested and photographed under constant settings with identical white balance using an Olympus BX51 microscope (Olympus, Center Valley, PA, USA) with the CCD camera digital imaging system (Diagnostic Instruments, Inc., Sterling Heights, MI, USA) under 20X magnification. The conidial size was represented by the area of conidia in the pictures that were measured by software SigmaScan Pro 5. The average pixel brightness intensities (BI) of the conidia in the pictures were measured using SigmaScan Pro 5 software. The melanin production was represented by the pigment intensity that was converted from the pixel brightness intensity using PI = 1 / BI.

Analysis of conidial productivity, conidiation pattern and conidiophore production

To measure conidial productivity, single conidium of wild type, knockout mutants and the complemented strains were inoculated on the centers of V8 PDA plates and allowed to grow for 7 days at 25 °C under constant dark and constant light conditions. Conidia were harvest and quantified as described by (Leng and Zhong 2012). The experiments were performed in triplicates.

To investigate the pattern of conidia formation, the conidia were inoculated on the slide culture with MM. After 5 days of growth, conidiation patterns were examined and photographs were taken using Olympus BX51 microscope with the CCD camera digital imaging system under the 20X magnification.

The conidiophore production was measured according to the methods described in (Chang et al. 2004). Briefly, single conidium of wild type and knockout mutant were inoculated on the centers of V8 PDA plates and allowed to grow for 7 days at 25 °C under constant dark and constant light conditions. The number of conidiophores per square centimeter of medium plates was counted with a dissecting microscope. The conidiophore production of wild type grown under constant dark conditions was used as a reference to calculate the conidiophore productivity rate.

Examination of premature germination

Conidial suspensions at 1.2×10^3 spores/mL were prepared from each culture grown on V8 PDA under constant dark and constant light for 3, 5, and 7 days after point inoculation with hundreds of conidia, respectively. Then, 0.1 mL of conidial suspension was spread on slides and the germ tube emergence was examined under a microscope. The percentage of germinated spores was calculated. This test was performed three times for each strain.

Pathogenicity test

Pathogenicity tests were performed by spray inoculation with conidial suspension on 10~12 days old seedlings of barley (cv. Bowman) plants (when the second leaves were fully expended) according to (Fetch and Steffenson 1999), except the concentration of the conidial suspension was at 1.5×10^3 conidia/mL. Inoculated plants were incubated in a humidity chamber for 20-24 hours, and then transferred into a greenhouse (23 ± 2 °C) and incubated for 6 days before the spot blotch disease was rated using the 1–9 rating scale of (Fetch and Steffenson 1999). For each

fungal strain, at least nine plants were used for inoculation and the experiment was repeated three times. The photographs of infected leaves were scanned using Epson Expression 10000XL (Epson America, Inc. Long Beach, CA, USA).

Spore viability test on barley leaves

To test spore viability on barley leaves, conidia (5×10^3 conidia/mL) of the wild type (ND90Pr), Δ*CsVosA* and complemented strains grown on V8 PDA for seven days were harvested and spray inoculated on 10~12 days old seedlings of barley cv. Bowman. The inoculated plants were misted with distilled water and then covered with a plastic bag to maintain high humidity. After 12 h of incubation under dark conditions at room temperature (23±2ºC), leaf segments were sampled and examined for spore viability under a compound microscope. The spore viability was calculated as the percentage of viable conidia in the total number of conidia examined. Only those conidia producing hyphae at least 5 times longer than the conidia at 12 hours post-incubation were considered viable. Three replicates (cones with three plants per cone) were used for each fungal strain and 100 conidia were examined for each replicate.

Examination of fungal infection process

To examine appressorium formation of the wild type and deletion mutants, seedlings of barley cv. Bowman were inoculated with a spore suspension (5×10^3 conidia/mL) prepared from each fungal strain. At 12 and 24 hours after inoculation (hai), leaf segments were sampled and subjected to treatments according to the method described by (Keogh et al. 1980). The stained

fungal structures were examined using an Olympus BX51 microscope (Olympus, Center Valley, PA, USA) and photographed by a CCD camera (Diagnostic Instruments, Inc., Sterling Heights, MI, USA). The average rate of appressorium formation was calculated for each fungal strain based on the percentage of appressorium-forming spores relative to the total number of germinated spores examined on three inoculated leaves.

RNA extraction and gene expression analyses

For expression analyses of *CsVosA* (protein ID: 22437), *CsTpsA* (protein ID: 200256), *CsOrlA* (protein ID: 35195), *CsTpsC* (protein ID: 38836), *CsTreA* (protein ID: 39633), and *CsTreB* (protein ID: 78439), RNA was extracted from conidia harvested from the culture in V8 PDA at the 7 days after inoculation (sample C), and mycelia grown in PDB at 12 and 48 hai (sample 12M and 48M) as well as a mixture of conidia and mycelia harvested from the culture in V8 PDA at 6 days after inoculation (sample 6DM). For expression analyses of *PKS18* (protein ID: 184740), *CsBrlA* (protein ID: 136667), *CsMedA* (protein ID: 219901), *CsStuA* (protein ID: 302496), and *CsWetA* (protein ID: 345897), total RNA was extracted from sample C, sample 12M, and sample 48M. For expression analyses of the two NRPS encoding genes (protein IDs 115356 and 140513), RNA was extracted from a mixture of mycelia harvested from the culture at 96 hai from different media including PDA, MM, V8 PDA, and water agar (sample 96M) as well as from inoculated barley leaves at 12 and 24 hours hai on bowman (sample 12B and 24B). All fungal materials were shock-frozen with liquid nitrogen immediately after harvesting. RNA was extracted using SV Total RNA Isolation System (Promega) and purified by treatment with DNase I (New England Biolabs). cDNA generation and RT-PCR procedure was the same as

previously described in (Leng and Zhong 2012). The β-actin-encoding gene (ACT) was amplified with the RT-Actin-F and RT-Actin-R primers (Table 1.1) and used as reference in all experiments. All gene expression experiments were repeated at least three times. The primer pairs for each gene used in each analysis are listed in Table 1.1.

Results

Identification of VosA homologs in *C. sativus*

Four candidate orthologs of VosA were identified from the draft genome sequence of *C. sativu*s (http://genome.jgi-psf.org/Cocsa1/Cocsa1.home.html) through homology search using the BLASTP algorithm and VosA of *A. nidulans* as a query. The ortholog with the highest score (452) and lowest E value ($8.34\times e^{-44}$) was identified as *CsVosA* (Fig. 1.1A) and the other three orthologs were designated as CsVeA, CsVelB and CsVelC, respectively, based on their similarities to other *velvet* proteins (VeA, VelB and VelC) in *A. nidulans*. Phylogenetic analysis indicated that the four *velvet* proteins of *C. sativus* belonged to four distinct clades, each containing the respective *velvet* protein of different fungi (Fig. 1.1B). The *CsVosA* gene contains 1050 base pairs without introns and encodes a protein (349 amino acids) with a highly conserved *velvet* domain, a characteristic of *velvet* gene family, as identified using Pfam (http://pfam.xfam. org/search) (Fig. 1.1Ahttp://www.ncbi.nlm.nih.gov/pmc/articles/PMC3285592/ - ppat.1002542.s001). A putative nuclear localization signal (pat4: 277 KKRR 280 or pat7: 274 PLAKKRR 280) was also identified by using the PSORT II program (http://psort. hgc.jp/form2. html).

Generation of gene knockout mutants and complemented strains

Three independent deletion mutants (Δ*CsVosA5*, Δ*CsVosA6* and Δ*CsVosA7*) as well as one ectopic strain Δ*CsVosAEC* were generated. By introducing the *CsVosA* gene back into one of the deletion mutants, Δ*CsVosA5*, three complemented strains (Δ*CsVosAC1*, Δ*CsVosAC2*, and Δ*CsVosAC3*) were obtained. These knockout mutants and complemented strains were confirmed by PCR amplification and Southern blot analyses. As shown in Fig. 1.2A and B, an amplicon (235 bp) was only present in the wild type (ND90Pr) and complemented strains but not in the knockout mutants when the *CsVosA*-specific primer pair SP-*CsVosA*-F and SP-*CsVosA*-R were used for PCR amplification. Using the primer *CsVosA*-F0 at the flanking region of *CsVosA* and the primer HYG2-R at the hygromycin resistance gene (*hph*) for PCR, the fragment (2,830bp) was only amplified from the knockout mutants but not from the wild type, indicating that *CsVosA* was replaced by *hph*. The deletion of *CsVosA* in Δ*CsVosA5* was further confirmed by Southern blot of the *Eco*RI-digested genomic DNA from the wild type and mutants using a probe amplified from the gene encoding sequence of *CsVosA* using primer pair SP-*CsVosA*-F and SP-*CsVosA*-R (Table 1.1). As indicated in Fig. 1.2C, the 9.6 kb fragment in the wild type strain (ND90Pr) was presented and no band was detected in the Δ*CsVosA* strain (Δ*CsVosA5*).

mRNA expression of *CsVosA* at different growth stages

As expected, no mRNA expression of *CsVosA* was observed in the deletion mutant (Δ*CsVosA5*) at the different growth stages (Fig. 1.3). However, mRNA expression of *CsVosA* was significantly higher in conidia than in vegetative mycelia in WT and the complemented strain (Fig. 1.3). Also, *CsVosA* showed a higher mRNA expression in the complemented strain

than in the WT at the three different growth stages. This is probably due to the fact that the complemented strain contained multiple copies of *CsVosA* as revealed by Southern blot analysis (Fig. 1.2C and data not shown).

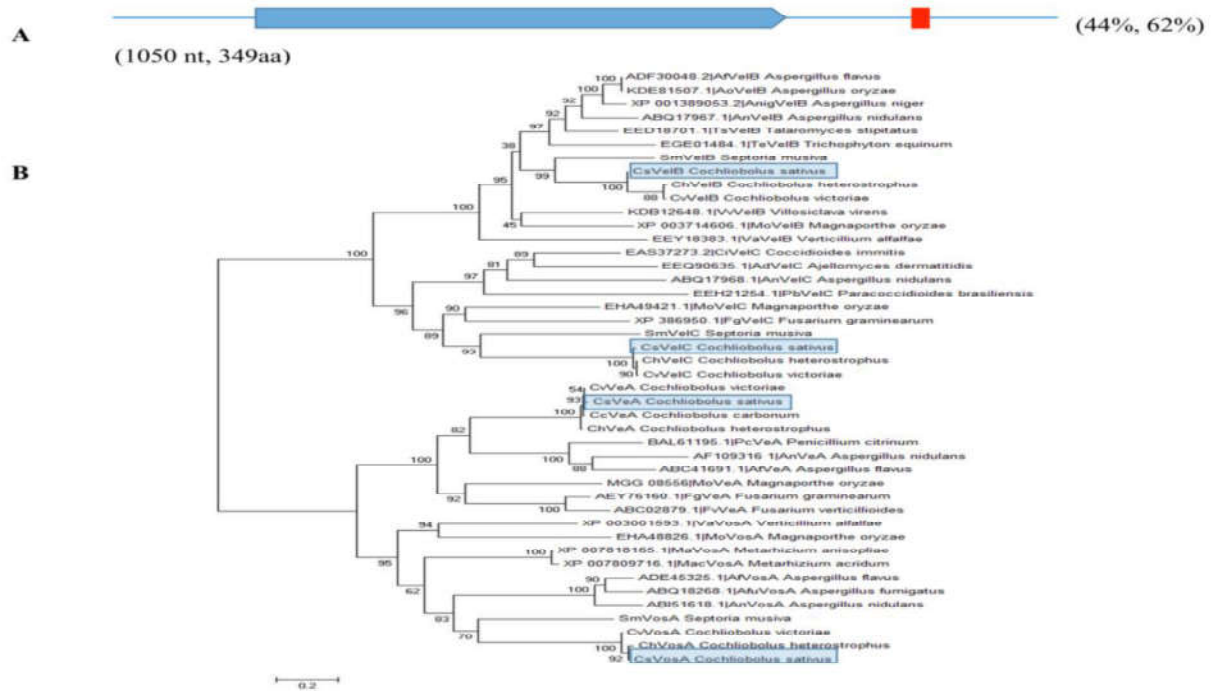

Fig. 1.1. The structure and phylogenetic tree of *C. sativus VosA* gene and its orthologs in other fungal species. **A.** Structural feature of *VosA* gene in *C. sativus*. The position of the conserved *velvet* factor domain and a putative nuclear localization signal (NLS) are indicated by a blue pentagon and a red rectangle, respectively. The nucleotide and amino acid length are noted in parentheses below the gene; the percent identity and similarity between *CsVosA* and its ortholog in *A. nidulans* are indicated on the right in parentheses. **B.** Phylogenetic tree for *CsVosA*. Phylogenetic tree was constructed by neighbor-joining method with 1000 bootstrap replicates, numbers on the branches represent the percentage of replicates supporting each branch. The *velvet* proteins of *C. sativus* are shaded. The scale bar represents 20% sequence divergence. The accession numbers in Genebank database or the protein IDs in DOE Joint Genome Institute of the genes are listed here: AF109316_1 for *AnVeA* in *Aspergillus nidulans,* ABC41691.1 for *AfVeA* in *Aspergillus flavus,* AEY76160.1 for *FgVeA* in *Fusarium graminearum,* ABC02879.1 for *FvVeA* in *Fusarium verticillioides,* BAL61195.1 for *PcVeA* in *Penicillium citrinum,* 1113718 for *ChVeA* in *Cochliobolus heterostrophus,* MGG_08556 for *MoVeA* in *Magnaporthe oryzae,* 96012 for *CcVeA* in *Cochliobolus carbonum,* 107450 for *CvVeA in Cochliobolus victoria,* 258482 for *CsVeA* in *Cochliobolus sativus,* ABQ17967.1 for *AnVelB* in *Aspergillus nidulans,* ADF30048.2 for *AfVelB* in *Aspergillus flavus,* KDE81507.1 for *AoVelB* in *Aspergillus oryzae,* KDB12648.1 for

VvVelB in *Villosiclava virens*, XP_001389053.2 for *AnigVelB* in *Aspergillus niger*, EEY18383.1 for *VaVelB* in *Verticillium alfalfa*, EGE01484.1 for *TeVelB* in *Trichophyton equinum*, EED18701.1 for *TsVelB* in *Talaromyces stipitatus*, XP_003714606.1 for *MoVelB* in *Magnaporthe oryzae*, 33742 for *ChVelB* in *Cochliobolus heterostrophus*, 38610 *for CsVelB* in *Cochliobolus sativus*, 38540 for *CvVelB* in *Cochliobolus victoria*, 151278 for *SmVelB* in *Septoria musiva*, ABQ17968.1 for *AnVelC* in *Aspergillus nidulans*, EAS37273.2 for *CiVelC* in *Coccidioides immitis*, EEQ90635.1 for *AdVelC* in *Ajellomyces dermatitidis*, EEH21254.1 for *PbVelC* in *Paracoccidioides brasiliensis*, EHA49421.1 for *MoVelC* in *Magnaporthe oryzae*, XP_386950.1 for *FgVelC* in *Fusarium graminearum*, 114528 for *ChVelC* in *Cochliobolus heterostrophus*, 119375 for *CsVelC* in *Cochliobolus sativus*, 31414 for *CvVelC* in *Cochliobolus victoria*, 148540 for *SmVelC* in *Septoria musiva*, ABI51618.1 for *AnVosA* in *Aspergillus nidulans*, ADE45325.1 for *AfVosA* in *Aspergillus flavus*, XP_007818165.1 for *MaVosA* in *Metarhizium anisopliae*, XP_007809716.1 for *MacVosA* in *Metarhizium acridum*, ABQ18268.1 for *AfuVosA* in *Aspergillus fumigatus*, XP_003001593.1 for *VaVosA* in *Verticillium alfalfa*, EHA48826.1 for *MoVosA* in *Magnaporthe oryzae*, 1067256 for *ChVosA* in *Cochliobolus heterostrophus*, 62627 for *CsVosA* in *Cochliobolus sativus*, 48009 for *CvVosA* in *Cochliobolus victoria*, 50595 for *SmVosA* in *Septoria musiva*.

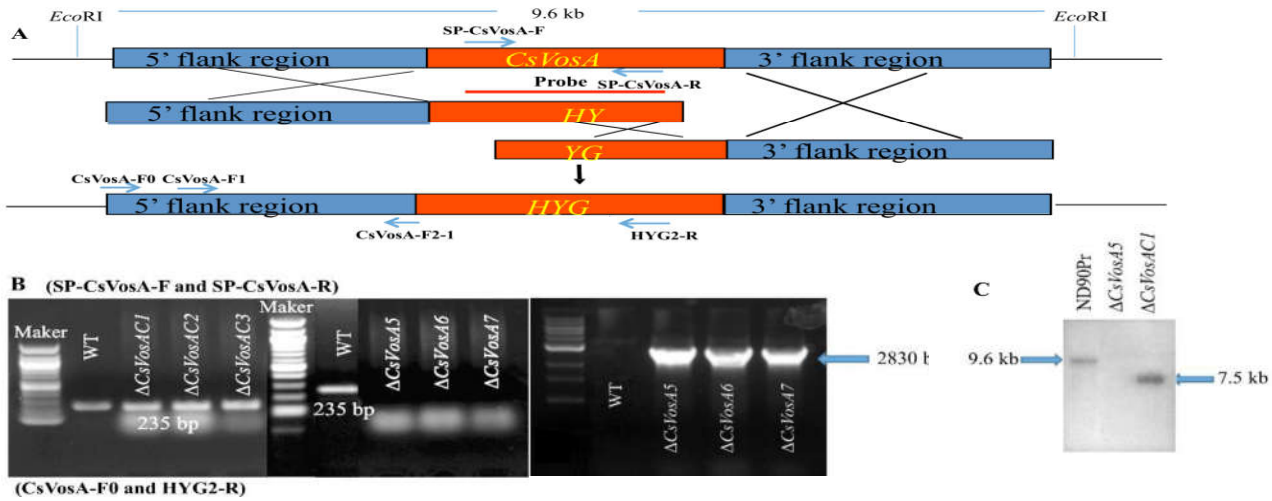

Fig. 1.2. Generation as well as PCR and Southern blot confirmation of Δ*CsVosA* and complemented strains in *Cochliobolus sativus*. **A.** Schematic representation of the replacement of the *CsVosA* gene by a 2.6-kb fragment carrying the *Escherichia coli* hygromycin phosphotransferase gene (*hph*) using the split-marker system. **B.** Polymerase chain reaction (PCR) amplification analysis of the wild type (ND90Pr), Δ*CsVosA* mutants (Δ*CsVosA5*, Δ*CsVosA6*, Δ*CsVosA7*) and complemented strains (Δ*CsVosAC1*, Δ*CsVosAC2*, Δ*CsVosAC3*) using primer pairs (SP-*CsVosA*-F/SP-*CsVosA*-R) and (*CsVosA*-F0/HYG2-R). **C.** Southern blot of *Eco*RI-digested genomic DNA from the wild type, Δ*CsVosA* mutant (Δ*CsVosA5*), and complemented strain (Δ*CsVosA*C1) using a probe amplified with primers *CsVosA*-F1 and *CsVosA*-F2-1 and labeled by ^{32}P. The 7.6-kb fragment in the wild type strain (ND90Pr) was replaced by the 5.3-kb fragment in the Δ*CsVosA5* strain.

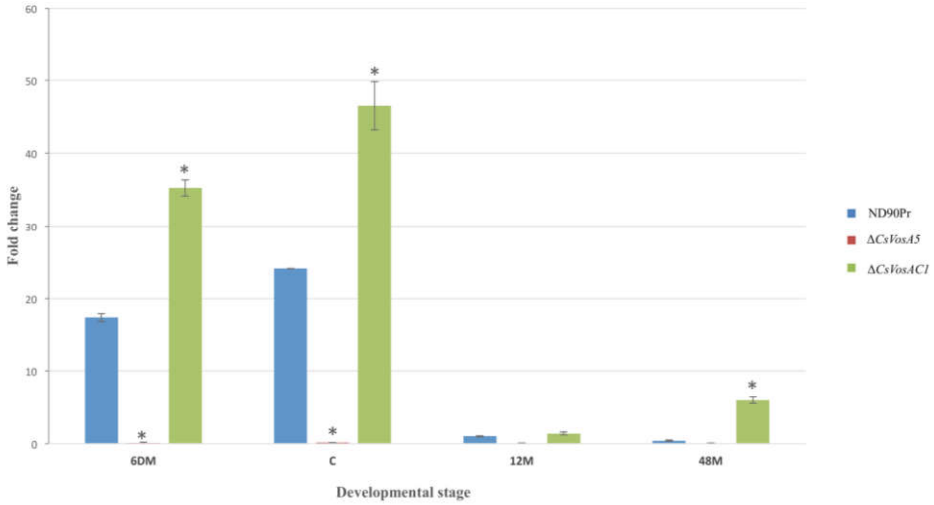

Fig. 1.3. Expression analyses of *CsVosA* in wild type and mutants at different developmental stages. Expression level relative to the sample 12M of WT strain is shown. Error bars represent range of fold change calculated according to standard deviation of ΔΔCt. The expression of the β-actin-encoding gene (*ACT*) was used as a reference. Asterisks indicate p-value <0.001 in T-test analyses in which each isolate was compared with corresponding wild type at the same sample type.
Sample 6DM: RNA was extracted from a mixture of conidia and mycelia harvested from the culture in V8 PDA at 6 dai
Sample C: RNA was extracted from conidia harvested from the culture in V8 PDA at the 7 dai
Sample 12M: RNA was extracted from mycelia grown in PDB at 12 hai
Sample 48M: RNA was extracted from mycelia grown in PDB at 48 hai

CsVosA regulates spore viability, trehalose accumulation, and tolerance to thermal and oxidative as well as ion stresses

As shown in Fig. 1.4A, the survival rate of conidia from Δ*CsVosA* grown for 10 or more days on MM were significantly reduced, while those of conidia from wild type and the complemented strain had little changes during 33 days of the incubation. Close microscopic examination further indicated that many of the mutant conidia *lost cytoplasm and totally collapsed* (data not shown). The amount of trehalose in the Δ*CsVosA* mutant was significantly reduced in conidia but significantly increased in mycelia compared to those from WT and the

complemented strain (Fig. 1.4B and 4C). To determine the role of *CsVosA* in regulating genes involved in synthesis and breakdown of trehalose, the expression levels of three genes (*CsTpsA*, *CsOrlA*, *CsTpsC* that are orthologous to *A*. *nidulans tpsA*, *orlA*, *tpsC*, which are involved in trehalose synthesis) and two genes (*CsTreA* and *CsTreB* that are orthologous to *A*. *nidulans treA* and *treB*, which are involved in trehalose breakdown) (Al-Bader et al. 2010; Ni and Yu 2007) were measured by quantitative real time PCR. The results showed that mRNA levels of *CsTpsA* and *CsOrlA* were significantly reduced in the Δ*CsVosA* mutant during asexual development (formation of conidia) compared to WT and complemented strain (Fig. 1.4D). However, mRNA levels of *CsTreA* (but not *CsTreB*) were significantly increased in mature conidia.

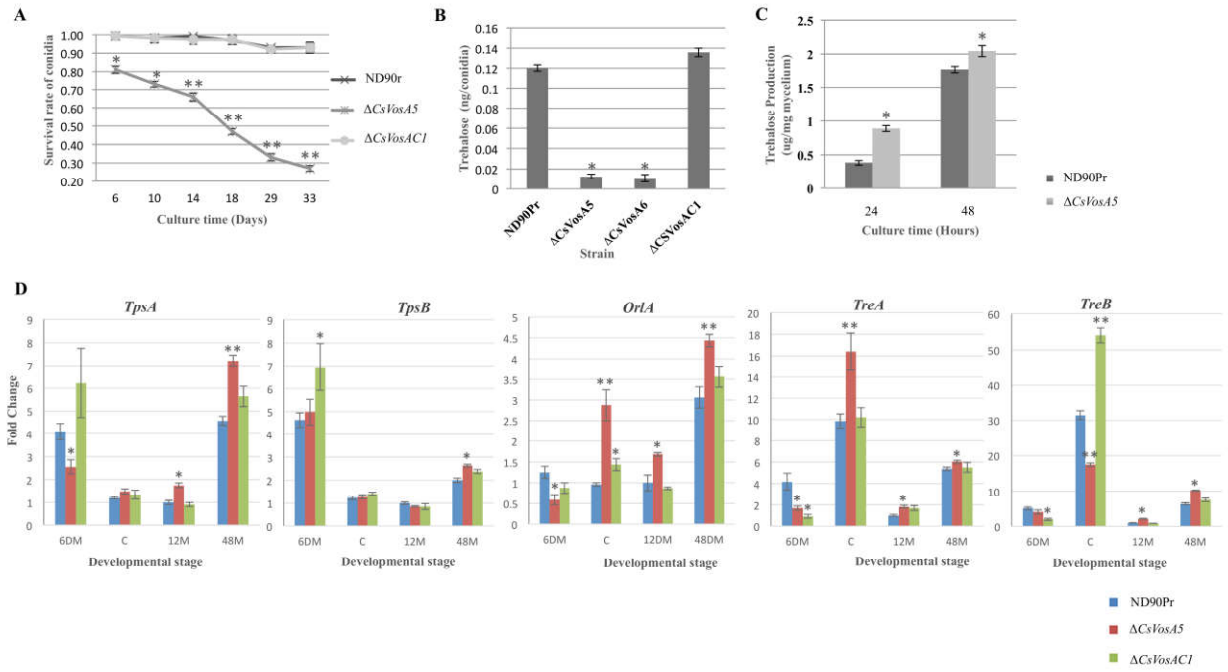

Fig. 1.4. Viability and trehalose content of conidia in wild type and mutant isolates. A. Viability of conidia of wild type (ND90Pr), ΔCsVosA and the complemented strain grown on V8 PDA at 25 °C for 6, 10, 14, 18, 29 and 33 days. The conidia were considered viable when they were able to germinate to produce germ tubes at least 5 times longer than the conidia after 12 hours of incubation on MM. The survival rate of conidia was calculated as the percentage of viable conidia in the total number of conidia examined. Error bars indicate the standard deviation. Single

asterisks indicate p-value <0.05, double asterisks indicate p-value <0.001 in T-test analyses in which each strain was compared with corresponding wild type at the same culture time. B. Trehalose content in conidia of wild type, ΔCsVosA and complemented strains. Trehalose was extracted from 105 conidia harvested from fungal cultures grown on V8 PDA for 6 days. The amount of glucose released from trehalose by trehalase was assayed with a glucose assay kit (Sigma) and used to calculate the amount of trehalose in conidia. Each sample not treated with trehalase served as a negative control. Three replicates were used for each fungal strain. Error bars indicate the standard deviation. Asterisks represent p-value <0.05 in T-test analyses when each isolate was compared with WT. C. Trehalose content in mycelia of wild type, ΔCsVosA and complemented strains. Trehalose was extracted from 30mg mycelia harvested from fungal cultures grown in PDB for 24 and 48 hours. The amount of glucose released from trehalose by trehalase was assayed with a glucose assay kit (Sigma) and used to calculate the amount of trehalose in mycelia. Each sample not treated with trehalase served as a negative control. Three replicates were used for each fungal strain. Error bars indicate the standard deviation. Asterisks represent p-value <0.05 in T-test analyses when each isolate was compared with WT. D. RNA expression of trehalose-related genes at different developmental stages. Expression level relative to the sample 12M of WT strain is shown. Error bars represent range of fold change calculated according to standard deviation of ΔΔCt. The expression of the β-actin-encoding gene (ACT) was used as a reference. Single asterisks indicate p-value <0.05, double asterisks indicate p-value <0.001 in T-test analyses in which each strain was compared with corresponding wild type at the same sample type.
Sample 6DM: RNA was extracted from a mixture of conidia and mycelia harvested from the culture in V8 PDA at 6 dai
Sample C: RNA was extracted from conidia harvested from the culture in V8 PDA at the 7 dai
Sample 12M: RNA was extracted from mycelia grown in PDB at 12 hai
Sample 48M: RNA was extracted from mycelia grown in PDB at 48 hai

The Δ*CsVosA* mutant conidia exhibited a drastic reduction in tolerance to heat (Fig. 1.5A and B), H_2O_2 (Fig. 1.5C), and ion (NaCl) (Fig. 1.5D) stresses than conidia of WT and complemented strains. Reintroduction of the *CsVosA* gene into the mutants restored the WT tolerance (Fig. 1.5).

CsVosA regulates asexual spore production and conidiogenesis pattern

The Δ*CsVosA* mutant strain produced 2.25 and 1.66 folds more conidia than the wild type on V8 PDA under both constant dark and light conditions, respectively (Fig. 1.6), indicating that

CsVosA represses spore production in *C*. *sativus*. In addition, the mutant produced more conidia under constant dark conditions than under constant light conditions, whereas the wild type produced a similar number of conidia under all these growth conditions (Fig. 1.6).

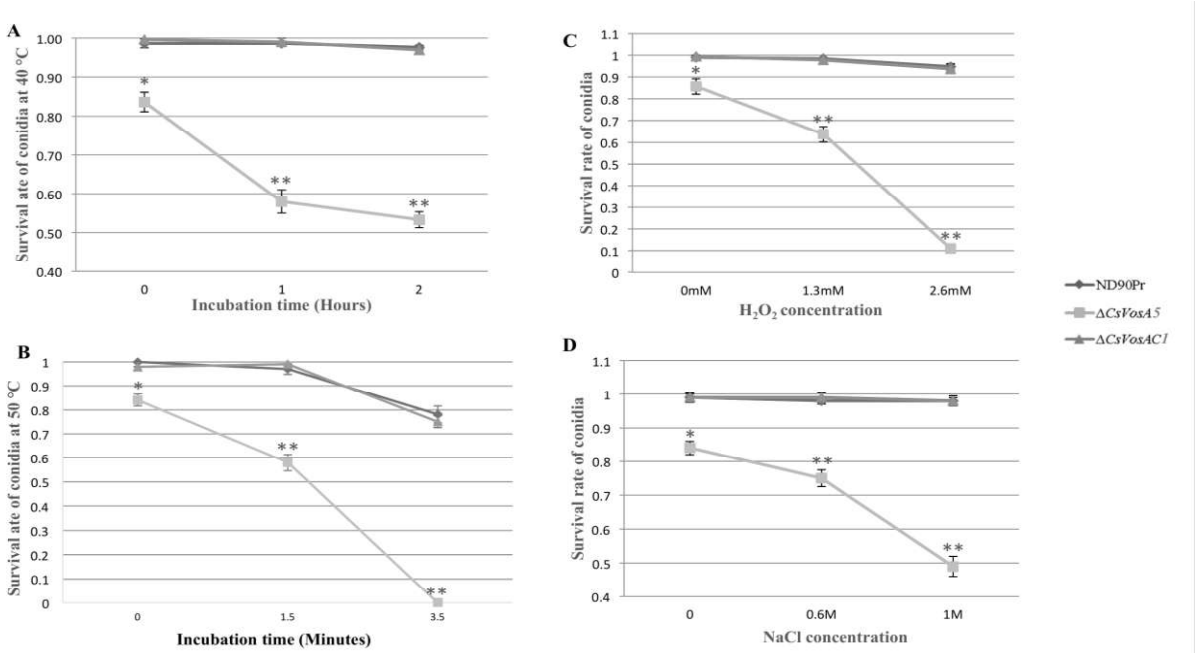

Fig. 1.5. Tolerance of wild type, Δ*CsVosA* and complemented strain to high temperature 40 °C, 50 °C, H_2O_2 stress, and NaCl stress. **A.** Conidia of each fungal strain harvested from cultures grown at 25 °C for 6 days on V8 PDA plates, were plated on MM and incubated at 40 °C for 0, 1, 2, 3 hours, respectively, and then returned to 25 °C for 12, 11, 10, and 9 hours before viability of conidia was examined. Single asterisks in indicate p-value <0.05, double asterisks indicate p-value <0.001 in T-test analyses in which each strain was compared with corresponding wild type at the same incubation time. **B.** Conidia of each fungal strain harvested from cultures grown at 25 °C for 6 days on V8 PDA plates, were incubated in water bath at 50 °C for 0, 1.5, 3.5 minutes, respectively, and then plated on MM and incubated at 25 °C for 12 hours before viability of conidia was examined. Single asterisks indicate p-value <0.05, double asterisks indicate p-value <0.001 in T-test analyses in which each strain was compared with corresponding wild type at the same incubation time. **C.** Conidia of each fungal strain harvested from cultures grown at 25 °C for 6 days on V8 PDA plates, were plated on MM plates containing different H_2O_2 concentrations (0, 1.3 and 2.6 mM) and incubated at 25 °C for 12 hours before viability of conidia was examined. Single asterisks indicate p-value <0.05, double asterisks indicate p-value <0.001 in T-test analyses in which each strain was compared with corresponding wild type at the same H_2O_2 concentration. **D.** Conidia of each fungal strain harvested from cultures grown at 25 °C for 6 days on V8 PDA plates, were plated on MM plates containing different NaCl concentrations (0, 0.6 and 1.0 M) and incubated at 25 °C for 12 hours before viability of conidia was examined.

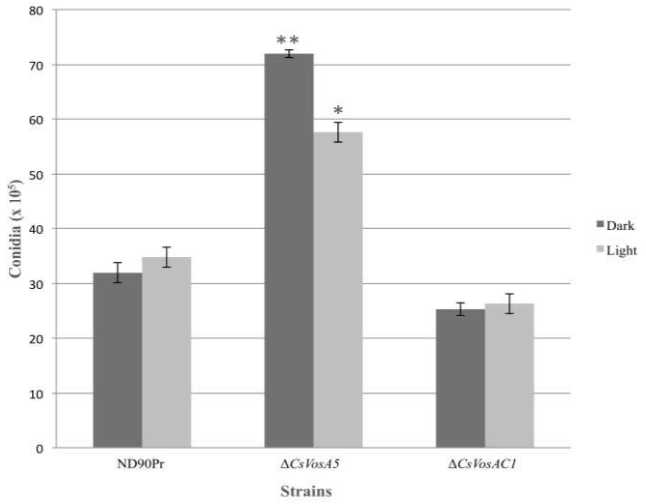

Fig. 1.6. Conidial productivity of wild type, knockout mutant and the complemented strains. The strains were grown on V8 PDA plates at 25 °C under constant dark and light conditions for 7 days, and then the conidia were harvested and quantified. Error bars indicate the standard deviation. Single asterisks indicate p-value <0.05, double asterisks indicate p-value <0.001 in T-test analyses in which each strain was compared with corresponding wild type under the same condition.

Further examination of conidiogenesis indicated that no significant differences in conidiophore production were observed between wild type and the Δ*CsVosA* mutant under the constant light conditions, but the mutant generated more conidiophores under constant dark conditions compared to the wild type (Table 1.2). More interestingly, the conidiation pattern was different between wild type and the knockout mutant. The wild type produced 3-5 conidia on a conidiophore in a sympodial fashion, while the Δ*CsVosA* mutant had conidiophores with multiple chains of conidia with the oldest conidium at the base and the youngest one emerging at the tip of the spore chain (Fig. 1.7). The wild type produced conidia in a sympodial pattern, one fashion of the holoblastic differentiation, while the Δ*CsVosA* mutant produced spores by two patterns of holoblastic differentiation: sympodial and acropetal.

Table 1.2. Conidiophore productivity of wild type (ND90Pr) and knockout mutant (Δ*CsVosA5*) under different conditions

Strains	Condition	Conidiophore production (%)
ND90Pr	Constant dark	100
ND90Pr	Constant light	94 ± 4.1
Δ*CsVosA5*	Constant dark	153 ± 7.9*
Δ*CsVosA5*	Constant light	98 ± 2.3

Single conidium of wild type and Δ*CsVosA5* were inoculated on the centers of V8 PDA plates and allowed to grow for 7 days at 25 °C under constant dark and constant light conditions. The number of conidiophores per square centimeter of medium plates was counted with a dissecting microscope. The conidiophore production of wild type grown under constant dark conditions was used as a reference to calculate the conidiophore productivity rate. Asterisk represents p-value <0.05 in T-test analysis when each isolate was compared with WT under constant dark conditions.

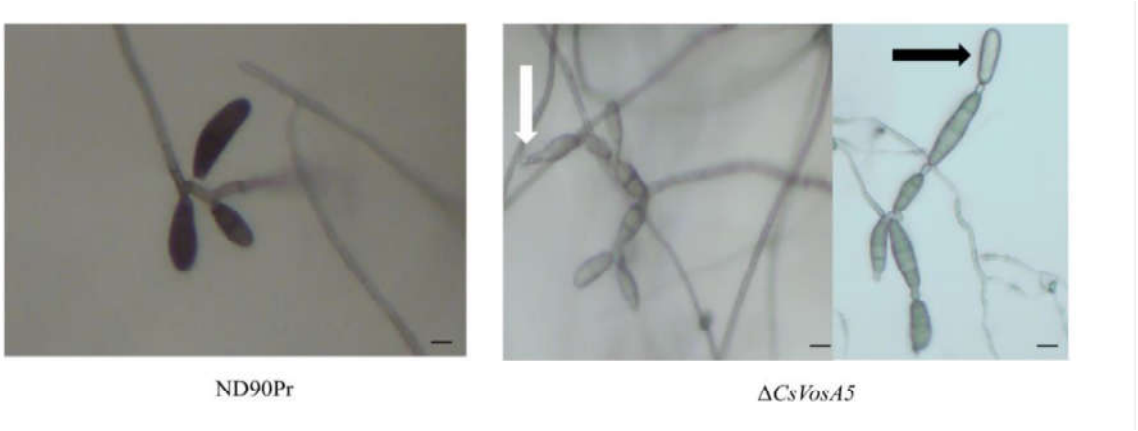

Fig. 1.7. Conidial developmental processes in *C*. *sativus* strains. Conidiogenesis patterns were examined under a light microscope. The white arrow points to a growing point of a new conidium and the dark arrow points to a younger conidium on the head of the older conidium. Note that wild type produces conidia in a traditional sympodial pattern whereas the knockout mutant generates conidia through both sympodial and acropetal patterns. bars = 20 μm.

To further investigate the molecular regulatory role of *CsVosA* in conidiation, we examined mRNA levels of four *C*. *sativus* genes (*CsBrlA* (protein ID: 136667), *CsWetA* (protein ID: 345897), *CsStuA* (protein ID: 302496) and *CsMedA* (protein ID: 219901) orthologous to b*rlA* (accession number M20631.1), *wetA* (accession number M60528.1), *stuA* (accession number

M83569.2), and m*edA* (accession number AF080599.1), which are involved in the regulatory pathway of sporulation and spore maturation in *A*. *nidulans*) (Adams et al. 1988; Marshall and Timberlake 1991; Miller et al. 1992). As shown in Fig. 1.8, *CsBrlA, CsStuA* and *CsWetA* were down-regulated while *CsMedA* was up-regulated in Δ*CsVosA5* conidia. However, a very low level of *CsBrlA* expression was detected in mycelia grown in PDB for 12 and 48 hours, indicating that this gene is preferably expressed in conidia. The expression levels of *CsWetA*, *CsStuA* and *CsMedA* were very low in mycelia after 12 hours of growth, but increased after 48 hours of growth. Also, the expression of *CsWetA*, *CsStuA* and *CsMedA* was up-regulated in Δ*CsVosA5* mycelia after 48 hours of growth in PDB as compared to WT and the complemented strain.

CsVosA regulates conidial size

Δ*CsVosA* conidia differed from WT conidia in size, shape, and septa production (Fig. 1.9). The wild type strain (ND90Pr) produced normal sized conidia measured at 15-28 × 80-120 μm (area value 6000~12000 in SigmaScan software) with 4-8 septa, and 4% or 12% small conidia measured at 7-14 × 15-30 μm (area value 2000~3000 in SigmaScan software) with 0-1 septa under constant dark and constant light conditions, respectively (Table 1.3). However, the Δ*CsVosA* mutant produced more small conidia and many large conidia measured at 20-35 x 120-250 μm (area value 12000~28000 in SigmaScan software) under both constant dark and continuous light conditions, respectively, compared to WT (Table 1.3). For these large conidia, the number of septa/conidium ranged from 0-8. However, no significant differences were found

in germination rate and responses to the stresses tested among the different sized conidia from each of the strains (data not shown).

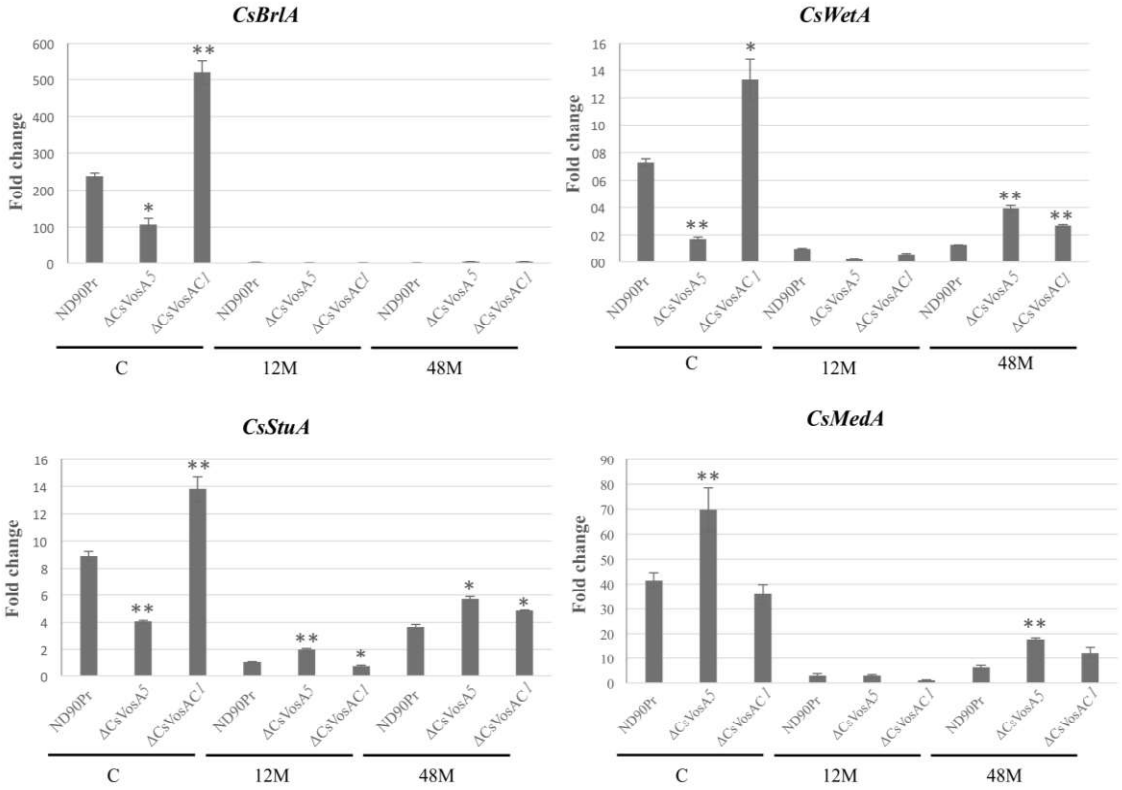

Fig. 1.8. RNA expression analyses of *CsBrlA*, *CsStuA*, *CsWetA* and *CsMedA* in wild type and mutants at different developmental stages. Expression level relative to the sample 12M of WT strain is shown. Error bars represent range of fold change calculated according to standard deviation of ΔΔCt. The expression of the β-actin-encoding gene (*ACT*) was used as a reference. Single asterisks indicate p-value <0.05, double asterisks indicate p-value <0.001 in T-test analyses in which each isolate was compared with corresponding wild type at the same sample type.
Sample C: RNA was extracted from conidia harvested from the culture in V8 PDA at the 7 dai
Sample 12M: RNA was extracted from mycelia grown in PDB at 12 hai
Sample 48M: RNA was extracted from mycelia grown in PDB at 48 hai

CsVosA is required for spore dormancy

The WT conidia of *C*. *sativus* would not germinate when they were attached to the conidiophores. However, the Δ*CsVosA* mutant conidia germinated when they were still attached to the conidiophores (Fig. 1.10). Premature germination rate was even higher for the *CsVosA* knockout mutants grown under light conditions than under dark conditions (Fig. 1.10). This indicates that *CsVosA* regulates spore dormancy. However, viability of the premature-germinated conidia was the same as that of the conidia that germinated after detachment from the conidiophore (data not shown), indicating the premature germination does not impair the conidial viability.

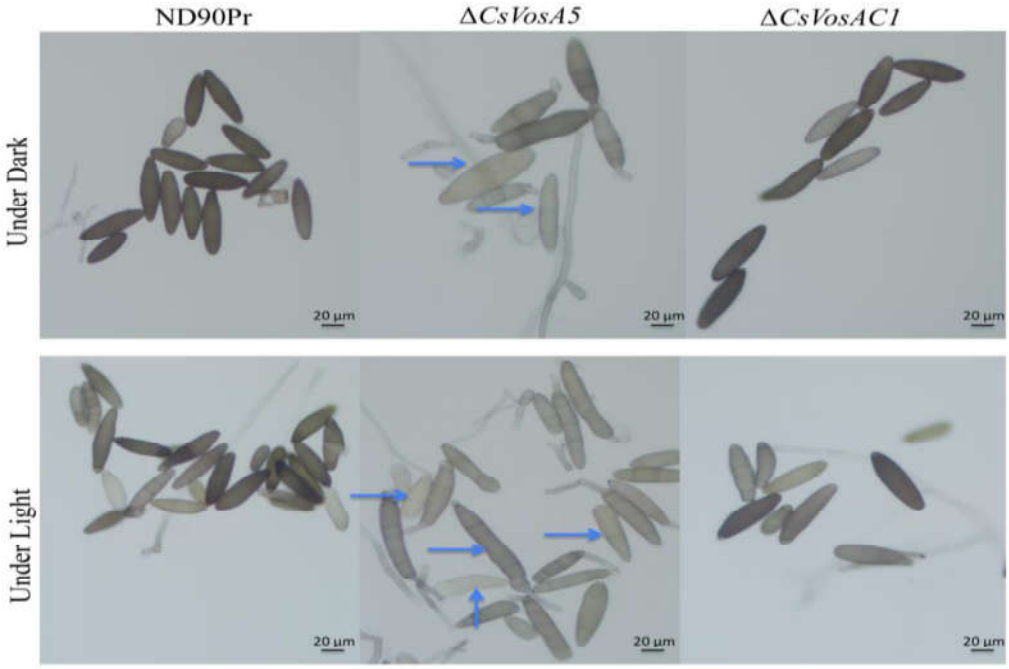

Fig. 1.9. Conidial morphology. The strains were grown on V8 PDA plates at 25 °C under constant dark and light conditions for 7 days, and then the conidia were harvested and photographed using Olympus BX51 microscope (Olympus, Center Valley, PA, USA) with the CCD camera digital imaging system (Diagnostic Instruments, Inc., Sterling Heights, MI, USA) under 20X magnification. Note WT and complemented strains have most of conidia with uniform size and regularly spaced septa. Arrows point to mutant conidia of irregular length and to compartments without septa or with irregularly placed septa.

CsVosA regulates pigmentation

The Δ*CsVosA* mutant conidia were lighter than WT conidia. However, mycelia of the mutant were darker than those of WT after 24 and 48 hours of growth in PDB (Fig. 1.11A and B). To investigate if *CsVosA* affects the expression of *PKS18*, the gene involved in biosynthesis of melanin in *C. sativus* (Leng et al. 2011), mRNA levels of *PKS18* in WT, Δ*CsVosA* mutant and complemented strains were examined using quantitative real time PCR. The results showed that *PKS18* was down-regulated in Δ*CsVosA* mutant conidia but significantly up-regulated in mycelia after 48 hours of growth in PDB (Fig. 1.11C).

Table 1.3. Percentage of different sized (small, normal and large) conidia of wild type (ND90Pr) and knockout mutant (Δ*CsVosA5*) under different condition

Strains	Condition	Small	Normal	Large
ND90Pr	Constant dark	4%	96%	0%
ND90Pr	Constant light	12%	88%	0%
Δ*CsVosA5*	Constant dark	29%	39%	32%
Δ*CsVosA5*	Constant light	14%	38%	48%

Normal conidia were measured at 15-28 × 80-120 µm (area value 6000~12000 in SigmaScan software) with 4-8 septa; small conidia were measured at 7-14 × 15-30 µm (area value 2000~3000 in SigmaScan software) with 0-1 septa; large conidia were measured at 20-35 x 120-250 µm (area value 12000~28000 in SigmaScan software) with 0-8 septa.

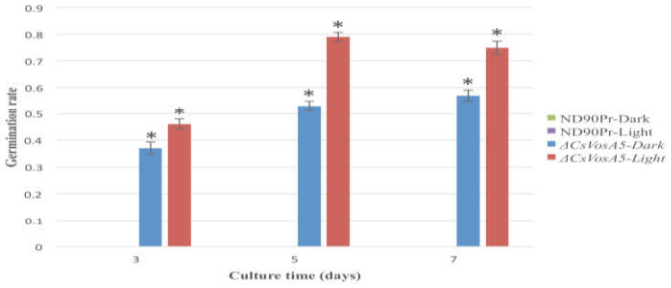

Fig. 1.10. Premature germination rate of mutant on V8 PDA under constant dark and light conditions at different time points. The germination rate was calculated as percentage of germinated conidia in the total number of conidia examined. Error bars indicate the standard deviation. Asterisks represent p-value <0.001 in T-test analyses when each isolate was compared with corresponding wild type under the same condition.

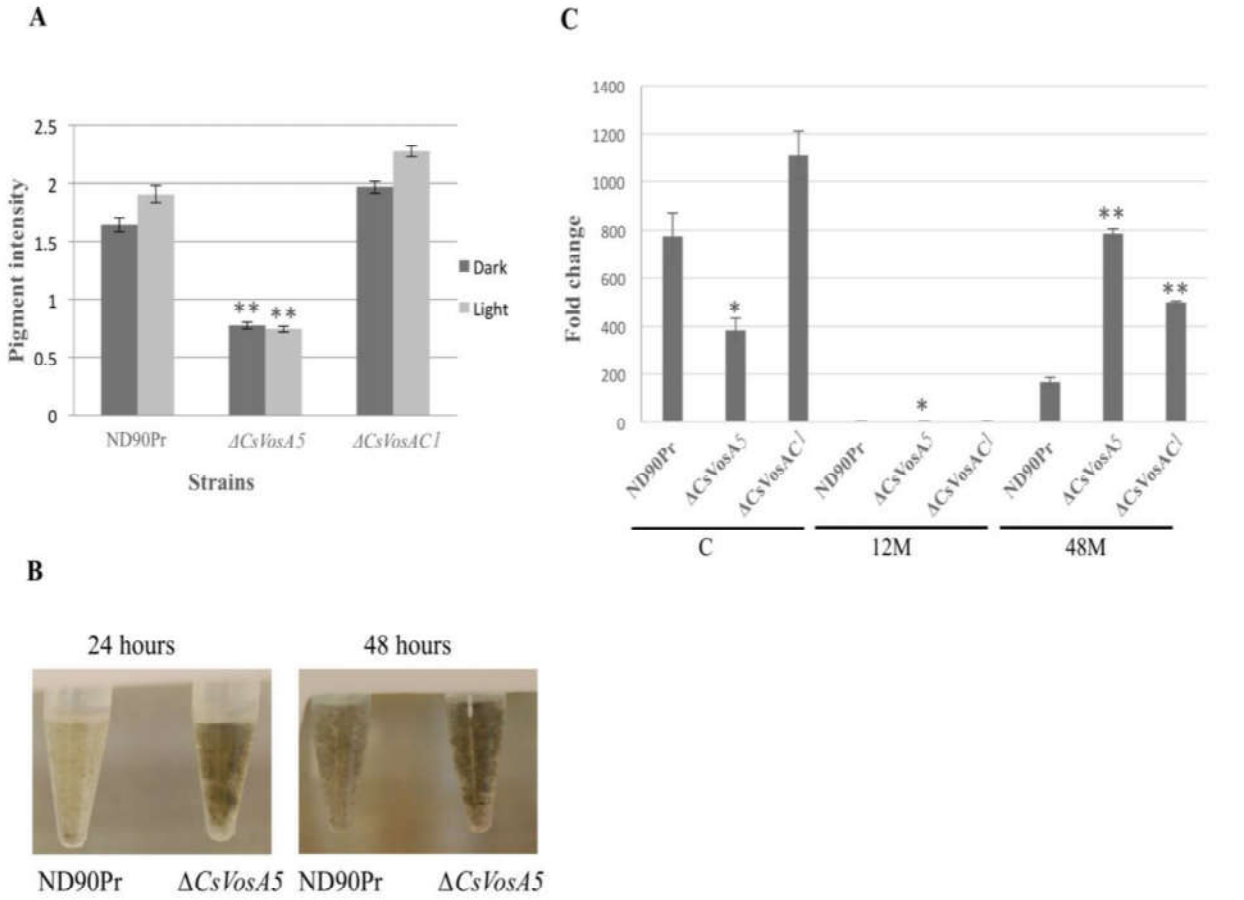

Fig. 1.11. *CsVosA* positively regulate conidial pigmentation of *C. sativus* but negatively regulate mycelial pigmentation of *C. sativus*. **A.** The strains were grown on V8 PDA plates at 25 °C under constant dark and light conditions for 7 days, and then the conidia were harvested and photographed using Olympus BX51 microscope (Olympus, Center Valley, PA, USA) with the CCD camera digital imaging system (Diagnostic Instruments, Inc., Sterling Heights, MI, USA) under 20X magnification. The software SigmaScan Pro 5 was used to estimate the color intensity of the conidia that represent the conidial melanin content. Error bars indicate the standard deviation. Single asterisks indicate p-value <0.05, double asterisks indicate p-value <0.001 in T-test analyses in which each isolate was compared with corresponding wild type under the same culture condition. **B.** Mycelial pellet were collected from cultures in PDB at 24 hours and 48 hours after inoculation with conidia and then photographed using digital camera (Nikon D80 with lens Af-S Micro NIKKOR 60 mm). **C.** RNA expression analysis of *PKS18* at different developmental stages. Expression level relative to the sample 12M of WT strain is shown. Error bars represent range of fold change calculated according to standard deviation of ΔΔCt. Single asterisks indicate p-value <0.05, double asterisks indicate p-value <0.001 in T-test analyses in which each isolate was compared with corresponding wild type at the same sample type.
Sample C: RNA was extracted from conidia harvested from the culture in V8 PDA at 7 dai.
Sample 12M: RNA was extracted from mycelia grown in PDB at 12 hai
Sample 48M: RNA was extracted from mycelia grown in PDB at 48 hai.

Roles of *CsVosA* in pathogenicity and virulence

Both WT and Δ*CsVosA* strains produced spot blotch symptoms on Bowman (Fig. 1.12A). However, the lesion number and size caused by the Δ*CsVosA* mutant were significantly different from those induced by the wild type (Fig.12B and C). The number of lesions produced by the mutant per leaf was significantly lower compared to WT under the same inoculation conditions (Fig.12B). The averaged lesion size of the mutant was 68% of that of WT (Fig.12C). Based on the 1–9 disease rating scale of (Fetch and Steffenson 1999), the infection responses caused by the wild type and *mutant strains* were rated as 7-8 and 5-6, respectively, at 6 days after inoculation (dai). No significant differences in pathogenicity and virulence were observed between WT and the complemented strain (Fig. 1.12B and C).

To determine which stage of the disease development is affected by *CsVosA*, the survival rate and appressorium formation of WT and mutant conidia on inoculated leaves of Bowman were examined under a microscope. The results showed that survival rate of the mutant conidia was significantly lower than that of WT conidia while no significant differences were observed between WT and complemented strain in this regard (Fig. 1.12D). However, conidia from both WT and mutants formed normal appressoria at 12 and 24 hai on the barley leaves, and no significant differences were observed between the Δ*CsVosA* and WT in appressorium formation frequencies for the germinated conidia (Fig. 1.12E).

mRNA expression levels of the two encoding genes for NRPSs (protein IDs 115356 and 140513) required for high virulence of isolate ND90Pr on Bowman (Condon et al. 2013) were measured in WT, Δ*CsVosA* and the complemented strain at different time points during host infection. The results showed that the two genes had significantly lower mRNA expression levels

in the Δ*CsVosA* mutant compared to WT and complemented strain, especially at 12 (for ID 115356) and 24 hai (for IDs 115356 and 140513) (Fig. 1.12F and G).

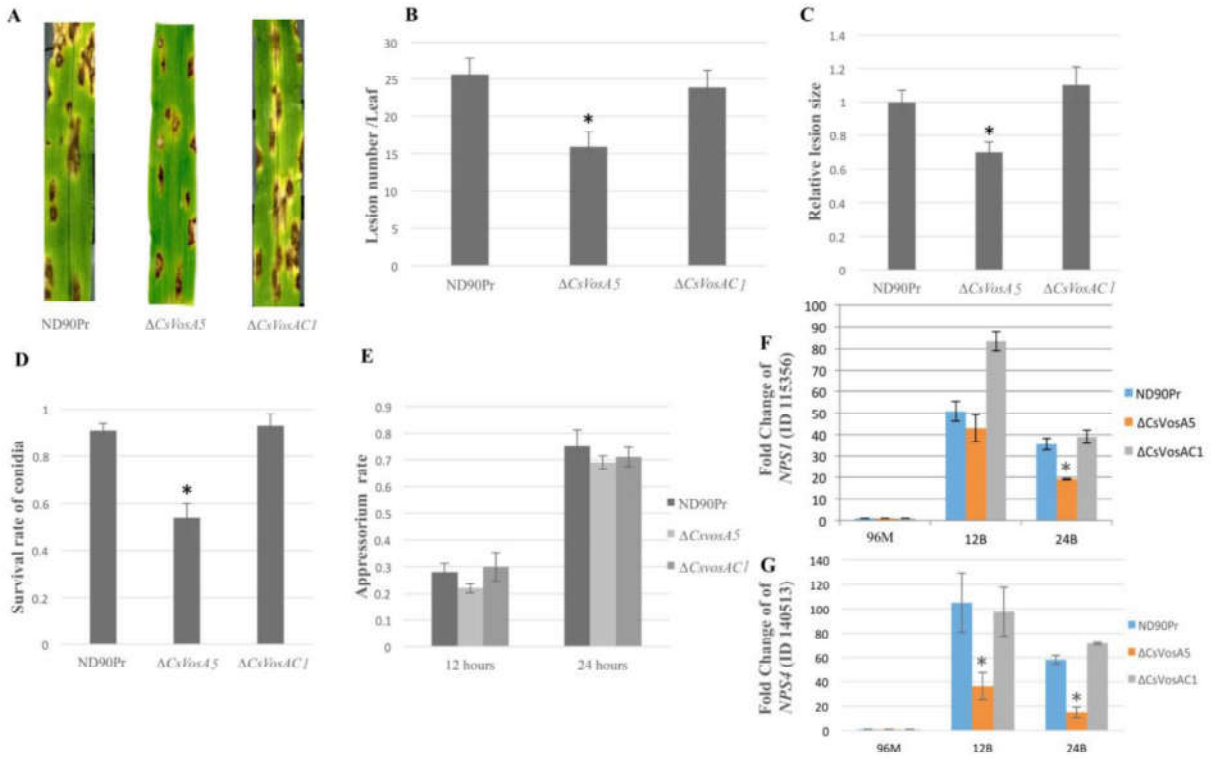

Fig. 1.12. Pathogenicity and virulence of wild type and mutants on barley cv. Bowman. **A.** Disease symptoms after spray-inoculation with conidia of the wild type (ND90Pr), knockout mutant (Δ*CsVosA*) and complementation strain (Δ*CsVosAC*). The photographs were taken at 6 dai. **B.** Quantification of lesion number. For each fungal strain, a total of 25 inoculated leaves were examined for lesion numbers at 6 dai and the average lesion number per leave was calculated. Error bars indicate the standard deviation. Asterisk represents p-value <0.05 in T-test analysis when each isolate was compared with wild type. **C.** Quantification of lesion size on leaves used in B. The average lesion size (length) caused by the WT strain was used as a control and relative lesion size was calculated for the knockout mutant (Δ*CsVosA*) and complementation strain (Δ*CsVosAC*). Error bars indicate standard deviation. Asterisk represents p-value <0.05 in T-test analysis when each isolate was compared with wild type. **D.** Viability of conidia on barley leaves. The survival rate was calculated as percentage of viable conidia in the total number of conidia examined. Error bars indicate the standard deviation. Asterisk represents p-value <0.05 in T-test analysis when each isolate was compared with wild type. **E.** Appressorial formation rate. The wild type and Δ*CsVosA* conidia were spray-inoculated on seedling leaves of barley cv. Bowman. After 12 and 24 hours after inoculation, the appressorium rate was calculated from the number of appressorium-forming conidia relative to the total number of conidia examined. Error bars indicate the standard deviation. **F.** RNA expression analyses of *NPS1* (ID 115356) during

infection of barley cv. Bowman. Expression levels relative to the sample 96M is shown. Error bars represent range of fold change calculated according to standard deviation of ΔΔCt. The expression of the β-actin-encoding gene (*ACT*) was used as a reference. Asterisks indicate p-value <0.05 in T-test analyses in which each isolate was compared with corresponding wild type at the same sample type. **G.** RNA expression analyses of *NPS4* (ID 140513) during infection of barley cv. Bowman. Expression levels relative to the sample 96M is shown. Error bars represent range of fold change calculated according to standard deviation of ΔΔCt. The expression of the β-actin-encoding gene (*ACT*) was used as a reference. Asterisks indicate p-value <0.05 in T-test analyses in which each isolate was compared with corresponding wild type at the same sample type. All experiments were repeated at least three times.
Sample 96M: RNA was extracted from a mixture of mycelia harvested from the culture at 96 hours after inoculation from different media including PDA, MM, V8 PDA, and water agar
Sample 12B: RNA was extracted from the inoculated barley leaves at 12 hai on Bowman
Sample 24B: RNA was extracted from the inoculated barley leaves at 24 hai on Bowman

Discussion

Although the *velvet* proteins are found to be conserved across filamentous fungi, their functions have been characterized in some species, especially for VosA and VelC, which were only studied in a few cases (Kim et al. 2014; Wang et al. 2014). In the present study, we identified and functionally characterized the homolog of VosA (*CsVosA*) in *C*. *sativus*. Our results revealed that *CsVosA* plays similar and unique roles in regulating fungal development, secondary metabolism and pathogenicity.

Deletion of *CsVosA* led to increased production of conidia under both constant dark and light conditions, suggesting that *CsVosA* negatively regulates conidial productivity, just as found in *A*. *nidulans* and *A*. *fumigatus* (Ni and Yu 2007; Park et al. 2012). The same effect was found for *VOS1* in *C*. *heterostrophus*, but the *VOS1* mutant had an increased conidial production only under constant dark conditions (Wang et al. 2014). These results indicate that the function of VosA/Vos1 can be different under different conditions even in certain related fungal species, like *C*. *sativus* and *C*. *heterostrophus*. Lights play different roles in conidiation of *C*. *sativus* and *C*.

heterostrophus. The wild type strain of *C*. *heterostrophus* produced more conidia under constant light conditions than under constant dark conditions (Wang et al. 2014), whereas no significant difference in conidial productivity was observed in *C*. *sativus* grown under these two conditions. In addition, the *C*. *sativus CsVosA* mutant produced more conidia under constant dark conditions than under constant light conditions (Fig. 1.6), indicating that *CsVosA* may have a stronger repression of conidiation in *C*. *sativus* under constant dark conditions than under constant light conditions.

We observed that the *CsVosA* mutant produced many larger conidia, whereas WT conidia were uniform in size with regularly spaced septa. (Wang et al. 2014) also showed that deletion of *VEL2* or *VOS1* affected conidium size and spacing of septa in *C*. *heterostrophus*. These results indicate VosA is a positive regulator of these processes. In *Fusarium verticillioides*, the cell wall defected mutants produced larger conidia due to the reduced resistance of cell wall to turgor pressure (Li et al. 2006). Osmotic stabilizers are able to reduce cellular turgor pressure and have been shown to restore cell wall defective mutants of *S*. *cerevisiae* (Levin and Bartlettheubusch 1992; Torres et al. 1991) and *A*. *nidulans* (Borgia et al. 1996) to the WT phenotypes. We examined conidial morphology of the wild type and Δ*CsVosA* grown on V8 PDA media containing the osmotic stabilizers (1.0 M sorbitol or 0.8 M sucrose), and failed to detect differences in conidial size between the mutant and WT (data not shown), indicating that *CsVosA* may regulate genes associated with biosynthesis of conidial cell wall components.

Our results showed that deletion of *CsVosA* results in a decreased amount of trehalose in conidia, and one of the genes involved in trehalose breakdown were up-regulated while two of the genes involved in trehalose biosynthesis was down-regulated in the *CsVosA* mutant, indicating that the corresponding protein is a positive regulator of trehalose biosynthesis. These

findings are consistent with those found for *A*. *nidulans*, *A*. *fumigatus* and *C*. *heterostrophus*, where *VosA* positively regulates conidial maturation and trehalose biosynthesis (Bayram et al. 2010; Park et al. 2012; Wang et al. 2014). However, the regulatory role of *VosA* in mycelial trehalose metabolism of *C*. *sativus* appeared to be different because deletion of *CsVosA* caused trehalose increase in mycelia compared to the wild type (Fig.4C).

We observed that Δ*CsVosA* conidia were hypersensitive to oxidative stress mediated by H_2O_2. This result matches those found for *VosA* in *C*. *heterostrophus* (Wang et al. 2014). In *C*. *heterostrophus*, VOS1 (orthologous to VosA) was found to regulate the expression of CAT3, one of three catalases in the genome central to decomposition of H_2O_2 and therefore protection from oxidative damage by ROS. *CsVosA* may have similar functions in controlling the expression of CAT3, but further studies are required to reveal the role of *CsVosA* in regulating CAT3 in *C*. *sativus*.

In *Cochliobolus* species, conidiogenesis follows a sympodial fashion in which conidia are normally produced by an expansion and swelling of the apex of the conidiophore, and after the formation of the first conidium, the active apical tip moves to the side to produce the next conidium. Multiple rounds of conidiation result in three to five spores borne sympodially on a conidiophore. However, in the *CsVosA* knockout mutant, we observed both sympodial and acropetal conidiation patterns. Sympodial conidiation generated initial conidia from the conidiophore while acropetal conidiation produced conidial chains with the youngest conidia emerging at the tip of the initial conidia. This result suggests that *CsVosA* regulates conidiogenesis.

Among the four *C*. *sativus* genes (*CsBrlA*, *CsWetA*, *CsStuA* and *CsMedA*), only *CsMedA* showed up-regulated expression while the others were down-regulated during conidiation of the

Δ*CsVosA* mutant (Fig.8). This result suggests that *CsVosA* negatively regulates *CsMedA* but positively controls the other three genes. A mutation at *MedA* in *A*. *nidulans* results in aberrant conidiophores with branching chains of metulae, delayed conidial differentiation, and frequent re-initiation of the secondary conidiophore (Busby et al. 1996; Clutterbuck 1969; Gemes and Clutterbuck 1994). The *REN1* (ortholog of *AnMedA*) mutants of *Fusarium oxysporum* lack normal conidiophores and phialides, producing rod-shaped cells in a single chain at the early stage of development and frequently form the cells in branching chains at the later stage of development while the wild type strain never forms conidia in a chain (Ohara et al. 2004). In *Magnaporthe grisea*, deletion of *ACR1* (ortholog of *AnMedA*) caused holoblastic acropetal pattern sporulation whereas the spore formation and differentiation in wild type occur in a typical holoblastic sympodial fashion (Lau and Hamer 1998). We hypothesize that *CsVosA* affects expression of *CsMedA* and others, leading to the occurrence of acropetal conidiation. More functional studies of this gene and other genes related to conidiation are needed to fully understand the conidial development in *C*. *sativus*.

In our study, we found that pigmentation (most likely due to production of melanin) and the expression levels of *PKS18*, the gene involved in biosynthesis of melanin in *C*. *sativus* (Leng et al. 2011) were decreased in conidia but increased in mycelia of the Δ*CsVosA* mutant, suggesting that VosA positively and negatively affects the melanin production in conidia and mycelia of *C*. *sativus*, respectively, by controlling the expression of genes involved in melanin biosynthesis. Previous studies showed that other *velvet* proteins regulate mycelial melanin production in fungi. For example, VeA positively regulates melanin biosynthesis in mycelia of *Mycosphaerella graminicola* (Choi and Goodwin 2011), but negatively controls mycelial melanin production in

Cochliobolus heterostrophus (Wu et al. 2012) and *Fusarium fujikuroi* (Wiemann et al. 2010). To my knowledge, it is the first time to show the regulatory role of VosA in melanin production.

Deletion of *CsVosA* led to a significant reduction in lesion number and size of the spot blotch disease caused by the mutant on barley plants. The fewer lesion numbers are probably due to the lower viability of the mutant conidia compared to the wild type conidia. The reduced virulence is probably due to the positive regulatory role of *CsVosA* in expression of the two genes for NRPSs involved in biosynthesis of an unknown secondary metabolite, which is required for high virulence on barley Bowman (Condon et al. 2013); Leng and Zhong, unpublished). Previous studies have shown that two of the *velvet* proteins, VeA and VelB, play important roles in regulating the production of secondary metabolites, including melanin in *Botrytis cinerea* (Yang et al. 2013) and *C. heterostrophus (Wu et al. 2012),* fumonisin and fusarin in *F. verticillioides* (Myung et al. 2009), sterigmatocystin in *A. nidulans,* trichothecene and zearalenone in *Fusarium graminearum*, and penicillin in *Penicillium chrysogenum* (Hoff et al. 2010; Kato et al. 2003). Wu et al. (2012) demonstrated that Vel1, the *VeA* ortholog in *C. heterostrophus*, is involved in regulation of biosynthesis of T-toxin, the host selective toxin (HST)/effector for pathogenicity of the pathogen. To our knowledge, this study is the first to demonstrate that VosA regulates genes for NRPS involved in virulence in ascomycete fungi.

Acknowledgements

This study was supported by the Triticeae-CAP project (2011-68002-30029) from the US Department of Agriculture National Institute of Food and Agriculture. We thank Dr. Xiwen Cai for helps in taking microscopic photographs of the fungal structures. The genome sequence data

of the *C*. *sativus* strain ND90Pr were produced and provided by the US Department of Energy Joint Genome Institute (http://genome.jgi.doe.gov/Cocsa1/Cocsa1.home. html).

References

Adams, T. H., Boylan, M. T., and Timberlake, W. E. 1988. *brla* is necessary and sufficient to direct conidiophore development in *Aspergillus nidulans*. Cell 54:353-362.

Ahmed, Y. L., Gerke, J., Park, H.-S., Bayram, Ö., Neumann, P., Ni, M., Dickmanns, A., Kim, S. C., Yu, J.-H., Braus, G. H., and Ficner, R. 2013. The velvet family of fungal regulators contains a DNA-binding domain structurally similar to NF-κB. PLoS Biol. 11:e1001750.

Al-Bader, N., Vanier, G., Liu, H., Gravelat, F. N., Urb, M., Hoareau, C. M. Q., Campoli, P., Chabot, J., Filler, S. G., and Sheppard, D. C. 2010. Role of trehalose biosynthesis in *Aspergillus fumigatus* development, stress response, and virulence. Infect. Immuni. 78:3007-3018.

Baba, S., Kinoshita, H., and Nihira, T. 2012. Identification and characterization of *Penicillium citrinum* VeA and LaeA as global regulators for ML-236B production. Curr. Genet. 58:1-11.

Bayram, O., and Braus, G. 2012. Coordination of secondary metabolism and development in fungi: the velvet family of regulatory proteins. FEMS Microbiol. Rev. 36:1-24.

Bayram, O., Valerius, O., Park, H. S., Irniger, S., Gerke, J., Ni, M., Han, K. H., Yu, J. H., and Braus, G. H. 2010. LaeA control of velvet family regulatory proteins for light-dependent development and fungal cell-type specificity. PLoS Genet. 6:e1001226.

Bayram, O., Krappmann, S., Ni, M., Bok, J., Helmstaedt, K., Valerius, O., Braus-Stromeyer, S., Kwon, N., Keller, N., Yu, J., and Braus, G. 2008. VelB/VeA/LaeA complex coordinates light signal with fungal development and secondary metabolism. Science 320:1504-1506.

Beck, E., Ludwig, G., Auerswald, E. A., Reiss, B., and Schaller, H. 1982. Nucleotide-sequence and exact localization of the neomycin phosphotransferase gene from transposon TN5. Gene 19:327-336.

Borgia, P., Miao, Y., and Dodge, C. 1996. The *orlA* gene from *Aspergillus nidulans* encodes a trehalose-6-phosphate phosphatase necessary for normal growth and chitin synthesis at elevated temperatures. Mol. Microbiol. 20:1287-1296.

Busby, T., Miller, K., and Miller, B. 1996. Suppression and enhancement of the *Aspergillus nidulans* medusa mutation by altered dosage of the bristle and stunted genes. Genetics 143:155-163.

Catlett, N. L., Lee, B.-N., Yoder, O. C., and Turgeon, B. G. 2003. Split-marker recombination for efficient targeted deletion of fungal genes. Fungal Genet. Newsl. 50:9–11.

Chang, M. H., Chae, K. S., Han, D. M., and Jahng, K. Y. 2004. The GanB G alpha-protein negatively regulates asexual sporulation and plays a positive role in conidial germination in *Aspergillus nidulans*. Genetics 167:1305-1315.

Chang, P. K., Scharfenstein, L. L., Li, P., and Ehrlich, K. C. 2013. *Aspergillus flavus* VelB acts distinctly from VeA in conidiation and may coordinate with FluG to modulate sclerotial production. Fungal Genet. Biol. 58-59:71-79.

Choi, Y. E., and Goodwin, S. B. 2011. *MVE1*, encoding the velvet gene product homolog in *Mycosphaerella graminicola*, is associated with aerial mycelium formation, melanin biosynthesis, hyphal swelling, and light signaling. Appl. Environ. Microb. 77:942-953.

Clutterbuck, A. J. 1969. A mutational analysis of conidial development in *Aspergillus nidulans*. Genetics 63:317-327.

Condon, B., Leng, Y. Q., Wu, D., Bushley, K., Ohm, R., Otillar, R., Martin, J., Schackwitz, W., Grimwood, J., MohdZainudin, N., Xue, C., Wang, R., Manning, V., Dhillon, B., Tu, Z., Steffenson, B., Salamov, A., Sun, H., Lowry, S., LaButti, K., Han, J., Copeland, A., Lindquist, E., Barry, K., Schmutz, J., Baker, S., Ciuffetti, L., Grigoriev, I., Zhong, S. B., and Turgeon, B. 2013. Comparative genome structure, secondary metabolite, and effector coding capacity across *Cochliobolus* pathogens. PLoS Genet. 9:e1003233..

Fetch, T. G., and Steffenson, B. J. 1999. Rating scales for assessing infection responses of barley infected with *Cochliobolus sativus*. Plant Dis. 83:213-217.

Gemes, D. H., and Clutterbuck, A. J. 1994. Enhancers of conidiation mutants in *Aspergillus nidulans*. Genetics 137:79-85.

Hoff, B., Kamerewerd, J., Sigl, C., Mitterbauer, R., Zadra, I., Kurnsteiner, H., and Kuck, U. 2010. Two components of a velvet-like complex control hyphal morphogenesis, conidiophore development, and penicillin biosynthesis in *Penicillium chrysogenum*. Eukaryot. Cell 9:1236-1250.

Jiang, J., Yun, Y., Liu, Y., and Ma, Z. 2012. *FgVELB* is associated with vegetative differentiation, secondary metabolism and virulence in *Fusarium graminearum*. Fungal Genet. Biol. 49:653-662.

Karakkat, B. B., Gold, S. E., and Covert, S. F. 2013. Two members of the *Ustilago maydis* velvet family influence teliospore development and virulence on maize seedlings. Fungal Genet. Biol. 61:111-119.

Kato, N., Brooks, W., and Calvo, A. M. 2003. The expression of sterigmatocystin and penicillin genes in *Aspergillus nidulans* is controlled by *veA*, a gene required for sexual development. Eukaryot. Cell 2:1178-1186.

Keogh, R. C., Deverall, B. J., and McLeod, S. 1980. Comparison of histological and physiological-response to *Phakopsora pachyrhizi* in resistant and susceptible soybean. T. Brit. Mycol. Soc. 74:329-333.

Kim, H.-J., Han, J.-H., Kim, K. S., and Lee, Y.-H. 2014. Comparative functional analysis of the velvet gene family reveals unique roles in fungal development and pathogenicity in *Magnaporthe oryzae*. Fungal Genet. Biol. 66:33-43.

Kim, H. K., Lee, S., Jo, S. M., McCormick, S. P., Butchko, R. A. E., Proctor, R. H., and Yun, S. H. 2013. Functional roles of *FgLaeA* in controlling secondary metabolism, sexual development, and virulence in *Fusarium graminearum*. PLoS One 8:15.

Kopke, K., Hoff, B., Bloemendal, S., Katschorowski, A., Kamerewerd, J., and Kuck, U. 2013. Members of the *Penicillium chrysogenum* velvet complex play functionally opposing roles in the regulation of penicillin biosynthesis and conidiation. Eukaryot. Cell 12:299-310.

Lan, N., Zhang, H., Hu, C., Wang, W., Calvo, A. M., Harris, S. D., Chen, S., and Li, S. 2014. Coordinated and Distinct Functions of Velvet Proteins in *Fusarium verticillioides*. Eukaryot. Cell 13:909-918.

Lau, G. W., and Hamer, J. E. 1998. Acropetal: A genetic locus required for conidophore architecture and pathogenicity in the rice blast fungus. Fungal Genet. Biol. 24:228-239.

Leng, Y. Q., and Zhong, S. B. 2012. Sfp-type 4 '-phosphopantetheinyl transferase is required for lysine synthesis, tolerance to oxidative stress and virulence in the plant pathogenic fungus *Cochliobolus sativus*. Mol. Plant Pathol. 13:375-387.

Leng, Y. Q., Wu, C. X., Liu, Z. H., Friesen, T. L., Rasmussen, J. B., and Zhong, S. B. 2011. RNA-mediated gene silencing in the cereal fungal pathogen *Cochliobolus sativus*. Mol. Plant Pathol. 12:289-298.

Levin, D. E., and Bartlettheubusch, E. 1992. Mutant in the *Saccharomyces cerevisiae pkc1*-gene display a cell cycle-specific osmotic stability defect. J. Cell Biol. 116:1221-1229.

Li, S. J., Myung, K., Guse, D., Donkin, B., Proctor, R. H., Grayburn, W. S., and Calvo, A. M. 2006. *FvVE1* regulates filamentous growth, the ratio of microconidia to macroconidia and cell wall formation in *Fusarium verticillioides*. Mol. Microbiol. 62:1418-1432.

Lopez-Berges, M. S., Hera, C., Sulyok, M., Schafer, K., Capilla, J., Guarro, J., and Di Pietro, A. 2013. The velvet complex governs mycotoxin production and virulence of *Fusarium oxysporum* on plant and mammalian hosts. Mol. Microbiol. 87:49-65.

Marshall, M. A., and Timberlake, W. E. 1991. *Aspergillus nidulans wetA* activates spore-specific gene-expression. Mol.Cell Biol. 11:55-62.

Mathre, D. E. 1997. Compendium of barley diseases. 2nd Edition. APS Press, St. Paul, MN:90.

Miller, K. Y., Wu, J. G., and Miller, B. L. 1992. *StuA* is required for cell pattern-formation in *Aspergillus*. Gene Dev. 6:1770-1782.

Myung, K., Li, S., Butchko, R. A. E., Busman, M., Proctor, R. H., Abbas, H. K., and Calvo, A. M. 2009. *FvVE1* regulates biosynthesis of the mycotoxins fumonisins and fusarins in *Fusarium verticillioides*. J. Agr. Food Chem. 57:5089-5094.

Ni, M., and Yu, J. H. 2007. A novel regulator couples sporogenesis and trehalose biogenesis in *Aspergillus nidulans*. PLoS One 2:e970.

Ohara, T., Inoue, I., Namiki, F., Kunoh, H., and Tsuge, T. 2004. *REN1* is required for development of microconidia and macroconidia, but not of chlamydospores, in the plant pathogenic fungus *Fusarium oxysporum*. Genetics 166:113-124.

Park, H. S., Bayram, O., Braus, G. H., Kim, S. C., and Yu, J. H. 2012. Characterization of the velvet regulators in *Aspergillus fumigatus*. Mol. Microbiol. 86:937-953.

Tamura, K., Stecher, G., Peterson, D., Filipski, A., and Kumar, S. 2013. MEGA6: molecular evolutionary genetics analysis version 6.0. Mol. Biol. Evol. 30:2725-2729.

Tinline, R. D., Strauffer, J. F., and Dickson, J. G. 1960. *Cochliobolus sativus* III. Effects of ultraviolet radiation. . Can. J. Bot. 38:275–282.

Torres, L., Martin, H., Garciasaez, M., Arroyo, J., Molina, M., Sanchez, M., and Nombela, C. 1991. A protein-kinase gene comlements the lytic phenotype of *Saccharomyces cerevisiae lyt2* mutatns. Mol. Microbiol. 5:2845-2854.

Valjavec-Gratian, M., and Steffenson, B. J. 1997a. Genetics of virulence in *Cochliobolus sativus* and resistance in barley. Phytopathology 87:1140-1143.

Valjavec-Gratian, M., and Steffenson, B. J. 1997b. Pathotypes of *Cochliobolus sativus* on barley in North Dakota. Plant Dis. 81:1275-1278.

Wang, W., Wu, D., Pan, H., and Turgeon, B. G. 2014. Vel2 and Vos1 hold essential roles in ascospore and asexual spore development of the heterothallic maize pathogen *Cochliobolus heterostrophus*. Fungal Genet. Biol. 70:113-124.

Webster, R. H., and Sil, A. 2008. Conserved factors Ryp2 and Ryp3 control cell morphology and infectious spore formation in the fungal pathogen *Histoplasma capsulatum*. Proc. Natl. Acad. Sci. USA 105:14573-14578.

Wiemann, P., Brown, D. W., Kleigrewe, K., Bok, J. W., Keller, N. P., Humpf, H. U., and Tudzynski, B. 2010. FfVel1 and FfLae1, components of a velvet-like complex in *Fusarium fujikuroi*, affect differentiation, secondary metabolism and virulence. Mol. Microbiol. 77:972-994.

Wiese, M. V. 1987. Compendium of wheat diseases. 2nd Ed. APS Press, St. Paul, Minn.:112.

Wu, D. L., Oide, S., Zhang, N., Choi, M. Y., and Turgeon, B. G. 2012. ChLae1 and ChVel1 regulate T-toxin production, virulence, oxidative stress response, and development of the maize pathogen *Cochliobolus heterostrophus*. PLoS Pathog. 8:e1002542.

Yang, Q., Chen, Y., and Ma, Z. 2013. Involvement of BcVeA and BcVelB in regulating conidiation, pigmentation and virulence in *Botrytis cinerea*. Fungal Genet. Biol. 50:63-71.

Zhong, S. B., Steffenson, B., Martinez, J., and Ciuffetti, L. 2002. A molecular genetic map and electrophoretic karyotype of the plant pathogenic fungus *Cochliobolus sativus*. Mol. Plant Microbe In. 15:481-492.

CHAPTER 2: COORDINATED AND INDEPENDENT FUNCTIONS OF *VELVET*-COMPLEX GENES IN FUNGAL DEVELOPMENT AND VIRULENCE OF THE FUNGAL CEREAL PATHOGEN *COCHLIOBOLUS SATIVUS*

Abstract

LaeA and *velvet* proteins regulate fungal development and secondary metabolism through formation of multimeric complexes in many fungal species, but their functions in the cereal fungal pathogen *Cochliobolus sativus* are not well understood. In this study, four *C*. *sativus* genes (*CsLaeA*, *CsVeA*, *CsVelB*, and *CsVelC*) orthologous to four components (*LaeA*, *VeA*, *VelB*, and *VelC*) of the *velvet* complexes, respectively, were identified, and knockout mutants for each of the genes were generated and characterized. Both Δ*CsVeA* and Δ*CsVelB* showed significantly reduction in aerial mycelia growth. Δ*CsVelB* also exhibited a hypermorphic conidiation phenotype with indeterminate growth of the conidial tip cells and premature germination of conidia. Δ*CsLaeA*, Δ*CsVeA*, and Δ*CsVelB* produced more conidia under constant light conditions than under constant dark conditions whereas the wild type had no differences under the two conditions. Under consistent light conditions, the three knockout mutants (Δ*CsLaeA*, Δ*CsVeA*, and Δ*CsVelB*) showed significantly reduced conidiation compared to the wild type; they produced more small sized conidia, especially under the constant dark conditions, and had less conidial pigmentation probably due to reduced expression of genes involved in melanin production as revealed by RNA expression assay for *PKS18*, one of the major genes involved in the melanin biosynthesis pathway in *C*. *sativus*. All knockout mutants (Δ*CsLaeA*, Δ*CsVeA*, Δ*CsVelB* and Δ*CsVelC*) showed some extent of reduction in virulence on susceptible barley plants compared to the wild type strain and the two NRPS genes involved in virulence of the fungus were down regulated at different levels. The results revealed the conserved and unique

roles of *velvet*-complex proteins as regulators in mediating fungal development and secondary metabolism in *C*. *sativus*.

Introduction

Spot blotch, caused by the ascomycete fungus *Cochliobolus sativus* (Ito & Kurib.) Drechs. ex Dastur. [anamorph: *Bipolaris sorokiniana* (Sacc.) Shoem.], is one of the most common and economically important diseases in barley. It can cause more than 30% yield loss and significantly impact the malting quality of barley (Wilcoxson et al. 1990). *C*. *sativus* is a polycyclic plant pathogen and the disease cycle begins when conidia (asexual spores) are landed on the leaf surface of barley or wheat (Braun and Howard 1994). Subsequently, the conidium germinates and develops an appressorium, a specialized infection structure, which assists in penetration into the leaves (Kumar et al. 2002). After successful penetration, the fungus produces infection hyphae to invade into the leaf mesophyll tissues to cause cell death of host (Santen et al. 2005). Then, necrosis and/or chlorosis appears in infected host cells and their neighboring non-infected cells, indicating that certain toxic compounds (virulence factor) released by the fungus diffuse into non-infected host cells (Kumar et al. 2002). Previous studies with pathotype 2 of *C*. *sativus* (ND90Pr) on the barley cv. Bowman have revealed the virulence factor is a secondary metabolite peptide synthesized by non-ribosomal peptide synthetases (NRPSs) (Condon et al. 2013). Based on the pathogen's life cycle and its infection process, the incidence and severity of the spot blotch disease are closely associated with (1) repetitive rounds of new infections; (2) the amounts of conidia produced during each round of conidiation; and (3) the productivity of virulence factor. Therefore, understanding the molecular regulation of conidiation and secondary metabolite biosynthesis in this fungus is a prerequisite for developing sustainable disease management strategies.

Recent studies revealed that LaeA and *velvet* proteins (VeA, VelB, VelC and VosA) act as global regulators of fungal development and secondary metabolism through formation of multimeric complexes, such as LaeA/VeA/VelB, VelB/VosA, VelB/VelB (Bayram et al. 2008; Bayram et al. 2010; Park et al. 2012a), VelC/VosA (Park et al. 2014), and VelC/VeA (Lan et al. 2014). These *velvet*-complex proteins are highly conserved in many fungal species and have been extensively studied in a number of fungi. LaeA was identified as a putative methyltransferase in *Aspergillus nidulans* (Bok and Keller 2004) and was reported to positively regulate the asexual development of *A*. *nidulans*, *Penicillium chrysogenum*, and *Fusarium fujikuroi* (Bayram et al. 2010; Kosalkova et al. 2009; Wiemann et al. 2010). In *Cochliobolus heterostrophus*, however, deletion of ChLae1 increases asexual sporulation and female sterility, reduces tolerance to oxidative stress and aerial hyphal growth (Wu et al. 2012). The other four components of *velvet*-complex are *velvet* superfamily proteins, which have been shown to be regulators in several fungal species by acting as transcription factors (Ahmed et al. 2013). VeA was first identified as a positive regulator of sexual sporulation and negative regulator of asexual development in *Aspergillus nidulans* (Kafer 1965). Similarly, in *C*. *heterostrophus*, ChVel1 positively regulates oxidative stress responses, sexual development, and aerial hyphal growth, but negatively controls asexual differentiation (Wu et al. 2012). Furthermore, in *Fusarium verticillioides*, deletion of FvVE1 suppresses aerial hyphal growth, reduces colony surface hydrophobicity, and activates conidiation with an increased ratio of macroconidia to microconidia (Li et al. 2006). In contrast, the VeA homologs in *Aspergillus flavus*, *P*. *chrysogenum* and *Fusarium graminearum* positively regulate asexual reproduction (Amaike and Keller 2009; Hoff et al. 2010; Merhej et al. 2012). VelB and VosA forms VelB/VosA and VelB/VelB dimers, positively controlling trehalose biosynthesis, spore viability and conidial germination but negatively controlling the conidia

production in *A*. *nidulans*, *C*. *heterostrophus* and *C*. *sativus* (Ni and Yu 2007; Park et al. 2012b; Wang et al. 2015; Wang et al. 2014). In another plant pathogen fungus *Magnaporthe grisea*, *MoVLEB* positively regulates the conidial germination and conidia production, whereas *MoVOSA* appears dispensable for the fungal development (Kim et al. 2014). VelC was studied only in a few fungal species. Deletion of VelC in *A*. *nidulans* increases conidiation but significantly reduces the number of sexual fruiting bodies (Park et al. 2014). Similarly, deletion of PcVelC in *P*. *chrysogenum* also increases conidiation (Kopke et al. 2013). In contrast, deletion of *MoVELC* in *M*. *oryzae* affects the cell wall integrity of appressoria, significantly decreases the conidia production, and reduces the conidial size (Kim et al. 2014).

LaeA and the *velvet*-complex proteins also play important roles in the regulation of secondary metabolism. For example, deletion of LaeA in *A*. *nidulans* blocks the expression of metabolic gene clusters, leading to reduced production of sterigmatocystin, penicillin, and lovastatin (Bok and Keller 2004). The VeA orthologs had been reported to control biosynthesis of various secondary metabolites such as aflatoxin, cyclopiazonic acid, and aflatrem in *A*. *flavus* (Duran et al. 2009), trichothecenes in *F*. *graminearum* (Merhej et al. 2012), and melanin in *Mycosphaerella graminicola* (Choi and Goodwin 2011). In *F*. *verticillioides,* Fvve1 and FvvelB positively regulate fumonisin production (Lan et al. 2014). In *P*. *chrysogenum*, PcLaeA, PcVelA, and PcVelC activate penicillin biosynthesis, whereas PcVelB represses this process. In *C*. *heterostrophus*, ChLae1 and ChVel1 positively regulate T-toxin biosynthesis but negatively control melanin biosynthesis in mycelia (Wu et al. 2012). In the fungal cereal pathogen *C*. *sativus*, CsVosA plays a positive and negative role in melanin production in conidia and mycelia, respectively, and positively regulates the biosynthesis of virulence related secondary metabolites (Wang et al. 2015).

All these studies indicate that although *velvet*-complex genes are conserved among many filamentous fungi, their functions on regulating fungal development and biosynthesis of secondary metabolites may be similar or different depending on the fungal species involved. In this study, we identified and characterized *CsLaeA, CsVeA*, *CsVelB* and *CsVelC* in *C*. *sativus* and showed their functions in regulating oxidative stress tolerance, aerial hyphal growth, asexual development, as well as production of melanin and virulence factors. By studying the single and double gene knockout mutants, we further explored the coordinated and distinct functions of these genes in fungal development and secondary metabolism and provided a comparative framework between the functions of *velvet*-complex genes in different fungal species.

Materials and methods

Fungal isolates, media and general growth conditions

In this study, the *C*. *sativus* isolate ND90Pr (ATCC 201652) was used as the wild type (WT). Unless mentioned otherwise, all isolates were grown on V8 potato dextrose agar (V8 PDA) under 12 hour fluorescent light each day at approximately 23 °C. Potato dextrose broth (PDB), minimal medium (MM) (Tinline et al. 1960), and water agar plates were also used for fungal growth in specific experiments.

Identification of the LaeA, VeA, VelB and VelC orthologs in *C. sativus*

The *A*. *nidulans* LaeA, VeA, VelB and VelC (accession number: CBF88745.1, AAD42946.1, ABQ17967.1, and ABQ17968.1) protein sequences were used to query the genome sequence of the *C*. *sativus* isolate ND90Pr (http://genome.jgi-psf.org/Cocsa1

/Cocsa1.home.html) using the BLASTP algorithm. cNLS Mapper program (http://nls-mapper.iab.keio.ac.jp/cgi-bin/NLS_Mapper_form.cgi) was used to predict the putative nuclear localization signal. The protein sequences of CsLaeA, VeA, VelB and VelC and their corresponding nucleotide sequences can be found in Energy Joint Genome Institute (http://genome.jgi-psf.org/Cocsa1 /Cocsa1.home.html) under the protein ID 175491, 101845, 173198, and 119375, respectively.

Gene replacement and complementation

Single or double *velvet*-complex genes were deleted and replaced by a 2.6-kb fragment carrying a hygromycin phosphotransferase gene (*hph*) or a fragment carrying the neomycin phosphotransferase II gene (*nptII*) using the split-marker system (Catlett et al. 2003). The transformation protocol was the same as previously described by Leng and Zhong (2012). Complementation was conducted with two methods. For complementation of Δ*CsLaeA* and Δ*CsVeA*, the coding region of the corresponding gene was cloned into the pSGATE1-G418-2 vector carrying the *nptII* gene for neomycin resistance (Leng et al. unpublished) using the Gateway cloning system. The constructed vectors containing Cs*LaeA* or Cs*VeA* gene were linearized by BxtXI and SacI digestion, respectively, and transformed into the corresponding single knockout mutant (*ΔCsLaeA9* and *ΔCsVeA9*). For complementation of Δ*CsVelB* and Δ*CsVelC*, a co-transformation method was applied. First, the coding region and flanking sequences containing promoter of the corresponding gene were cloned into the pGEM®-T Easy vector. Second, the constructed T Easy vector and the plasmid G418 carrying the *nptII* gene for neomycin resistance were linearized by NdeI and *Eco*RI digestion, respectively, and then were

co-transformed into the single knockout mutant (*ΔCsVelB3* or *ΔCsVelC2*). The primers used for gene deletion and complementation are listed in Table 2.1. The procedure for Southern blot and PCR confirmation was the same as previously described in Leng and Zhong (2012). The enzymes used for digestion of the wild type genomic DNA were indicated in Appendix A. Sequences of primers for hybridization probe and PCR confirmation are listed in Table 2.1.

Table 2.1. Primers used in this study

Primer	Sequence 5' to 3'	Purpose
CsLaeA-F1	AAACGAGAAACCGCCCTAAT	**Generation of knockout mutants**
CsLaeA-F2-1	CACTGGCCGTCGTTTTACAACGTCGGCGAAAAACTGGTGGTAGA	
CsLaeA-F3	TCATGGTCATAGCTGTTTCCTGTGCGCTAACCTTTGCACCTCTG	
CsLaeA-F4	CCAAAGGGAAGCAAAGAATG	
CsVeA-F1	ACCGAACCCATCAACGTTAC	
CsVeA-F2-1	CACTGGCCGTCGTTTTACAACGTCGCATGGAGGAAGAAGTTTGC	
CsVeA-F3	TCATGGTCATAGCTGTTTCCTGTGTTTTGTCGCGTGATTTACGA	
CsVeA-F4	GGGTATGTTGCGAAGTGGTT	
CsVelB-F1	CTCTCTCGAATCTGCCAACC	
CsVelB-F2-1	CACTGGCCGTCGTTTTACAACGTCTGCTGTCGATCTCGTTGAAA	
CsVelB-F3	TCATGGTCATAGCTGTTTCCTGTGGATTCCCATTCGCAAAGATG	
CsVelB-F4	ACGCGGATCCAAAGTACAAT	
CsVelC-F1	CCAGATACGTACAGGGTCGT	
CsVelC-F2-1	CACTGGCCGTCGTTTTACAACGTCAGTGGATCGAAGGTAGCTGG	
M13F	GACGTTGTAAAACGACGGCCAGTG	
M13R	CACAGGAAACAGCTATGACCATGA	
HY	GGATGCCTCCGCTCGAAGTA	
YG	CGTTGCAAGACCTGCCTGAA	
nptIIF	TGAATGAACTGCAGGACGAG	
nptIIR	AATATCACGGGTAGCCAACG	

Table 2.1. Primers used in this study (continued)

Primer	Sequence 5' to 3'	Purpose
CsLaeA-F0	CCTGACGACATCTACCACGA	**PCR and Southern confirmation**
CsVeA-F0	ACCGAACCCATCAACGTTAC	
CsVelB-F0	CACGATTTTGTTTTCGCAGA	
CsVelC-F0	CACTTATCGCTGTCCTGGTC	
HYG2-R	ATGTTGGCGACCTCGTATT	
nptIIR	AATATCACGGGTAGCCAACG	
SP-LaeA-L	ATCCTCGATGTAGGCTGTGG	
SP-LaeA-R	TGGTTTGAGGTGACTGGACA	
SP-VeA-L	AACCAGCCCCAGTATTCACA	
SP-VeA-R	AGCCAGGGTCGTAGCTGTAA	
SP-VelB-L	CACTATGTCGCCACAACGAT	
SP-VelB-R	ATTCTGCACAACCCACCAAC	
SP-VelC-L	CCAGATACGTACAGGGTCGT	
SP-VelC-R	AGCTCGGAGTATATGCAGGT	
CP-LaeA-F1	GGGGACAAGTTTGTACAAAAAAGCAGGCTCTGT ACCGAATGACGACACG	**Generation of complimented strains**
CP-LaeA-R	GGGGACCACTTTGTACAAGAAAGCTGGGTGTTGT GGTGTCACCGAAATG	
CP-VeA-F1	GGGGACAAGTTTGTACAAAAAAGCAGGCTACCA CAGCCCTACACACACA	
CP-VeA-R	GGGGACCACTTTGTACAAGAAAGCTGGGTCGGT AGCTGCATAGTCGTCA	
CP-CsVelB-F-2	GCACAGGTGATGTGGAGAGA	
CP-CsVelB-R-2	ACGCGGATCCAAAGTACAAT	
CP-CsVelC-F4	TCGATCCATCCAATCCAGCA	
CP-CsVelC-R	TCCTTCCTTTCTTTGTGCGC	
CsNPS1-F1	GTCGACTGCCATCTGGAAAC	
CAN1-F2-2	TGCGGGGTCATCTTAAAAAC	
CsNPS4-RT-F3	ACAGGATCATTGGCCAGTTC	
CsNPS4-RT-R3	AAGGAGGACTTTGGCCATTT	
08856-F	GTGGTGTCATGGCATACGAG	
PKS18F4-KO	AGTGAGGAAGGAGCCATGAA	
RT-Actin-F	GTATGGGCCAAAAGGACTCA	
RT-Actin-R	CACGCAGCTCGTTGTAGAAG	

Assays of oxidative stresses

To evaluate the sensitivity of conidia to oxidative stress, conidia of each fungal strain grown on V8 PDA for 6 days were harvested and plated on MM plates supplemented with different concentrations (0, 1.3 and 2.6 mM) of H2O2, and then incubated at 25 °C for 12 hours before the conidial viability rate was calculated. The conidial viability was calculated as the percentage of viable conidia in the total number of conidia examined. Only those conidia producing hyphae at least 5 times longer than the conidia at 12 hours post-incubation were considered viable. Three replicates were used for each fungal strain and 100 conidia were examined for each replicate.

To evaluate the sensitivity of mycelium to oxidative stress, a small mycelial plug (1 mm × 1 mm) of each fungal strain grown on V8 PDA for 3 days was cut and placed on the center of V8 PDA supplemented with H_2O_2 at final concentrations of 0, 4, 6, and 8 mM. After 7 days of incubation at room temperature, the radial diameter of the fungal colony was measured. Three replicates were used for each strain.

Analysis of conidial productivity, conidiation pattern and conidiophore production

To measure conidial productivity, single conidium of wild type, knockout mutants and the complemented strains were inoculated on the center of V8 PDA plates and allowed to grow for 7 days at 25 °C under constant dark and constant light conditions. Conidia were harvested and quantified as described by Leng and Zhong (2012). The experiments were performed in triplicates.

To investigate the pattern of conidia formation, the conidia were inoculated on the slide culture with MM. After 5 days of growth, conidiation patterns were examined and photographs

were taken using Olympus BX51 microscope (Olympus, Center Valley, PA, USA) with the CCD camera digital imaging system (Diagnostic Instruments, Inc., Sterling Heights, MI, USA) under the 20X magnification.

To measure the conidiophore production, single conidium of wild type and knockout mutant was inoculated on the center of V8 PDA plates and allowed to grow for 7 days at 25 °C under constant dark and constant light conditions, respectively. The number of conidiophores per square centimeter of medium plates (only the conidiation sections were considered for Δ*CsVeA9* and Δ*CsVelB3*) was counted with a dissecting microscope. The conidiophore production of wild type grown under constant dark conditions was used as a reference to calculate the conidiophore productivity rate.

Examination of conidial size and melanin production

To examine the size and pigmentation of conidia, wild type and mutants were grown on V8 PDA under constant dark and constant light conditions for 7 days. Conidia of each strain were harvested and photographed using an Olympus BX51 microscope (Olympus, Center Valley, PA, USA) with the CCD camera digital imaging system (Diagnostic Instruments, Inc., Sterling Heights, MI, USA) under 20X magnification. The average conidial size was calculated based on the area of conidia on the pictures that were measured by the software SigmaScan Pro 5 (Systat Software Inc., San Jose, CA, USA). The average pixel brightness intensities (BI) of the conidia on the pictures were also measured using the SigmaScan Pro 5 software. The pigment intensity (PI) was converted from the pixel brightness intensity using PI = 1/BI.

Spore viability test on barley leaves

To test spore viability on barley leaves, conidia of the wild type, knockout mutants and complemented strains grown on V8 PDA at 25 ºC for seven days were harvested and spray inoculated on 10~12 days old seedlings of barley cv. Bowman (1 mL per leave at 5×10^3 conidia mL^{-1}). The inoculated plants were misted with distilled water and then covered with a black plastic bag to maintain high humidity. After 12 hours of incubation under dark conditions at room temperature (23 ± 2ºC), barley leaves were sampled and examined for spore viability under a compound microscope. The spore viability was calculated as the percentage of viable conidia in the total number of conidia examined. Only those conidia producing hyphae at least 5 times longer than the conidia after 12 hours of incubation on barley leaves were considered viable since the *CsVelB* mutant conidia germinated when they were attached to the conidiophores but they failed to grow on barley leaves. Three replicates (barley leaves) were used for each fungal strain and 100 conidia were examined for each replicate.

Pathogenicity test

Pathogenicity tests were performed by spray inoculation with conidial suspension on 10~12 days old seedlings of barley (cv. Bowman) plants (when the second leaves were fully expended) according to Fetch and Steffenson (1999), except the concentration of the conidial suspension and the sprayed amount per leave was at 1.5×10^3 conidia/mL and 0.5 ml, respectively. Inoculated plants were incubated in a humidity chamber for 20-24 hours, and then transferred into a greenhouse (23 ± 2 °C) and incubated for 7 days before the spot blotch disease was rated using the 1–9 rating scale of Fetch and Steffenson (1999). For each fungal strain, at least nine

plants were used for inoculation and the experiment was repeated three times. The photographs of infected leaves were taken using digital camera (Nikon D80 with lens Af-S Micro NIKKOR 60 mm).

RNA extraction and gene expression analyses

For expression analyses of *PKS18* (Leng et al. 2012), total RNA was extracted from conidia harvested from the culture of each strain grown on V8 PDA under constant dark for 7 days. For expression analyses of the NRPS encoding genes (protein IDs 115356 and 140513), RNA was extracted from a mixture of mycelia harvested from the culture at 96 hai from different media including PDA, MM, V8 PDA, and water agar (sample M96) as well as from inoculated barley leaves at 12, 24, and 48 hours hai on bowman (sample 12hai, 24 hai, and 48 hai). RNA was extracted using SV Total RNA Isolation System (Promega, Madison, WI) and purified by treatment with DNase I (New England Biolabs, Ipswich, MA). cDNA generation and RT-PCR procedure was the same as previously described in Leng and Zhong (2012). The β-actin-encoding gene (ACT) was amplified with the RT-Actin-F and RT-Actin-R primers (Table 2.1) and used as reference in all RNA expression experiments. The primer pairs for each gene used in each analysis are listed in Table 2.1.

Results

Identification of the LaeA, VeA, VelB and VelC orthologs in C. sativus

The candidate orthologs were identified from the draft genome sequence of *C. sativus* (http://genome.jgi-psf.org/Cocsa1/Cocsa1.home.html) through ortholog search using the

BLASTP algorithm with LaeA, VeA, VelB and VelC of *A*. *nidulans* as queries. Based on the highest scores and the lowest E values, four protein sequences were identified and designated as CsLaeA, CsVeA, CsVelB and CsVelC, respectively. The *CsLaeA* gene contains 1,445 base pairs with 7 introns and encodes a protein (368 amino acids) with a highly conserved methyltransferase domain, a characteristic of the *LaeA* genes, as identified using Pfam (http://pfam.xfam. org/search) (Fig. 2.1). The other three genes (*CsVeA*, *CsVelB* and *CsVelC*) contain 1,800, 1,089, and 1,476 base pairs, respectively, and one intron exists in *CsVelC*. The *velvet* domain was identified in all three proteins using Pfam (Fig. 2.1). For CsVeA and CsVelC, a putative monopartite nuclear localization signal (NLS) and bipartite nuclear localization signal (NLS) was identified, respectively, using the cNLS Mapper program (http://nls-mapper.iab.keio.ac.jp/cgi-bin/NLS_Mapper_form.cgi) (Fig. 2.1).

Generation of gene knockout mutants and complemented strains

Knockout mutants were generated for all four genes (*CsLaeA*, *CsVeA*, *CsVelB* and *CsVelC*) and at least three independent deletion mutants as well as one ectopic strain were generated for each of them. By introducing the *velvet*-complex gene back into the corresponding deletion mutant, at least three complemented strains were obtained for each gene. These knockout mutants and complemented strains were confirmed by PCR amplification and Southern blot analyses, although only one from each was selected and presented in this manuscript. Δ*CsLaeA9*, Δ*CsVeA9*, Δ*CsVelB3* and Δ*CsVelC2* were single gene knockout mutants with the corresponding gene deleted, respectively; Δ*CsLaeAVeA2* was a double gene knockout mutant with both *CsLaeA* and *CsVeA* deleted; Δ*CsLaeAVelB3* was a double gene knockout mutant with both *CsLaeA* and

CsVelB deleted; and Δ*CsVelBVeA6* was a double knockout mutant with both *CsVeA* and *CsVelB* deleted. As shown in Appendix A and Appendix B (A), an amplicon was only present in the wild type (ND90Pr) and complemented strains but not in the knockout mutants when the *Csvelvet*-specific primer pair SP-Cs*velvet*-F and SP-Cs*velvet*-R were used for PCR amplification. Using the primer Cs*velvet*-F0 at the flanking region of *Csvelvet* and the primer HYG2-R or nptIIR at the hygromycin resistance gene (*hph*) or the neomycin resistance gene (*nptII*) for PCR, the fragments were only amplified from the knockout mutants but not from the wild type [Appendix B (B)], indicating that *Csvelvet* genes were replaced by *hph* in the single knockout mutants and also by *nptII* in the double gene knockout mutants. The deletion of *Csvelvet* genes in all mutants were further confirmed by Southern blot of the enzyme-digested genomic DNA from the wild type and mutants using the probes amplified from the Cs*velvet* gene encoding sequences using primer pair SP-Cs*velvet*-F and SP-Cs*velvet*-R (Table 2.1). As indicated in Appendix A (E-F), the fragments in the wild type strain and complemented strain were detected while no hybridization signals were observed in the knockout mutants.

Morphology and aerial mycelium growth of mutants on V8 PDA

Under the dark conditions, Δ*CsVeA9* and Δ*CsVelB3* as well as their derived double knockout mutants (Δ*CsLaeAVeA2*, Δ*CsLaeAVelB3*, and Δ*CsVelBVeA6*) showed restricted mycelia growth compared with WT and other mutants on V8 PDA (Fig. 2.2A and Supplemental Fig. 2.3A). Only some specific sections (conidiation sections) of the Δ*CsVeA9* and Δ*CsVelB3* cultures produce conidia under the constant dark conditions (Fig. 2.2A). In addition, the WT, Δ*CsLaeA9* and Δ*CsVelC2* developed long, thick, white aerial mycelia under the constant dark or

light conditions, whereas Δ*CsVeA9* and Δ*CsVelB3* as well as their derived double knockout mutants showed significant reduction in the amount of produced aerial mycelia, leading to a flat surface of the mutants (Fig. 2.2A&B and Supplemental Fig. 2.3A). Complementation with the corresponding genes to the single knockout mutants restored the WT phenotype (data not shown).

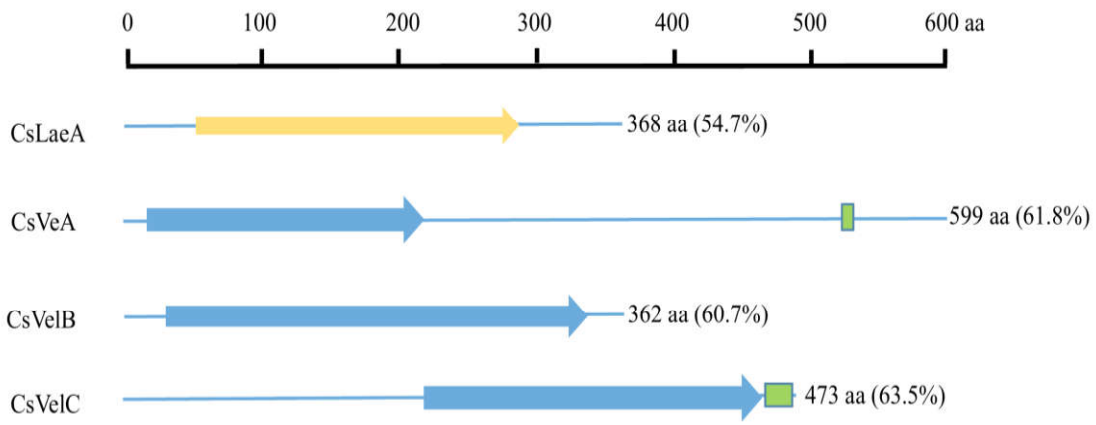

Fig. 2.1. The domain architecture of *velvet*-complex proteins in *C*. *sativus*. The position of the conserved methyltransferase domain for CsLaeA and the *velvet* domain for *velvet* proteins (CsVeA, CsVelB, and CsVelC) are indicated by yellow and blue arrows, respectively. The putative nuclear localization signals (NLS) are indicated by green pentagons in CsVeA and CsVelC. The amino acid lengths are noted on the right of each protein. The percentage identity between the proteins in *C*. *sativus* and *A*. *nidulans*. was indicated in parentheses.

Velvet-complex genes regulate responses to oxidative stress

Except for the *CsVelC* knockout mutants, the conidia of other *velvet*-complex geneknockout mutants exhibited different levels of reduction in tolerance to H_2O_2 stress than those of WT (Fig. 2.3A). The conidia of *CsVelB* knockout mutants (Δ*CsVelB3*, Δ*CsLaeAVelB3* and Δ*CsVelBVeA6*) were more sensitive to H_2O_2 stress than those of *CsLaeA* and *CsVeA* mutants (Δ*CsLaeA9*, Δ*CsVeA9* and Δ*CsLaeAVeA2*). We also investigated the sensitivity of mycelia to oxidative stress.

As indicated in Fig. 2.3B, the mycelia of *velvet*-complex knockout mutants (except Δ*CsVelC* mutants) exhibited slower growth at the same concentration of H_2O_2 compared to the WT. However, in contrast to conidia, the mycelia of *CsLaeA* mutants (Δ*CsLaeA9*, Δ*CsLaeAVeA2* and Δ*CsLaeAVelB3*) were more sensitive to oxidative stress than those of *CsVeA* and *CsVelB* mutants (Δ*CsVeA9*, Δ*CsVelB3* and Δ*CsVelBVeA6*). The *CsLaeA* mutants were completely inhibited for growth on PDA with 6mM of H_2O_2 whereas the *CsVeA* and *CsVelB* mutants stopped the growth on PDA with 8mM of H_2O_2 (Fig. 2.3B).

Velvet-complex genes regulate conidia production and conidiogenesis pattern

Under constant dark conditions, Δ*CsVeA9* and Δ*CsVelB3* as well as their derived double knockout mutants (Δ*CsLaeAVeA2*, Δ*CsLaeAVelB3*, and Δ*CsVelBVeA6*) showed a significant increase in conidial production (Fig. 2.4A), whereas the *CsLaeA* and *CsVelC* mutants produced similar amount of conidia compared to WT. In contrast, under constant light conditions, Δ*CsLaeA9*, Δ*CsVeA9* and Δ*CsVelB3* mutants were significantly decreased in conidial production. The derived double knockout mutants (Δ*CsLaeAVeA2,* Δ*CsLaeAVelB3,* and Δ*CsVelBVeA6*) produced similar amount of conidia as the *CsLaeA* mutant. Δ*CsVelC*2 produced similar amount of conidia just like WT (Fig. 2.4A). In addition, all mutants except Δ*CsVelC2* produced more conidia under constant dark conditions than under constant light conditions (Fig. 2.4A).

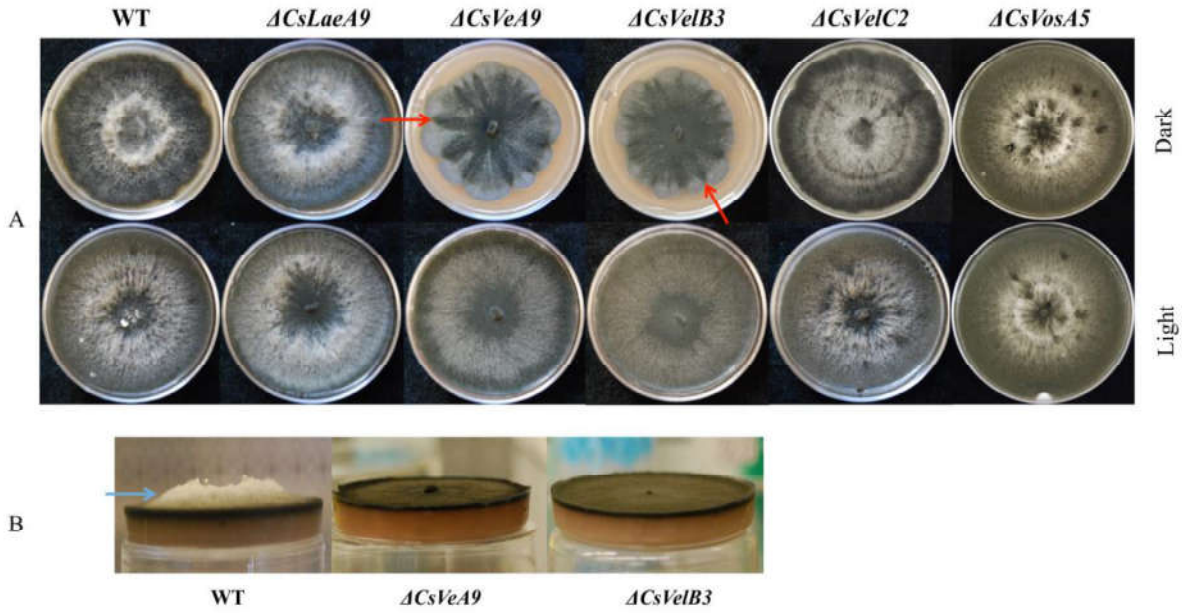

Fig. 2.2. *CsVeA* and *CsVelB* influence the culture morphology and aerial mycelial growth. **A.** Cultures of wild type (WT) and five single gene knockout mutants grown on V8 PDA under constant dark and constant light conditions. The conidiation sections of Δ*CsVeA9* and Δ*CsVelB3* was indicated by red arrows. **B.** Side view of plate cultures of WT strain and two knockout mutants (Δ*CsVeA9* and Δ*CsVelB3*) grown under constant light conditions on V8 PDA. The long, thick white aerial mycelia (indicated by blue arrow) were observed in WT, but not in the mutants.

Further examination of conidiogenesis indicated that significant differences in conidiophore production were observed between wild type and the mutants under the constant dark and light conditions (Table 2.2). Especially for the *CsVeA* and *CsVelB* mutants, the conidiophore production was significantly increased under constant dark conditions and significantly decreased under constant light conditions. More interestingly, the *CsVelB* mutant exhibited conidiation pattern different from WT. The wild type and other mutants (Δ*CsLaeA9*, Δ*CsVeA9* and Δ*CsVelC*2) produced 3-5 conidia on a conidiophore in a sympodial fashion, while Δ*CsVelB3* had conidiophores with multiple chains of conidia with the oldest conidium at the base and the youngest one emerging at the tip of the spore chain (Fig. 2.4B), as reported for Δ*CsVosA5* in Wang et al. (2015)

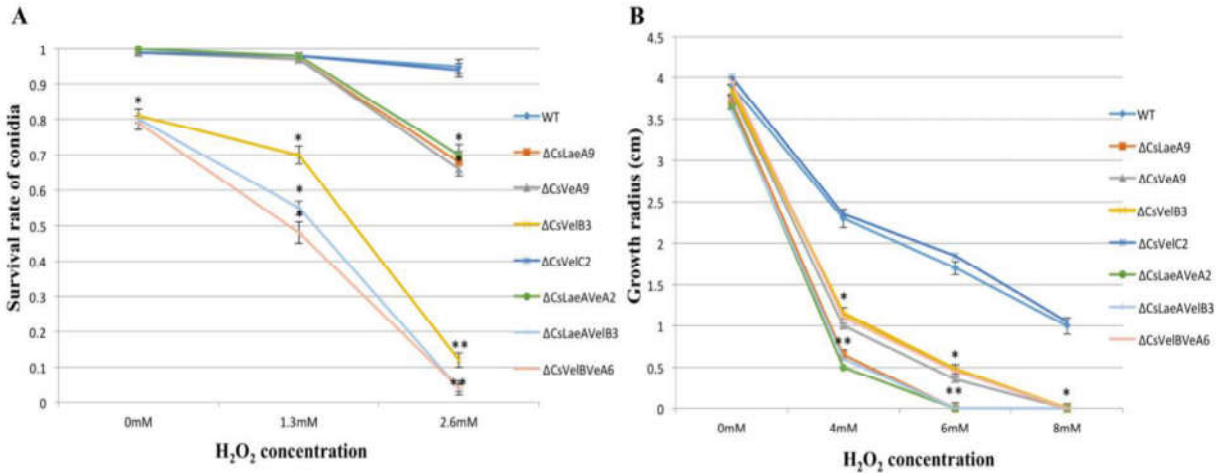

Fig. 2.3. Tolerance of wild type and *velvet*-complex gene knockout mutants to H_2O_2 stress. **A.** Conidia of each fungal strain were harvested from cultures grown at 25 °C for 6 days on V8 PDA plates, plated on MM plates containing H_2O_2 at different concentrations (0, 1.3 and 2.6 mM) and incubated at 25 °C for 12 hours before examination for viability under a microscope. Error bars indicate the standard deviation. **B.** Mycelia plug of each fungal strain harvested from cultures grown at 25 °C for 3 days on V8 PDA plates, were plated on MM plates containing different H_2O_2 concentrations (0, 4, 5, 6 and 8 mM) and incubated at 25 °C for 6 days before culture radius was measured. Error bars indicate the standard deviation. Single asterisks in A and B indicate p-value <0.05, double asterisks in A and B indicate p-value <0.001 in T-test analyses in which each strain was compared with corresponding wild type at the same H_2O_2 concentration.

Table 2.2. Conidiophore productivity of wild type and knockout mutants under different light conditions

Strains	**Conidiophore production (%)**	
	Constant dark	**Constant light**
WT	100	94 ± 4.1
Δ*CsLaeA9*	90 ± 4.7*	32 ± 3.3*
Δ*CsVeA9*	685 ± 24.4**	57 ± 5.3*
Δ*CsVelB3*	468± 20.6**	52 ± 3.7*
Δ*CsVelC2*	96 ± 2.3	98 ± 1.1

Single conidium of wild type and mutant strains were inoculated on the centers of V8 PDA plates and allowed to grow for 7 days at 25 °C under constant dark and constant light conditions. The number of conidiophores per square centimeter of medium plates (only the conidiation sections were considered for Δ*CsVeA9* and Δ*CsVelB3*) was counted with a dissecting microscope. The conidiophore production of wild type grown under constant dark conditions was used as a reference (100%) to calculate the conidiophore productivity rate. Single asterisks indicate p-value <0.05, double asterisks indicate p-value <0.001 in T-test analysis when each isolate was compared with WT under constant dark conditions.

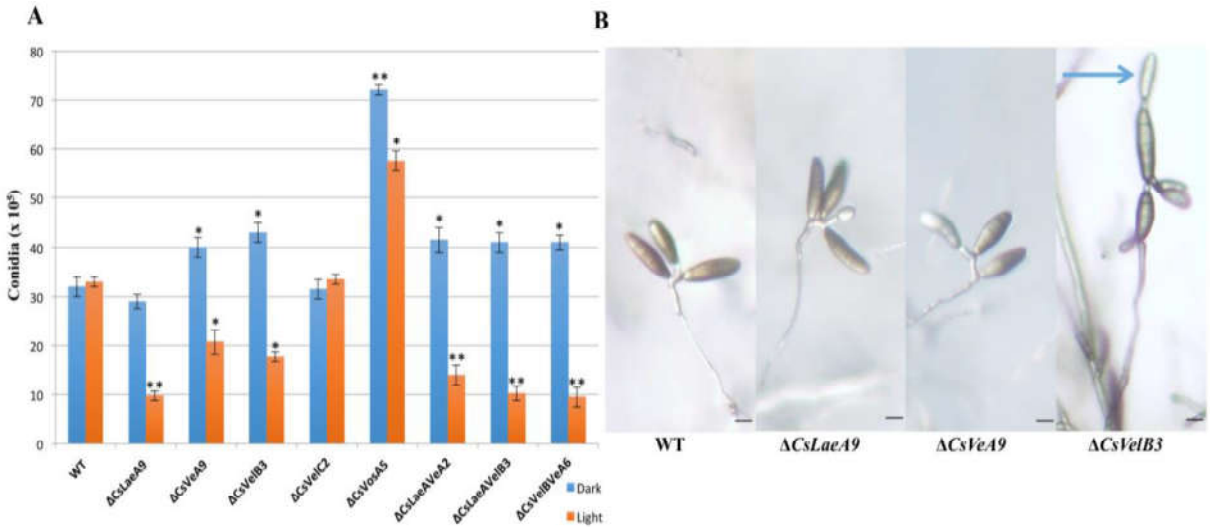

Fig. 2.4. Conidial productivity and conidial developmental processes in *C. sativus* strains. **A.** Conidial productivity of wild type and knockout mutants. The strains were grown on V8 PDA plates at 25 °C under constant dark and light conditions for 7 days, and then the conidia were harvested and quantified. Error bars indicate the standard deviation. Single asterisks indicate p-value <0.05, double asterisks indicate p-value <0.001 in T-test analyses in which each strain was compared with corresponding wild type under the same condition. **B.** Conidial developmental processes in *C. sativus* strains. Conidiogenesis patterns were examined under a light microscope. The blue arrow points to a new emerging conidium on the head of the older conidium. Note that wild type produces conidia in a traditional sympodial pattern whereas the *CsVelB* mutant generates conidia through both sympodial and acropetal patterns. Bars = 20 µm.

Velvet-complex genes regulate conidial morphology

The conidia of mutants (except Δ*CsVelC2*) differed from those of WT in size, shape, septa production and compartmentalization [Fig. 2.5 and Appendix C (B)]. The wild type strain (ND90Pr) and *CsVelC* mutant produced normal sized conidia measured at 15-28 × 80-120 µm (area value 3,000~4,500 in SigmaScan software) with 4-8 septa, and having very few small sized conidia measured at 7-14 × 15-30 µm (area value 500~1,500 in SigmaScan software) with 0-1 septa under constant dark and constant light conditions (Table 2.3). However, the knockout mutants for *CsLaeA*, *CsVeA*, and *CsVelB* produced much more small conidia under constant dark and/or constant light conditions, compared to WT (Table 2.3). Similar to the *CsVosA* mutant,

Δ*CsVelB3* also produced some large conidia measured at 20-30 x 120-200 μm (area value 8,000~10,000 in SigmaScan software), but only under constant light conditions (data not shown).

The WT conidia of *C*. *sativus* would not germinate when they were attached to the conidiophores. However, conidia of Δ*CsVelB3* and its derived double knockout mutants (Δ*CsLaeAVelB3* and Δ*CsVelBVeA6*) germinated even when they were still attached to the conidiophores [Fig. 2.5 and Appendix C (B)]. This indicates that *CsVelB* is involved in regulating spore dormancy.

Velvet-complex genes regulate pigmentation

As showed in Fig. 2.6A, all single gene knockout mutants except for Δ*CsVelC2* showed different levels of reduction in pigmentation, with Δ*CsVelB3* and its derived double knockout mutants (Δ*CsLaeAVelB3* and Δ*CsVelBVeA6*) showing the highest level of reduction. Δ*CsVeA9* and double knockout mutant Δ*CsLaeAVeA2* had a similar level of reduction in pigmentation. To investigate if the *velvet*-complex genes affect the expression of *PKS18*, the gene involved in biosynthesis of melanin in *C*. *sativus* (Leng et al. 2011), mRNA levels of *PKS18* in WT and five single knockout mutants were examined using quantitative real time PCR. The results showed that *PKS18* expression was down regulated in the mutant conidia (Fig. 2.6B), consistent with the pigment intensity levels measured by SigmaScan Pro 5 (Fig. 2.6A).

Table 2.3. Percentage of small sized conidia of wild type and knockout mutants under different light conditions

	Dark	Light
WT	6.4 ± 1.1	8.1 ± 2.0
Δ*CsLaeA9*	53.4 ± 3.1**	6.3 ± 0.8
Δ*CsVeA9*	79.6 ± 9.2**	29.3 ± 2.9**
Δ*CsVelB3*	45.5 ± 5.4**	27.4 ± 5.3**
Δ*CsVelC2*	5.0 ± 0.8	4.4 ± 2.1
Δ*CsVosA5*	29.0 ± 4.3**	14.0 ± 2.2*
Δ*CsLaeAVeA2*	86.4 ± 6.9**	25.4 ± 4.7**
Δ*CsLaeAVelB3*	82.6 ± 8.6**	20.3 ± 3.1**
Δ*CsVelBVeA6*	92.8 ± 8.3**	28.1 ± 2.2**

Percentage of small sized conidia of wild type and knockout mutants under different conditions. Normal sized conidia were measured at 15-28 × 80-120 μm (area value 3000~4500 in SigmaScan software) with 4-8 septa, whereas the small sized conidia were measured at 7-14 × 15-30 μm (area value 500~1500 in SigmaScan software) with 0-2 septa. Single asterisks indicate p-value <0.05, double asterisks indicate p-value <0.001 in T-test analysis when each isolate was compared with WT under constant dark or constant light conditions.

Roles of *velvet*-complex genes in pathogenicity and virulence

WT and all mutants produced spot blotch symptoms on Bowman (Fig. 2.7A). However, the virulence of Δ*CsVeA9* and Δ*CsVelB3* was significantly reduced while the virulence of the Δ*CsLaeA9* and Δ*CsVelC2* strains was slightly reduced as compared to the wild type. The virulence of the double knockout mutants (Δ*CsLaeAVeA2* and Δ*CsLaeAVelB3*) were slightly lower than or similar to the virulence observed for the single gene knockout mutants (Δ*CsVeA9* and Δ*CsVelB3*) while the double knockout mutant Δ*CsVelBVeA6* was the lowest in virulence compared to all other gene knockout mutants (Fig. 2.7A and B). The complemented strains for each of single gene knockout mutants restored the virulence to WT (data not shown).

To determine which stage of the disease development is affected by *velvet*-complex genes, the viability of WT and mutants conidia inoculated on leaves of Bowman were examined under a

microscope. The results showed that the viability of conidia from Δ*CsVelB3* and its derived double knockout mutants was significantly lower than conidia of WT while no significant differences were observed between WT and other mutants along with the complemented strain for Δ*CsVelB3* on barley leaves (Fig. 2.7C).

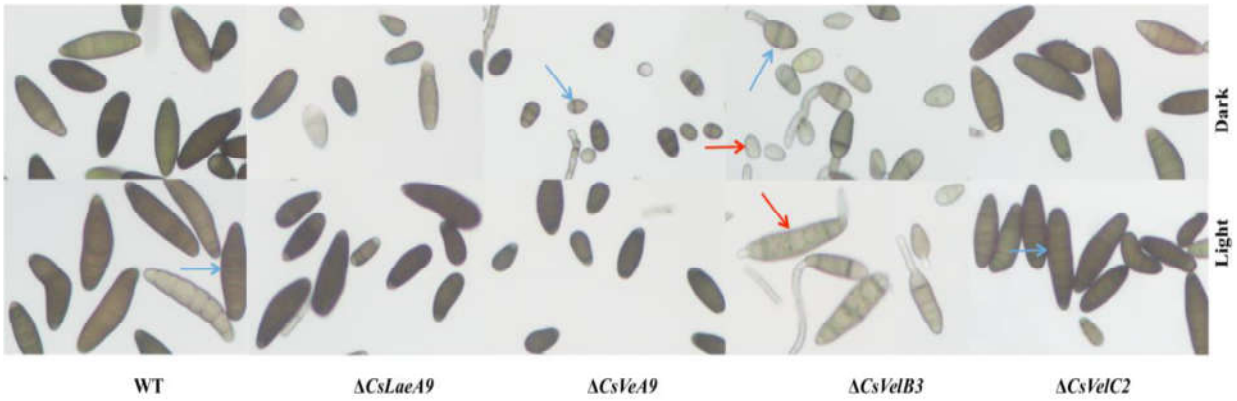

Fig. 2.5. Conidial morphology of wild type and knockout mutants. The strains were grown on V8 PDA plates at 25 °C under constant dark and light conditions for 7 days, and then the conidia were harvested and photographed using Olympus BX51 microscope (Olympus, Center Valley, PA, USA) with the CCD camera digital imaging system (Diagnostic Instruments, Inc., Sterling Heights, MI, USA) under 20X magnification. The septa are indicated by blue arrows, and the unnormalized compartments are indicated by red arrows.

To investigate whether the *velvet*-complex regulates the two *NRPS* genes (protein IDs 115356 and 140513) required for high virulence of isolate ND90Pr on Bowman (Condon et al. 2013), their mRNA expression levels were measured in WT and the *velvet*-complex single gene knockout mutants at different time points during host infection. The results indicated that the two *NRPS* genes had the lowest levels of expression in Δ*CsVeA9* and Δ*CsVelB3* whereas their expression levels in Δ*CsLaeA9* and Δ*CsVelC2* were only slightly reduced (Fig. 2.8A and B), consistent with the disease ratings.

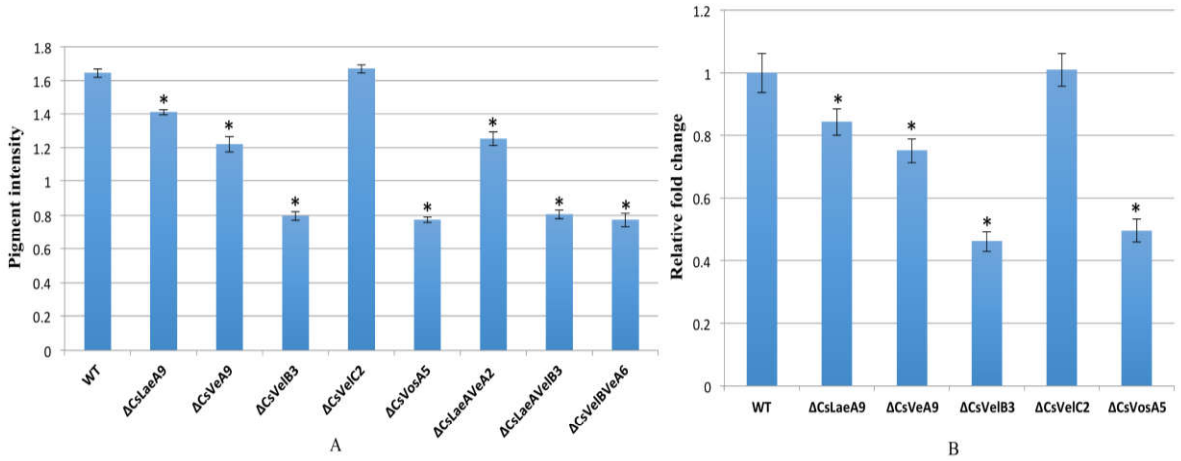

Fig. 2.6. *Velvet*-complex genes positively regulate conidial pigmentation of *C*. *sativus*. **A.** The strains were grown on V8 PDA plates at 25 °C under constant dark for 7 days, and then the conidia were harvested and photographed using Olympus BX51 microscope (Olympus, Center Valley, PA, USA) with the CCD camera digital imaging system (Diagnostic Instruments, Inc., Sterling Heights, MI, USA) under 20X magnification. The software SigmaScan Pro 5 was used to estimate the color intensity of the conidia that represent the conidial melanin content. Error bars indicate the standard deviation. Single asterisks indicate p-value <0.05 in T-test analyses in which each isolate was compared with WT. **B.** RNA expression analysis of *PKS18* in conidia. The RNA was extracted from conidia harvested from the culture grown on V8 PDA under constant dark conditions at 7 days after plating for each strain. Expression level relative to the sample of WT strain is shown. Error bars represent range of fold change calculated according to standard deviation of ΔΔCt. Single asterisks indicate p-value <0.05 in T-test analyses in which each isolate was compared with WT.

Discussion

The LaeA protein and *velvet* proteins are highly conserved among various fungi and they have been identified in many plant fungal pathogens (Bayram and Braus 2012). In this study, we identified CsLaeA, CsVeA, CsVelB and CsVelC in the cereal fungal pathogen *C*. *sativus*, which contain the methyltransferase domain and the *velvet* domain, respectively, indicating they are candidate orthologs of the LaeA and *velvet* proteins. The nuclear localization signals (NLSs) identified in CsVeA and CsVelC support their possible functions as transcription factors (Ahmed et al. 2013). Although the NLS was not identified in CsVelB, the transportation of CsVelB into

nuclei may depend on the formation of heterodimers with CsVeA protein, as indicated in *A. nidulans* (Bayram et al. 2008).

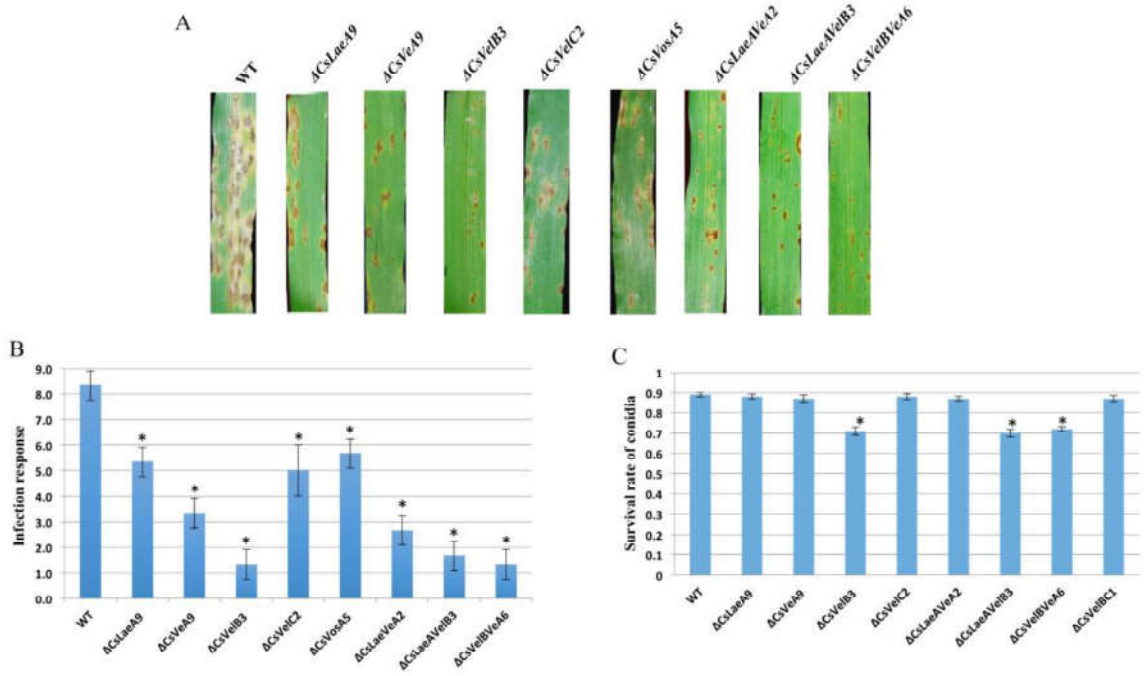

Fig. 2.7. Pathogenicity tests of wild type (WT) and gene knockout mutants on barley cv. Bowman. **A.** Disease symptoms after spray-inoculation with conidia of the wild type and gene knockout mutants. The photographs were taken at 7 days after inoculation (DAI). **B.** Disease infection responses caused by each fungal strain on Bowman. For each fungal strain, the second leaves of 9 inoculated plants were rated at 7 DAI using a 1-9 scale developed by Fetch and Steffenson (1999). Error bars indicate the standard deviation. An asterisk represents p-value <0.05 in T-test analysis when each isolate was compared with wild type. **C.** Conidial viability of WT and mutants on barley leaves. The viability was calculated as percentage of viable conidia in the total number of conidia examined at 12 hours after inoculation. Error bars indicate the standard deviation. Asterisk represents p-value <0.05 in T-test analysis when each isolate was compared with WT.

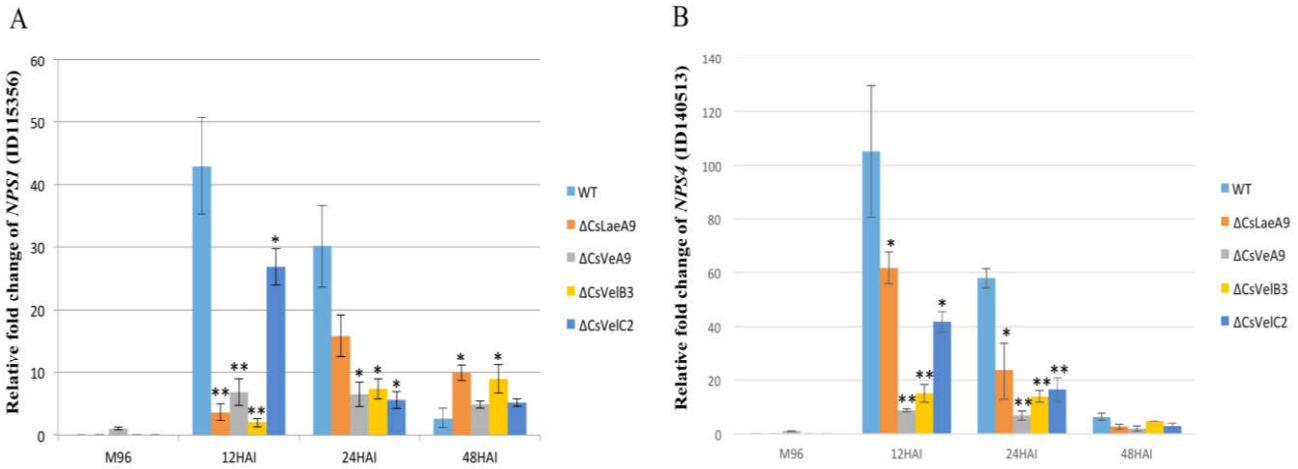

Fig. 2.8. RNA expression analyses of the two genes *NPS1* (ID 115356) and *NPS4* (ID 140513) involved in virulence on barley cv. Bowman. **A.** RNA expression analyses of *NPS1* (ID 115356) during infection of barley cv. Bowman. Expression levels relative to the sample M96 from WT is shown. Error bars represent range of fold change calculated according to standard deviation of ΔΔCt. The expression of the β-actin-encoding gene (*ACT*) was used as a reference. Single asterisks indicate p-value <0.05, double asterisks indicate p-value <0.001 in T-test analyses in which each isolate was compared with corresponding wild type at the same sample type. **B.** RNA expression analyses of *NPS4* (ID 140513) during infection of barley cv. Bowman. Expression levels relative to the sample M96 from WT is shown. Error bars represent range of fold change calculated according to standard deviation of ΔΔCt. The expression of the β-actin-encoding gene (*ACT*) was used as a reference. Single asterisks indicate p-value <0.05, double asterisks indicate p-value <0.001 in T-test analyses in which each isolate was compared with corresponding wild type at the same sample type. All experiments were repeated at least three times.
Sample M96: RNA was extracted from a mixture of mycelia harvested from the culture at 96 hours after inoculation from different media including PDA, MM, V8 PDA, and water agar
Sample 12hai: RNA was extracted from the inoculated barley leaves at 12 hai on Bowman
Sample 24hai: RNA was extracted from the inoculated barley leaves at 24 hai on Bowman
Sample 48hai: RNA was extracted from the inoculated barley leaves at 48 hai on Bowman

Previous studies show that LaeA, VeA, and VelB were positively involved in regulating the growth of aerial mycelia. For example, no or few aerial mycelial growth was observed on the cultural surface of the *VeA* knockout mutant of *Mycosphaerella graminicola* (Choi and Goodwin 2011), the *LaeA* and *VeA* mutants of *C. heterostrophus* (Wu et al. 2012) and *Penicillium citrinum* (Baba et al. 2012), the *LaeA*, *VeA* and *VelB* knockout mutants of *F. oxysporum* (Lopez-Berges et al. 2013), and the *VeA* and *VelB* mutants of *Fusarium graminearum* (Jiang et al. 2011; Lee et al.

2012). Similarly, we showed that deletion of *CsVeA* and *CsVelB* led to abolishment of the aerial mycelia growth under both constant dark and light conditions. However, the *CsLaeA* and *CsVelC* knockout mutants produced the similar amount of aerial mycelia as the wild type, suggesting they are not involved in this process in *C*. *sativus*. In addition, the phenotypes of the *LaeA* plus *VeA* or *VelB* double knockout mutants were the same as the Δ*CsVeA* or Δ*CsVelB*, suggesting *CsVeA* and *CsVelB* are epistatic to *CsLaeA* in regulation of aerial mycelial growth.

Reactive oxygen species (ROS) play key roles in plant-pathogen interactions and thus we tested the sensitivities of each knockout mutant to oxidative stress at both conidia and mycelia stage. It is observed that the conidia and mycelia of Δ*CsLaeA*, Δ*CsVeA*, and Δ*CsVelB* were hypersensitive to oxidative stress mediated by H_2O_2, indicating these genes are required to provide the protection from oxidative damage by ROS. Interestingly, the major genes involved in responses to the oxidative stress are different in conidia and mycelia. Based on the results listed in Fig. 2.3, *CsVelB* mainly regulates the sensitivity to oxidative stress in conidia while *CsLaeA* is mainly involved in mycelial responses to the oxidative stress; *CsVeA* plays less important role in this process. The molecular mechanisms underlying these changes and differences are unknown in *C*. *sativus*. In *C*. *heterostrophus*, the expression of CAT3, one of three catalases in the genome central to decomposition of H_2O_2, was regulated by *lae1* (*ChLaeA*), *vel1* (*ChVeA*), *vel2* (*ChVelB*), and *vos1* (*ChVosA*) genes. The *velvet*-complex genes in *C*. *sativus* may have similar functions in controlling the expression of CAT3, but further studies are needed.

The *velvet*-complex genes negatively or positively regulate conidia production in various fungal species. For example, *VeA* in *A*. *nidulans* negatively regulated conidiation whereas *VelB* positively regulated this process in *A*. *nidulans* (Kim et al. 2002; Park et al. 2012). In addition, *FgVe1* and *FfVel1* positively regulate conidiation in *F*. *graminearum* (Merhej et al., 2012) and *F*.

fujikuroi (Wiemann et al., 2010), respectively. In *M*. *oryzae*, *MoVEA*, *MoVELB* and *MoVELC* positively regulate conidia production (Kim et al. 2014). In *P*. *chrysogenum*, *velvet*-complex genes are known to play functionally opposing roles in conidiation: *PcVelA* and *PcVelC* inhibits conidiation while *PcLaeA*, *PcVelB* and *PcVosA* promote conidiation (Kopke et al., 2013). In *C*. *sativus*, *CsVosA* was found to suppress conidia production (Wang et al. 2015). In this study, we showed that *CsLaeA*, *CsVeA*, and *CsVelB* positively regulated conidial production under light conditions. However, interestingly, under dark conditions, *CsVeA*, and *CsVelB* negatively regulated conidia production. To our knowledge, this is the first report to show that the same *velvet* gene plays opposing roles under different light conditions in the same fungus.

Light plays important role in balancing between asexual and other differentiation processes in various fungi. In *A*. *nidulans*, sexual development is induced under dark conditions and repressed under light conditions, while asexual sporulation is regulated in a contrasting way in response to a light/dark signal (Bayram et al. 2008; Bayram et al. 2010). In addition, the differentiation processes in *Botrytis cinerea* are strictly regulated by the light regime: dark conditions promote sclerotial development while light induces conidiation (Schumacher et al. 2012). Similar light regulations were observed in *C*. *heterostrophus* and *P*. *chrysogenum*: these two fungi produce much more conidia under light than under dark conditions, indicating light promotes the conidiation (Wu et al. 2012; Kopke et al. 2013). The molecular mechanism underlying this light regulation can be partly explained by the regulatory function of VeA in these fungi. In *A*. *nidulans*, VeA is transferred to the nucleus only under the dark to turn on genes involved in sexual development. Deletion of VeA suppresses the sexual development and promotes the asexual development (Bayram et al. 2008; Bayram et al. 2010). In *B*. *cinerea,* deletion of the VeA uncouples the developmental program (sclerotial development and

conidiation) from this light control, making the *BcVeA* mutant produce more conidia than wild type under both light and dark conditions. Similarly, deletion of VeA and VelB in *C. heterostrophus* produced more conidia than wild type under dark and light conditions (Wu et al. 2012). For *C. sativus*, the light regulation through VeA in wild type was absent and the wild type produces the same amount of conidia under both dark and light conditions. However, deletion of VeA induces the light response and leads to production of significantly different numbers of conidia under dark and light conditions. We speculate that there is another protein that can sense the lights and regulate conidiation in *C. sativus* but is suppressed by VeA in the wild type. When VeA was deleted, this protein was activated to sense the light and regulate the conidiation, resulting in differences in conidial production under different light conditions. However, the exact molecular mechanism is not known and more studies are needed to better understand the conidiation process and the light regulation in this fungus.

In *Cochliobolus* species, conidiogenesis follows a sympodial fashion in which 3 to 5 conidia are normally produced by an expansion and swelling of the apex of the conidiophore. In this pattern, all produced conidia were attached on the conidiophore. This pattern was observed in wild type and the three mutants, Δ*CsLaeA9*, Δ*CsVeA9* and Δ*CsVelC*2. However, both sympodial and acropetal conidiation patterns were observed in *CsVelB* knockout mutant, like the *CsVosA* knockout mutant (Wang et al. 2015), in which the new conidia were produced on the tips of older conidia, formed on the apex of the conidiophore. These results suggest that *CsVelB* and *CsVosA* suppress the acropetal conidiogenesis pattern in *C. sativus* whereas the other *velvet*-complex genes are independent for this process.

Previous studies showed that *velvet*-complex proteins regulate melanin production in various fungi. For example, LaeA in *C. heterostrophus* represses the production of mycelial

melanin (Wu et al. 2012). VeA positively regulates melanin biosynthesis in mycelia of *Mycosphaerella graminicola* (Choi and Goodwin 2011), but negatively controls mycelial melanin production in *C*. *heterostrophus* (Wu et al. 2012) and *Fusarium fujikuroi* (Wiemann et al. 2010). VosA in *C*. *sativus* negatively regulates the mycelial melanin production but positively regulate the conidial melanin production (Wang et al. 2015). In this study, we found that conidial pigmentation (most likely due to production of melanin) and the expression levels of *PKS18*, the gene involved in biosynthesis pathway of melanin in *C*. *sativus* (Leng et al. 2012), were decreased in the *CsLaeA*, *CsVeA*, and *CsVelB* knockout mutants, suggesting that these three genes positively control melanin production in conidia of *C*. *sativus*, probably by regulating the expression of genes involved in melanin biosynthesis. Our results indicate the *CsVelB* and *CsVosA* play more important roles in regulating melanin production of conidia than *CsLaeA* and *CsVeA*.

Our pathogenicity tests indicated that deletion of each of the four genes (*CsLaeA*, *CsVeA*, *CsVelB* and *CsVelC*) led to a significant reduction in virulence of the mutants on barley plants. Since the appressorium production and infection structure formation were not impacted in the mutants (data not shown), the reduced virulence is probably due to the decreased expression of the two genes for NRPSs involved in biosynthesis of an unknown secondary metabolite, which is required for high virulence on barley Bowman (Condon et al. 2013; Leng and Zhong, unpublished). Previous studies have shown that LaeA (Bok and Keller, 2004; Perrin et al., 2007) and the *velvet* proteins promote transcription of NRPS genes. For example, expression of NRPS (NRPS2/sidE) for biosynthesis of a putative siderophore was greatly reduced in the Δ*laeA* mutant of *Aspergillus fumigatus* under inducing iron-deficient conditions (Perrin et al., 2007). In *F*. *oxysporuma*, the LaeA, VeA, and VelB proteins play important roles in biosynthesis of three

secondary metabolites, ferricrocin, triacetylfusarinine C and beauvericin (BEA), which are synthesized by NRPSs (Lopez-Berges et al. 2013). Our previous study also showed that *CsVosA* positively regulates the two NRPS-encoding genes involved in virulence in *C. sativus* (Wang et al. 2015). These data indicate the conserved function of *velvet*-complex proteins in this process. In our study, it was also observed that the Δ*CsVeA* and Δ*CsVelB* and their derived double knockout mutants were most significantly reduced in virulence and in expression of the NRPS genes, suggesting that these two genes are mainly involved in regulating the virulence.

In summary, the *velvet*-complex proteins can coordinately and independently regulate the fungal development and secondary metabolism of the fungal cereal pathogen *C. sativus*. The working model of *velvet*-complex proteins is illustrated in Fig. 2.9. In regulating aerial mycelia growth, only CsVeA and CsVelB are involved. The conidiogenesis pattern, trehalose production (data not shown) and spore dormancy are only regulated by *CsVelB* and *CsVosA*. However, all the *velvet*-complex proteins were coordinately involved in virulence probably through regulation of the NRPS genes, although CsVeA and CsVelB make more contributions to this process than *CsLaeA* and *CsVelC*.

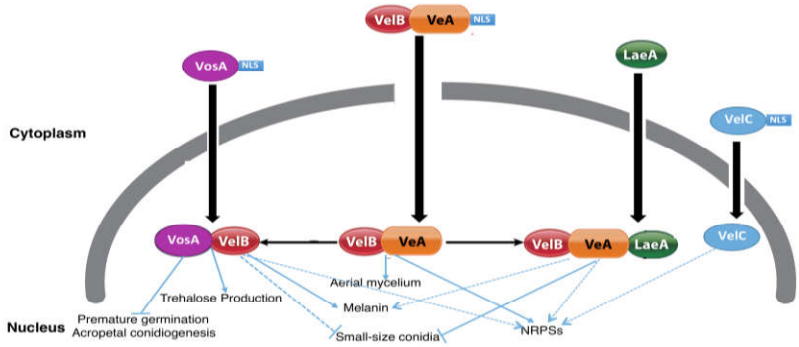

Fig. 2.9. Working model of *velvet*-complex proteins in *C. sativus*. The solid lines indicate the major promotion or suppression effects of proteins whereas the dotted lines indicate the minor effects.

Acknowledgements

This study was partially supported by the Triticeae-CAP project (2011-68002-30029) from the US Department of Agriculture National Institute of Food and Agriculture. The authors thank Dr. Justin D. Faris and Dr. Timothy F. Friesen for supplying equipment and facilities for the Southern blot analysis. We also thank Dr. Xiwen Cai for providing help in microscopic observation of the fungal infection structures. The sequence data of the *C*. *sativus* strain ND90Pr were produced and provided by the US Department of Energy Joint Genome Institute (http://genome.jgi.doe.gov/Cocsa1/Cocsa1.home.html).

References

Ahmed, Y. L., Gerke, J., Park, H. S., Bayram, Ö., Neumann, P., Ni, M., Dickmanns, A., Kim, S. C., Yu, J. H., Braus, G. H., and Ficner, R. 2013. The velvet family of fungal regulators contains a DNA-binding domain structurally similar to NF-κB. PLoS Biol. 11:e1001750.

Amaike, S., and Keller, N. P. 2009. Distinct roles for VeA and LaeA in development and pathogenesis of *Aspergillus flavus*. Eukaryot. Cell 8:1051-1060.

Baba, S., Kinoshita, H., and Nihira, T. 2012. Identification and characterization of *Penicillium citrinum* VeA and LaeA as global regulators for ML-236B production. Curr. Genet. 58:1-11.

Bayram, O., and Braus, G. 2012. Coordination of secondary metabolism and development in fungi: the velvet family of regulatory proteins. FEMS Microbiol. Rev. 36:1-24.

Bayram, O., Krappmann, S., Ni, M., Bok, J., Helmstaedt, K., Valerius, O., Braus-Stromeyer, S., Kwon, N., Keller, N., Yu, J., and Braus, G. 2008. VelB/VeA/LaeA complex coordinates light signal with fungal development and secondary metabolism. Science 320:1504-1506.

Bayram, O. S., Bayram, O., Valerius, O., Park, H. S., Irniger, S., Gerke, J., Ni, M., Han, K. H., Yu, J. H., and Braus, G. H. 2010. LaeA control of velvet family regulatory proteins for light-dependent development and fungal cell-type specificity. PLoS Genet. 6: e1001226

Beck, E., Ludwig, G., Auerswald, E.A., Reiss, B., Schaller, H. 1982. Nucleotide-sequence and exact localization of the neomycin phosphotransferase gene from transposon TN5. Gene 19:327-336.

Bok, J. W., and Keller, N. P. 2004. LaeA, a regulator of secondary metabolism in *Aspergillus* spp. Eukaryot. Cell 3:527-535.

Borgia, P., Miao, Y., Dodge, C. 1996. The *orlA* gene from *Aspergillus nidulans* encodes a trehalose-6-phosphate phosphatase necessary for normal growth and chitin synthesis at elevated temperatures. Mol. Microbiol. 20:1287-1296.

Braun, E. J., and Howard, R. J. 2015. Adhesion of fungal spores and germlings to host plant surfaces. Protoplasma 181:202-212

Catlett, N. L., Lee, B.-N., Yoder, O. C., and Turgeon, B. G. 2003. Split-marker recombination for efficient targeted deletion of fungal genes. Fungal Genet. Newsl. 50:9–11.

Chang, P. K., Scharfenstein, L. L., Li, P., Ehrlich, K. C. 2013. *Aspergillus flavus* VelB acts distinctly from VeA in conidiation and may coordinate with FluG to modulate sclerotial production. Fungal Genet. Biol. 58-59:71-79.

Choi, Y. E., and Goodwin, S. B. 2011. MVE1, encoding the velvet gene product homolog in *Mycosphaerella graminicola*, is associated with aerial mycelium formation, melanin biosynthesis, hyphal swelling, and light signaling. Appl. Environ. Microb. 77:942-953.

Condon, B., Leng, Y., Wu, D., Bushley, K., Ohm, R., Otillar, R., Martin, J., Schackwitz, W., Grimwood, J., MohdZainudin, N., Xue, C., Wang, R., Manning, V., Dhillon, B., Tu, Z., Steffenson, B., Salamov, A., Sun, H., Lowry, S., LaButti, K., Han, J., Copeland, A., Lindquist, E., Barry, K., Schmutz, J., Baker, S., Ciuffetti, L., Grigoriev, I., Zhong, S., and Turgeon, B. 2013. Comparative genome structure, secondary metabolite, and effector coding capacity across *Cochliobolus* pathogens. PLoS Genet. 9:e1003233.

Duran, R. M., Cary, J. W., and Calvo, A. M. 2009. The role of VeA in *Aspergillus flavus* infection of peanut, corn and cotton. TOMYCJ. 3:27-36.

Fetch, T. G., and Steffenson, B. J. 1999. Rating scales for assessing infection responses of barley infected with *Cochliobolus sativus*. Plant Dis. 83:213-217.

Hoff, B., Kamerewerd, J., Sigl, C., Mitterbauer, R., Zadra, I., Kurnsteiner, H., and Kuck, U. 2010. Two components of a velvet-like complex control hyphal morphogenesis, conidiophore development, and penicillin biosynthesis in *Penicillium chrysogenum*. Eukaryot. Cell 9:1236-1250.

Jiang, J., Liu, X., Yin, Y., and Ma, Z. 2011. Involvement of a velvet protein FgVeA in the regulation of asexual development, lipid and secondary metabolisms and virulence in *Fusarium graminearum*. PLoS One 6 :e28291.

Kafer, E. 1965. Origins of translocations in *Aspergillus nidulans*. Genetics 52:217-232.

Kato, N., Brooks, W., Calvo, A. M. 2003. The expression of sterigmatocystin and penicillin genes in *Aspergillus nidulans* is controlled by *veA*, a gene required for sexual development. Eukaryot. Cell 2:1178-1186.

Keogh, R. C., Deverall, B. J., and McLeod, S. 1980. Comparison of histological and physiological-response to *Phakopsora pachyrhizi* in resistant and susceptible soybean. T. Brit. Mycol. Soc. 74:329-333.

Kim, H. J., Han, J. H., Kim, K. S., and Lee, Y. H. 2014. Comparative functional analysis of the velvet gene family reveals unique roles in fungal development and pathogenicity in *Magnaporthe oryzae*. Fungal Genet. Biol. 66:33-43.

Kim, H. S., Han, K. Y., Kim, K. J., Han, D. M., Jahng, K. Y., Chae, K. S. 2002. The *veA* gene activates sexual development in *Aspergillus nidulans*. Fungal Genet. Biol. 37:72-80.

Kopke, K., Hoff, B., Bloemendal, S., Katschorowski, A., Kamerewerd, J., and Kuck, U. 2013. Members of the *Penicillium chrysogenum* velvet complex play functionally opposing roles in the regulation of penicillin biosynthesis and conidiation. Eukaryot. Cell 12:299-310.

Kosalkova, K., Garcia-Estrada, C., Ullan, R. V., Godio, R. P., Feltrer, R., Teijeira, F., Mauriz, E., and Francisco Martin, J. 2009. The global regulator LaeA controls penicillin biosynthesis, pigmentation and sporulation, but not roquefortine C synthesis in *Penicillium chrysogenum*. Biochimie 91:214-225.

Kumar, J., Schafer, P., Huckelhoven, R., Langen, G., Baltruschat, H., Stein, E., Nagarajan, S., and Kogel, K. H. 2002. *Bipolaris sorokiniana*, a cereal pathogen of global concern: cytological and molecular approaches towards better control. Mol. Plant Pathol. 3:185-195.

Lan, N., Zhang, H., Hu, C., Wang, W., Calvo, A. M., Harris, S. D., Chen, S., and Li, S. 2014. Coordinated and distinct functions of velvet proteins in *Fusarium verticillioides*. Eukaryot. Cell 13:909-918.

Lee, J., Myong, K., Kim, J. E., Kim, H. K., Yun, S. H., and Lee, Y. W. 2012. FgVelB globally regulates sexual reproduction, mycotoxin production and pathogenicity in the cereal pathogen *Fusarium graminearum*. Microbiology 158:1723-1733.

Leng, Y. Q., and Zhong, S. B. 2012. Sfp-type 4 '-phosphopantetheinyl transferase is required for lysine synthesis, tolerance to oxidative stress and virulence in the plant pathogenic fungus *Cochliobolus sativus*. Mol. Plant Pathol. 13:375-387.

Leng, Y. Q., Wu, C. X., Liu, Z. H., Friesen, T. L., Rasmussen, J. B., and Zhong, S. B. 2011. RNA-mediated gene silencing in the cereal fungal pathogen *Cochliobolus sativus*. Mol. Plant Pathol. 12:289-298.

Levin, D. E., and Bartlettheubusch, E. 1992. Mutant in the *Saccharomyces cerevisiae pkc1*-gene display a cell cycle-specific osmotic stability defect. J. Cell Biol. 116:1221-1229.

Li, S. J., Myung, K., Guse, D., Donkin, B., Proctor, R. H., Grayburn, W. S., and Calvo, A. M. 2006. *FvVE1* regulates filamentous growth, the ratio of microconidia to macroconidia and cell wall formation in *Fusarium verticillioides*. Mol. Microbiol. 62:1418-1432.

Lopez-Berges, M. S., Hera, C., Sulyok, M., Schafer, K., Capilla, J., Guarro, J., and Di Pietro, A. 2013. The velvet complex governs mycotoxin production and virulence of *Fusarium oxysporum* on plant and mammalian hosts. Mol. Microbiol. 87:49-65.

Merhej, J., Urban, M., Dufresne, M., Hammond-Kosack, K. E., Richard-Forget, F., and Barreau, C. 2012. The *velvet* gene, *FgVe1*, affects fungal development and positively regulates trichothecene biosynthesis and pathogenicity in *Fusarium graminearum*. Mol. Plant Pathol. 13:363-374.

Myung, K., Li, S., Butchko, R. A. E., Busman, M., Proctor, R. H., Abbas, H. K., Calvo, A. M., 2009. FvVE1 regulates biosynthesis of the mycotoxins fumonisins and fusarins in *Fusarium verticillioides*. J. Agr. Food Chem. 57:5089-5094.

Ni, M., and Yu, J. H. 2007. A novel regulator couples sporogenesis and trehalose biogenesis in *Aspergillus nidulans*. PLoS One 2:e970.

Park, H. S., Nam, T. Y., Han, K. H., Kim, S. C., and Yu, J. H. 2014. VelC positively controls sexual development in *Aspergillus nidulans*. PLoS One 9:e89883.

Park, H. S., Ni, M., Jeong, K. C., Kim, Y. H., and Yu, J. H. 2012a. The role, interaction and regulation of the *velvet* regulator VelB in *Aspergillus nidulans*. PLoS One 7:e45935.

Park, H. S., Bayram, O., Braus, G. H., Kim, S. C., and Yu, J. H. 2012b. Characterization of the *velvet* regulators in *Aspergillus fumigatus*. Mol. Microbiol. 86:937-953.

Perrin, R. M., Fedorova, N.D., Bok, J. W., Cramer, R. A., Wortman, J. R., Kim, H. S., Nierman, W. C., Keller, N. P. 2007. Transcriptional regulation of chemical diversity in *Aspergillus fumigatus* by LaeA. PLoS Pathog. 3:e50.

Santen, K., Marttila, S., Liljeroth, E., and Bryngelsson, T. 2005. Immunocytochemical localization of the pathogenesis-related PR-1 protein in barley leaves after infection by *Bipolaris sorokiniana*. Physiol. Mol. Plant P. 66:45-54.

Schumacher, J., Pradier, J. M., Simon, A., Traeger, S., Moraga, J., Collado, I. G., Viaud, M., Tudzynski, B. 2012. Natural variation in the VELVET gene *bcvel1* affects virulence and light-dependent differentiation in *Botrytis cinerea*. PLoS One 7:e47840.

Tinline, R. D., Strauffer, J. F., and Dickson, J. G. 1960. *Cochliobolus sativus* III. Effects of ultraviolet radiation. Can. J. Bot. 38:275–282.

Torres, L., Martin, H., Garciasaez, M., Arroyo, J., Molina, M., Sanchez, M., Nombela, C. 1991. A protein-kinase gene comlements the lytic phenotype of *Saccharomyces cerevisiae lyt2* mutatns. Mol. Microbiol. 5:2845-2854.

Wang, R., Leng, Y., and Zhong, S. 2015. The regulatory gene *VosA* affects conidiogenesis and is involved in virulence of the fungal cereal pathogen *Cochliobolus sativus*.

Wang, W., Wu, D., Pan, H., and Turgeon, B. G. 2014. Vel2 and Vos1 hold essential roles in ascospore and asexual spore development of the heterothallic maize pathogen *Cochliobolus heterostrophus*. Fungal Genet. Biol. 70:113-124.

Wiemann, P., Brown, D. W., Kleigrewe, K., Bok, J. W., Keller, N. P., Humpf, H. U., and Tudzynski, B. 2010. FfVel1 and FfLae1, components of a velvet-like complex in *Fusarium fujikuroi*, affect differentiation, secondary metabolism and virulence. Mol. Microbiol. 77:972-994.

Wilcoxson, R. D., Rasmusson, D. C., and Miles, M. R. 1990. Development of barley resistant to spot blotch and genetics of resistance. Plant Dis. 74:207-210.

Wu, D. L., Oide, S., Zhang, N., Choi, M. Y., and Turgeon, B. G. 2012. ChLae1 and ChVel1 regulate T-toxin production, virulence, oxidative stress response, and development of the maize pathogen *Cochliobolus heterostrophus*. PLoS Pathog. 8:e1002542.

Yang, Q., Chen, Y., Ma, Z. 2013. Involvement of BcVeA and BcVelB in regulating conidiation, pigmentation and virulence in *Botrytis cinerea*. Fungal Genet. Biol. 50:63-71.

CHAPTER 3: GENOME-WIDE ASSOCIATION MAPPING OF SEEDLING RESISTANCE TO TWO DIFFERENT PATHOTYPES OF *COCHLIOBOLUS SATIVUS* IN A USDA BARLEY CORE COLLECTION

Abstract

Spot blotch, caused by *Cochliobolus sativus*, is an economically important disease of barley in many regions of the world and is best controlled through the deployment of resistant cultivars. In the Upper Midwest region of the USA, the durable spot blotch resistance derived from the barley line ND B112 has been widely used in barley breeding programs and it is still effective against the three pathotypes (0, 1, and 2) of *C*. *sativus* identified so far in the region. However, a new pathotype (pathotype 3) of the fungus was identified in North Dakota, which can overcome the ND B112 resistance. To identify genetic loci conferring resistance to pathotype 3 (represented by isolate ND4008) and pathotype 2 (represented by isolate ND90Pr) of *C*. *sativus*, a world-wide barley core collection consisting of 2,062 accessions from USDA were phenotyped at the seedling stage with the two isolates (ND4008 and ND90Pr). Genome-wide association analyses were conducted with the 1,480 barley accessions having both phenotype and genotype data. Two QTL (Rcs-qtl-6H-P3 and Rcs-qtl-1H-P3) for resistance to ND4008 were detected on chromosome 6H and 1H, respectively, and one QTL (Rcs-qtl-1H-P2) for resistance to ND90Pr was identified on the short arm of chromosome 1H, using the 1,480 barley accessions (Whole_Panel). One QTL (Rcs-qtl-3H-P3) on chromosome 3H and one QTL (Rcs-qtl-2H-P3) on chromosome 2H for resistance to ND4008 were only identified when two-row barley accessions (Two-row_Panel) and six-row barley accessions (Six-row_Panel) were analyzed separately. Rcs-qtl-1H-P2 was also detected in the Two-row_Panel, but one QTL (Rcs-qtl-6H-P2) for resistance to ND90Pr located on chromosome 6H was only detected in the Six-row_Panel. Rcs-qtl-1H-P2 is

coincident with the QTL (*Rcs6*) previously identified by bi-parental mapping, while Rcs-qtl-6H-P2, Rcs-qtl-6H-P3, Rcs-qtl-1H-P3, Rcs-qtl-3H-P3 and Rcs-qtl-2H-P3 are novel loci conferring resistance to spot blotch. Our results indicate that subpopulation-specific association analysis is necessary and valuable when a worldwide barley population is used.

Introduction

Spot blotch, caused by *Cochliobolus sativus* (Ito and Kurib.) Drechsl. ex Dastur [(anamorph: *Bipolaris sorokiniana* (Sacc. in Sorok.) Shoem.)], is one of the most common and economically important diseases in barley. The disease occurs in many regions of the world, but is particularly severe in the Upper Midwest region of the USA and Prairie Provinces of Canada. It can cause more than 30% yield losses and significantly impact the malting quality of barley (Fetch and Steffenson 1994). Three pathotypes (0, 1 and 2) of *C*. *sativus* were previously identified based on virulence patterns on three barley differential lines (ND 5883, Bowman, and ND B112) in the Upper Midwest region (Valjavec-Gratian and Steffenson 1997b). Pathotype 0 isolates show low virulence on all three barley lines. Pathotype 1 isolates exhibit high virulence on ND 5883 but low virulence on Bowman and ND B112, while pathotype 2 isolates show high virulence on Bowman but low virulence on ND 5883 and NDB112. Recently, *C*. *sativus* isolates with high virulence on ND B112 and Bowman have been identified in Manitoba of Canada (Ghazvini and Tekauz 2007) and North Dakota of USA (Gyawali 2010). The Canadian isolates possessing unique virulence on ND B112 and Bowman were designated as virulence groups 7.7.7.5, 7.7.5.1 and 6.3.5.0 (Ghazvini and Tekauz 2007), while the North Dakota isolates were classified as pathotype 3 (Gyawali 2010; Zhong et al. 2015). Emergence of these new pathotypes poses a potential threat to barley production because nearly all six-row barley cultivars in the

region carry spot blotch resistance derived from ND B112, while many two-row barley cultivars share the spot blotch resistance source from Bowman (Steffenson et al. 1996). Furthermore, Bowman is highly susceptible to pathotype 2 isolates of *C*. *sativus* (Fetch and Steffenson 1994; Valjavec-Gratian and Steffenson 1997a), making the situation even worse for two-row barleys.

In the past years, great efforts have been made to identify various sources of spot blotch resistance and to characterize genetic loci conferring the resistance using the bi-parental mapping method. Wilcoxson et al. (1990) first studied genetics of spot blotch resistance in populations derived from crosses of five spot blotch resistant barley lines (Minn 33, Minn 65-241, Minn 65-243, Minn 65-244, and Minn 7) with the susceptible cultivar Larker, and revealed that spot blotch resistance is conditioned by one or two major genes. Using the doubled haploid (DH) populations developed by crossing the resistant cultivar Morex with three susceptible cultivars (Steptoe, Dicktoo, and Harrington), respectively, Steffenson et al. (1996) and Bilgic et al. (2005) mapped QTL for resistance to the pathotype 1 (represented by isolate ND85F) on chromosomes 1H, 3H and 7H, respectively. Using a doubled haploid population derived from the Calicuchima-sib/Bowman-BC cross, Bilgic et al. (2006) mapped the genetic loci conferring resistance to pathotype 1 and 2 on chromosome 4H and 1H, respectively. Several other research groups also conducted QTL analysis for spot blotch resistance at the seedling stage. Bovill et al. (2010) identified two QTL for resistance to the isolate SB61 on chromosome 5HL and 7HS using four populations [VB9524/ ND11231-12 (VB/ND-12), ND11231-11/WI2875-17 (ND-11/WI), TR251/Gairdner (TR/GA) and WPG84 12-9-2-1/Lindwall (WP/LI)]. In addition, Grewal et al. (2012) mapped three QTL (*QRcss1, QTcss3, and QRcss5*) on chromosome 1H, 3H, and 5H for resistance to three different isolates (WRS1909, WRS1908, and SK1-1) using a DH population from the cross between CDC Bold and TR251.

Although the traditional bi-parental mapping approach is effective for identification of QTL for resistance to diseases, the main disadvantage of this method is that only a very limited genetic diversity of the species is captured since only two genotypes are used as parents in the population. Furthermore, the genetic resolution of bi-parental mapping is often at a range of 10 cM to 30 cM because of the restricted number of meiotic events that are captured in the bi-parental mapping population (Bilgic et al. 2006; Laido et al. 2014). Association mapping (AM), which uses the linkage disequilibrium (LD) pattern in a large population of unrelated individuals (Risch 2000), provides an alternative method for identifying QTL. With AM, one can utilize diverse germplasm panels, including worldwide collections, and therefore the genetic diversity of the mapping population is greatly increased. Besides, in AM populations, recombination events occurred throughout their evolutionary history, contributing to the breakage of LD blocks within the genome. Thus, LD decays much faster in AM populations than in bi-parental mapping populations (Rafalski 2002), greatly increasing the map resolution. Considering all of these advantages, AM has been successfully used in various plant species to identify markers associated with many different traits, including resistance to spot blotch. AM has been conducted with a collection of 318 wild barley lines (Roy et al. 2010), US barley breeding germplasm (Zhou and Steffenson 2013) and Virginia Tech winter barley lines (Berger et al. 2013) and QTL for spot blotch resistance to pathotype 1 (ND85F) were detected on barley chromosome 1H, 3H, and 7H, respectively. More recently, a total of 2,417 barley accessions selected from the USDA National Small Grains Collection (NSGC) were genotyped using the Infinium iSelect SNP assay through the Triticeae Coordinated Agricultural Project (http://www.triticeaecap.org/). Munoz-Amatriain et al. (2014) analyzed the LD pattern and population structure of these barley accessions and demonstrated the utility of this barley core collection for locating genetic loci

affecting phenotypes by genome-wide association mapping. Using this same barley core collection, Tamang et al. (2015) detected 21 putative novel loci significantly associated with resistance or susceptibility to the spot form net blotch disease caused by four different isolates of *Pyrenophora teres* f. *maculata*.

The objective of this study was to identify genetic loci that contribute to the resistance to pathotype 3 and pathotype 2 of the spot blotch fungus *C*. *sativus* in the USDA barley core collection with the association mapping approach. Identification of markers associated with the resistance loci will facilitate the marker-assisted selection of spot blotch resistance in barley breeding programs.

Materials and methods

Plant materials

A total of 2,062 barley accessions consisting of cultivars, breeding lines, landraces, and genetic stocks were obtained from the National Small Grain Collection, Aberdeen, Idaho. Five barley genotypes (Bowman, ND 5883, ND B112, ND 23329, and ND 23345) were included as checks. Bowman, ND 5883, and ND B112 are three barley differential lines used for differentiating pathotype 0, 1 and 2 isolates of the fungal pathogen *C*. *sativus* (Valjavec-Gratian and Steffenson 1997b). ND 23329 and ND 23345 are the two barley lines exhibiting moderate resistance to the pathotype 3 isolate ND4008 in a previous study (Gyawali 2010).

Spot blotch phenotyping

Two isolates, ND90Pr and ND4008, which represent pathotype 2 and 3 of *C*. *sativus*, respectively, were used to evaluate the reactions of barley lines to spot blotch at the seedling stage. Fungal inoculum preparation, inoculation, and plant incubation were performed according to the procedure described in Leng et al. (unpublished). Three independent replicates were used in each inoculation for each isolate and the mean of the three replicates was used for further analysis. The disease was rated 7 days after inoculation using the 1 to 9 rating scale described by Fetch and Steffenson (1999).

SNP genotyping and data analysis

A total of 2,417 barley accessions were genotyped with the barley 9k Illumina Infinium iSelect assay through the Triticeae Coordinated Agriculture Project (T-CAP). The data were deposited in the Triticeae Toolbox (T3) website (http://malt.pw.usda.gov/t3/sandbox/barley/). The SNP genotyping and data curation were described in Munoz-Amatriain et al. (2014). The genotyping data, consisting of 6,244 SNPs that passed the quality control, were extracted for the final association panel (1,480 unique barley accessions). The iSelect consensus map developed in Munoz-Amatriain et al. (2014) was used as reference for the genetic positions of the selected SNP markers. Based on the genotyping data and genetic map, the marker coverage, polymorphic information content (PIC) values, minor allele frequency (MAF), and gene diversity were calculated for each SNP in all association-mapping panels using JMP Genomics statistical suite v6.0 (Cary, North Carolina). Markers with minor allele frequency (MAF) < 0.05 or with missing calls $> 20\%$ accessions were removed for further analyses.

Linkage disequilibrium analysis

The JMP Genomics statistical suite v6.0 was used to calculate the linkage disequilibrium (LD) parameter squared correlation coefficient (r^2) between SNP markers. First, a hundred thousand pairwise r^2 values were calculated between randomly selected unlinked markers in each barley panel. The parametric 95th percentile of the distribution of these r^2 values was calculated in RStudio v0.98.1091 (RStudio, Inc. Boston, MA) and used as a threshold. All LD values beyond this critical r^2 value were considered to be the result of genetic linkage. Then, the r^2 values between all SNP markers in each panel were calculated. LD decay was quantified by plotting pair-wise r^2 values against the distance (cM) between adjacent SNP loci. By fitting smoothing spline line, r^2 values were regressed on the genetic distances. The intersection of the smoothing spline-fitting curve at the critical LD threshold was estimated to be the LD decay in terms of genetic distance. To better understand the LD pattern in each chromosome, the LD decay was also investigated in each chromosome in the Whole_Panel. Furthermore, to investigate the LD pattern of the detected QTL region, LD was also analyzed and presented as a heat map for all markers around the QTL region.

Population structure analysis

The Multidimensional Scaling (MDS) and the Principal Component Analysis (PCA) were used to establish the matrix (Q) for correcting population structure in association analysis. MDS and PCA were conducted in JMP Genomics. To adequately represent the full data set in the smallest possible number of dimensions, the “elbow” location in two plots (Badness-of-Fit Criterion vs. Number of Dimensions and Distance Correlation vs. Number of Dimensions) was

selected as the number of dimensions for establishing the matrix Q1. The first principal components (PCs) explaining approximately 25% cumulative variation were chosen to construct the Q2 matrix.

Genome-wide association analysis

The underlying regression statistic of association analysis was: $Y = X\alpha + Q\beta + v + e$, where Y is a vector of phenotypic values, α is a vector of fixed effects from SNP markers, β is a vector of fixed effects regarding population structure, v is a vector of the random effects pertaining to the relationships among the lines using marker data, and e is a vector of residuals. X is the matrix of genotypes at the SNP markers. Q is the matrix of significant multiple dimensions (Q1) generated by the MDS or significant principal components (Q2) generated by PCA. The variances of the random effects were assumed to be $Var(v) = 2RV_g$, where R is the familial relationship matrix estimated from the Identity by State (IBS), which calculates the probability that two lines share the same copy of an allele, and V_g is the genetic variance. $Var(e) = V_R$, where V_R is the residual variance (Yu et al. 2006). Based on this regression, six different models (Naïve, IBS, MDS, PCA, PCA+IBS, MDS+IBS) were conducted on all three panels using two sets of phenotyping data. To select the best model with the least statistic inflation (type I error), the lowest mean square difference (MSD) values between cumulative and observed *p* values of all marker loci were calculated in each model. The principle here is that the ideal model should have a uniform distribution of cumulative vs. observed *p* values. More away from this uniform distribution of the model, the MSD value of this model will be bigger. Thus, the best model should exhibit the smallest MSD value. The method of calculating MSD was modified from

Mamidi et al. 2011. Briefly, all marker *p* values were ranked from the smallest to largest, and then the following formula was used:

$$\mathbf{MSD} = \left\{\sum_{\mathbf{i=1}}^{\mathbf{n}} [\mathbf{p_i} - \left(\frac{\mathbf{i}}{\mathbf{n}}\right)]^{\mathbf{2}}\right\} / \mathbf{n}$$

where i is the rank number, p_i is the ith ranked *p* value, and n is the total number of markers.

After the best model was selected, positive false discovery rate (pFDR; *q* value) was calculated (Storey 2002) for that model using the PROC MULTTEST procedure in the Statistical Analysis System (SAS 9.2) software. The *q* value at 0.1 was considered to be the threshold of the significance of the association between markers and disease resistance.

Results

Association mapping panels

Of the 2,062 barley accessions phenotyped (Leng et al. unpublished), only 1,480 accessions were used in this study because of duplicated genotypes and missing genotype data for some accessions (Munoz-Amatriain et al. 2014). These 1,480 barley accessions were from 97 countries and were comprised of 650 landraces, 624 cultivars/breeding lines, 15 genetic stocks and 191 accessions of uncertain improvement status (Leng et al. unpublished). They formed the Whole_Panel. To detect the resistance loci in two-row and six-row barley accessions separately, the Whole_Panel was divided into two subpopulations, the Two-row_Panel, containing 621 two-row barley lines, and the Six-row_Panel, containing 857 six-row barley lines.

Phenotyping and genotyping data

In all three panels, 22.5% to 28.3% of the accessions showed resistant (mean disease rating of 1.0-4.0) or intermediate reactions (mean disease rating of 4.1-6.0) to ND4008, whereas 86.7% to 89.3% of the accessions showed resistant or intermediate reactions to ND90Pr (Fig. 3.1). These results are consistent with the phenotyping distributions of the whole 2,062 barley accessions described in Leng et al. (unpublished).

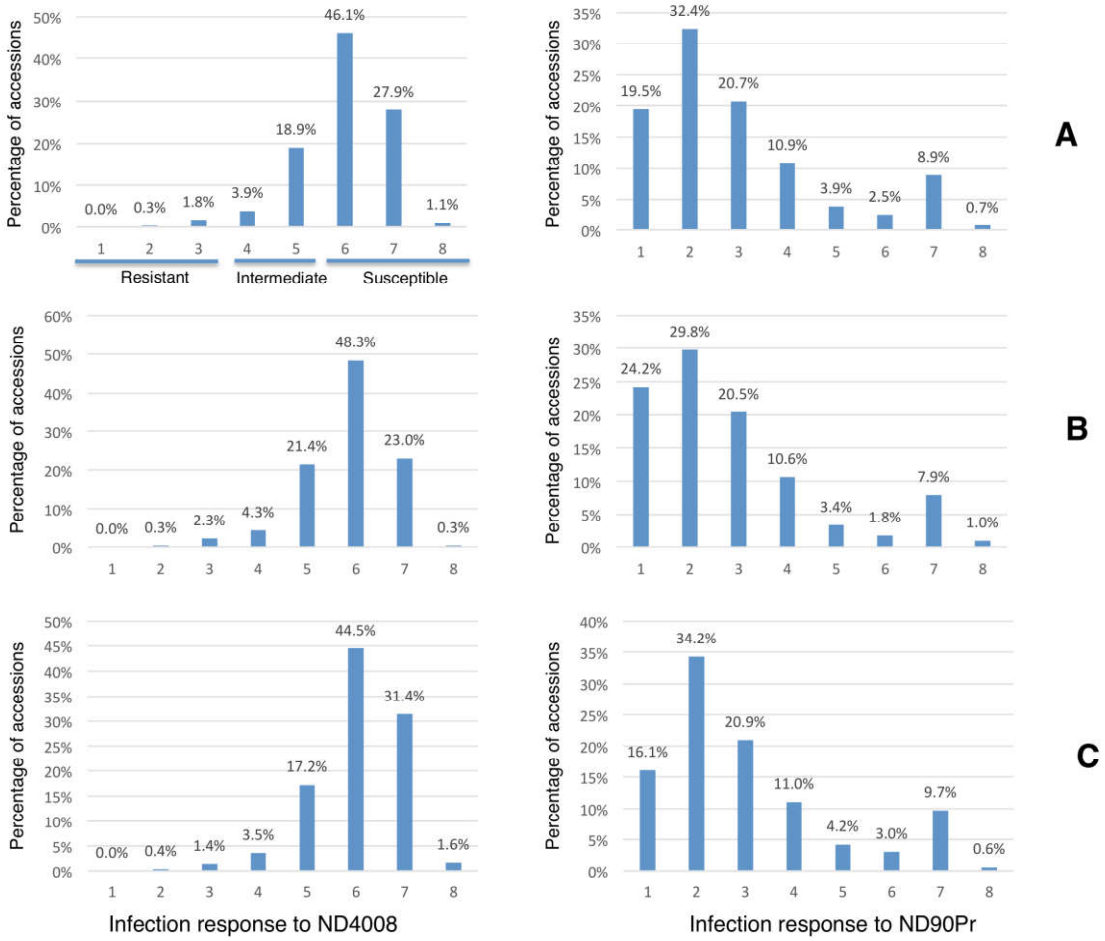

Fig. 3.1. Frequency distribution of the mean spot blotch infection responses to pathotype 3 (ND4008) and pathotype 2 (ND90Pr) in three panels. **A.** Whole_Panel, **B.** Two-row_Panel, and **C.** Six-row_Panel. The y-axis represents the percentage of accessions with mean infection response in the respective rating intervals: 1 (1.0-2.0); 2 (2.1-3.0); 3 (3.1-4.0); 4 (4.1-5.0); 5 (5.1-6.0); 6 (6.1-7.0); 7 (7.1-8.0); 8 (8.1-9.0).

Of the 6,224 SNP markers obtained from the Triticeae toolbox database, 4,968 SNP markers were located on the iSelect consensus genetic map developed by Munoz-Amatriain et al. (2014) and used for further analysis in the study. After removal of the SNPs with missing calls in > 20% accessions or minor allele frequency (MAF < 0.05), 4,747, 4,558, and 4,446 SNP markers were finally used in association analysis for the Whole_Panel, Two-row_Panel, and Six-row_Panel, respectively.

In the Whole_Panel, the 4,747 SNP markers were distributed over all 7 chromosomes with an average spacing of 0.23 cM. The coverage of SNP markers varies among chromosomes with a minimum of 3.22 SNP markers per centimorgan on 1H and a maximum of 5.09 markers per centimorgan on 5H. Marker coverage for each chromosome is listed in Table 3.1. Similar SNP marker coverage was observed for Two-row_Panel and Six-row_Panel (data not shown). PIC values for all SNPs in Whole_Panel ranged from 0.09 to 0.38 with an average of 0.31 and 82.5% of the markers displaying PIC values exceeding 0.25, demonstrating these markers are highly informative and useful. The average PIC values for Two-row_Panel and Six-row_Panel are 0.30. Gene diversity for the three panels ranged from 0.10 to 0.50 with an average of 0.39 for Whole_Panel, 0.38 for Two-row_Panel and 0.37 for Six-row_Panel, respectively.

Linkage disequilibrium analysis

The LD decays in terms of genetic distances were calculated at 1.1, 1.6, and 0.8 cM for the three panels (Whole_Panel, Two-row_Panel, and Six-row_Panel), respectively. The results indicate that the LD decays much faster in six-row barley than in two-row barley although the significance thresholds were similar between the two panels (Fig. 3.2).

LD analyses were also performed for each chromosome in the Whole_Panel. Providing the LD threshold for each chromosome is the same as it is for the whole genome, the results showed that the LD decay was similar for chromosome 1H to chromosome 6H, ranging from 1.16 cM to 2.18 cM, whereas the LD decay for chromosome 7H was much higher (4.07 cM) than those for the other chromosomes (Fig. 3.2).

Table 3.1. Statistics of single nucleotide polymorphism markers on barley chromosomes in the Whole_Panel

Chromosome	Genetic Distance (cM)	Markers	Marker coverage*
1H	145.82	470	3.22
2H	179.41	825	4.60
3H	164.42	733	4.46
4H	129.68	489	3.77
5H	185.05	942	5.09
6H	139.39	646	4.63
7H	168.94	642	3.80
All	1112.71	4747	4.27

* Marker coverage indicates the number of markers per centimorgan (cM) on the genetic map.

Population structure

The MDS were first conducted for the three panels. Based on two plots (Badness-of-Fit Criterion vs. Number of Dimensions and Distance Correlation vs. Number of Dimensions), two dimensions were selected in each panel to establish the matrix Q1. PCA was also implemented to evaluate population structure and establish the Q matrix. For the Whole_Panel, 28.5% of the variation was explained by the first four principal components, where 12.2%, 7.0%, 5.2%, and 4.1% of the variation were explained by the first to the fourth component, respectively. Therefore, the Q2 matrix in this panel was established using these four principal components.

Similarly, the Q2 matrix was established by the first five principal components explaining 27.6% of the variation for the Two-row_Panel and by the first three principal components explaining 25.7% of the variation for the Six-row_Panel.

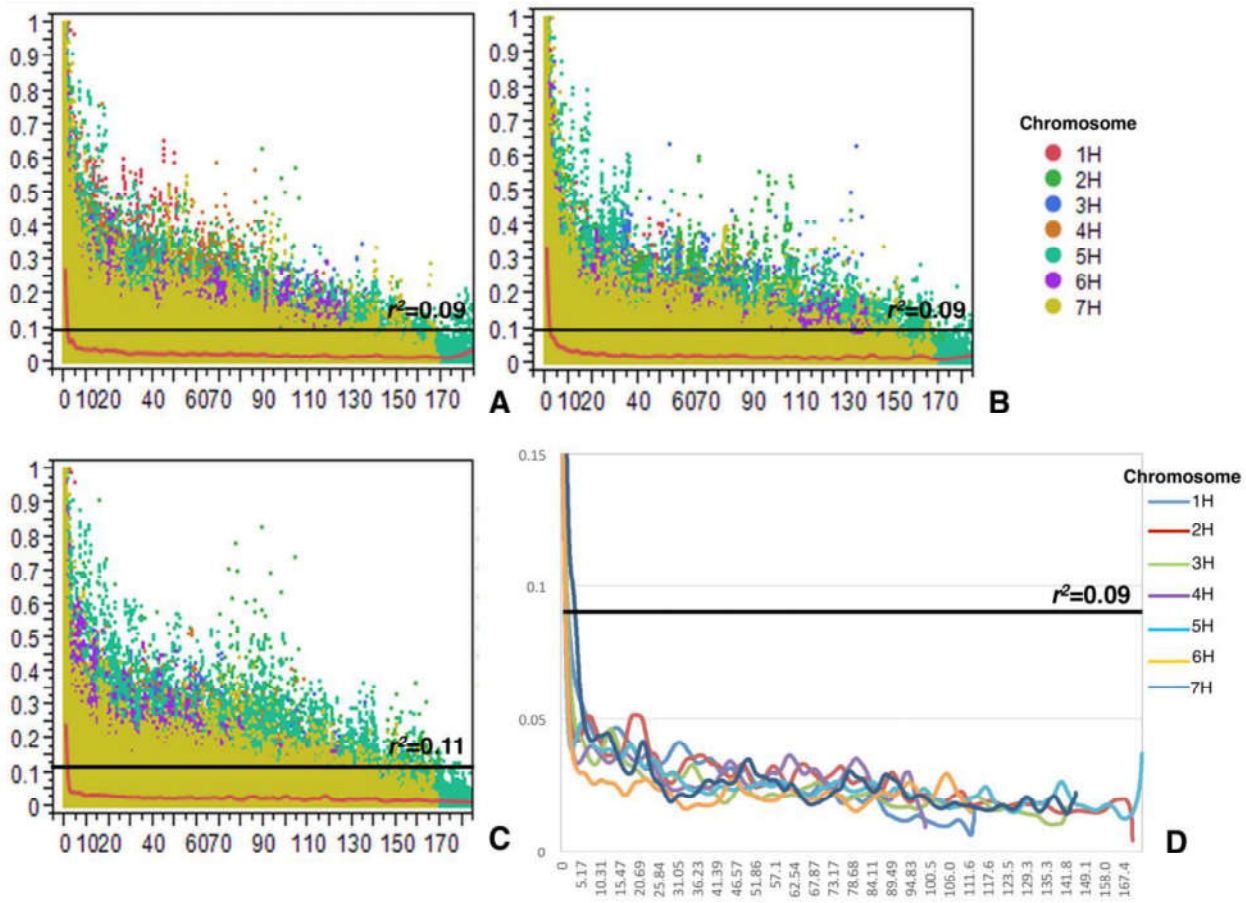

Fig. 3.2. Linkage disequilibrium (r^2) decay over genetic distance (cM) for whole genome and for each chromosome. **A-C.** Linkage disequilibrium (r^2) decay over genetic distance (cM) for whole genome in **A.** Whole_Panel, **B.** Two-row_Panel, and **C.** Six-row_Panel. The threshold of r^2 values are represented as dark solid lines. The smoothing spline curves were fitted in JMP Genomics as red solid lines to infer the decay of LD. **D.** Linkage disequilibrium (r^2) decay over genetic distance (cM) for each chromosome in Whole_Panel. The threshold of r^2 value is represented as dark solid line. The smoothing spline fittings were conducted in JMP Genomics and then illustrated in Excel as colorful solid lines to infer the decay of LD for each chromosome. The LD decays for each chromosome from 1H to 7H are: 2.18, 1.63, 1.81, 1.38, 1.16, 1.26, 4.07 centimorgan (cM), respectively.

Genome-wide association mapping of resistance to spot blotch

The genotypic and phenotypic data were evaluated using six different models as described above. The best model should exhibit the least MSD value, which has the least inflation. Analyses of the MSD values of each model using the phenotyping data obtained from the pathotype 3 isolate ND4008 indicated that the naïve model and the models only corrected by population structure (MDS or PCA) showed much higher MSD values, ranging from 0.044379 to 0.383375, indicating the high inflation of these models. However, the models corrected for the relationship component (IBS) or the models corrected for both relationship and structure component had much lower MSD values, ranging from 0.000085 to 0.000124 (Table 3.2). Based on these results, the mixed model K (IBS) was selected to conduct SNP marker–traits associations for the Whole_Panel and Six-row_Panel, while the mixed model Q+K (IBS+PCA) was selected to conduct SNP marker–traits associations for the Two-row_Panel. For association mapping with the phenotyping data obtained from the pathotype 2 isolate ND90Pr, similar MSD value patterns in different association models were observed (data not shown), thus the same models were selected for association analysis in each panel for isolate ND90Pr.

Table 3.2. Mean square difference (MSD) values in different association models using single nucleotide polymorphism (SNP) markers and phenotyping data obtained with the *Cochliobolus sativus* pathtype 3 isolate ND4008

Model	MSD		
	Whole_Panel	Two-row_Panel	Six-row_Panel
Naïve	0.113794	0.383375	0.084402
IBS	0.000085	0.001699	0.000361
PCA	0.078032	0.096533	0.044379
MDS	0.082829	0.097948	0.068605
IBS+PCA	0.000124	0.001382	0.000450
IBS+MDS	0.000231	0.001545	0.000567

QTL for resistance to pathotype 3 isolate ND4008

As listed in Table 3.3 and illustrated in Fig. 3.3A, four QTL (Rcs-qtl-1H-P3, Rcs-qtl-2H-P3, Rcs-qtl-3H-P3 and Rcs-qtl-6H-P3) were identified conferring seedling resistance to isolate ND4008. The most significant one (Rcs-qtl-6H-P3) is located on the short arm of 6H at 16.16 to 16.66 cM, with five markers (SCRI_RS_129888, SCRI_RS_20187, SCRI_RS_202723, SCRI_RS_139713 and SCRI_RS_139715) being significantly associated with it in the Two-row_Panel. Two of the markers (SCRI_RS_20187 and SCRI_RS_202723) were also significantly associated with Rcs-qtl-6H-P3 in the Whole_Panel and the Six-row_Panel. The five markers detected in the Two-row_Panel exhibited similar *p* values and explained 2.9% to 3.1 % of the phenotypic variation. LD pattern among these markers was examined and the markers were divided into two groups based on the LD pattern. One group contained three markers (SCRI_RS_129888, SCRI_RS_139713, and SCRI_RS_139715) mapped at 16.16-16.26 cM of 6H. LD among these three markers was very strong, ranging from 0.56 to 1.0. The other group contained two markers (SCRI_RS_20187 and SCRI_RS_202723) located at 16.56-16.66 cM of 6H. LD between these two markers was extremely strong at 0.81. However, the LD between these two groups was weak, with the r^2 values ranging from 0.23 to 0.30 (Fig. 3.4A).

The QTL (Rcs-qtl-1H-P3) on chromosome 1H (142.74 cM) was only identified in the Whole_Panel. Only one marker (SCRI_RS_152664) was significantly associated with this QTL, which explained 1.8% of the phenotypic variation. LD analysis of this QTL region didn't detect strong LD (r^2 >0.6) between SCRI_RS_152664 and its neighboring markers.

The QTL (Rcs-qtl-3H-P3) on chromosome 3H (66.15 cM) was only detected in the Two-row_Panel. Only one significant marker (BOPA1_5960_1302) was significantly associated with

this QTL, explaining 3.8% of the phenotypic variation. LD analysis of this QTL region indicated that BOPA1_5960_1302 showed very weak LD (r^2 <0.28) with all neighboring markers.

The QTL (Rcs-qtl-2H-P3) on chromosome 2H (164.4 cM) was only identified in the Six-row_Panel. Only one marker (SCRI_RS_152664) was significantly associated with Rcs-qtl-2H-P3, which explained 1.6% of the phenotypic variation. This marker was also detected in the Whole_Panel with a low *p* value of 7.52E-04 but a relative higher *q* value of 0.319. LD analysis indicated strong LD (0.88) between SCRI_RS_152664 and another marker SCRI_RS_174077, which is located at the same position (164.4 cM) on 2H. However, SCRI_RS_174077 was associated with spot blotch resistance at a non-significant level in the Six-row_Panel with the *p* value of 3.21E-04 but the *q* value of 0.27.

QTL for resistance to pathotype 2 isolate ND90Pr

GWAS was also conducted on the phenotype data obtained with the pathotype 2 isolate ND90Pr. As listed in Table 3.3 and illustrated in Fig. 3.3B, two QTL (Rcs-qtl-1H-P2 and Rcs-qtl-6H-P2) were identified conferring resistance to ND90Pr. Four markers (BOPA1_6949_895, SCRI_RS_119312, BOPA2_12_30933, and SCRI_RS_148560) were significantly associated with the QTL (Rcs-qtl-1H-P2) located on the short arm of 1H (6.68~14.2 cM) in the Two-row_Panel, and one of them (SCRI_RS_119312) was also significantly associated with Rcs-qtl-1H-P2 in the Whole_Panel. Among the four markers detected in the Two-row_Panel, BOPA1_6949_895 exhibited extremely low *q* value at 2.85E-12 and explained 10.4% of the phenotypic variation. LD (as measured by r^2) among these markers were extremely weak ranging from 5.7E-05 to 0.16 (Fig. 3.4B). The other QTL (Rcs-qtl-6H-P2) located on 6H was only detected in the Six-row_Panel and only one marker (BOPA2_12_10278, 59.9 cM) explaining

2.3% of the phenotypic variation was significantly associated with this QTL. LD analysis indicated that BOPA2_12_10278 exhibited extremely low LD (r^2 <0.05) with any of the neighboring markers.

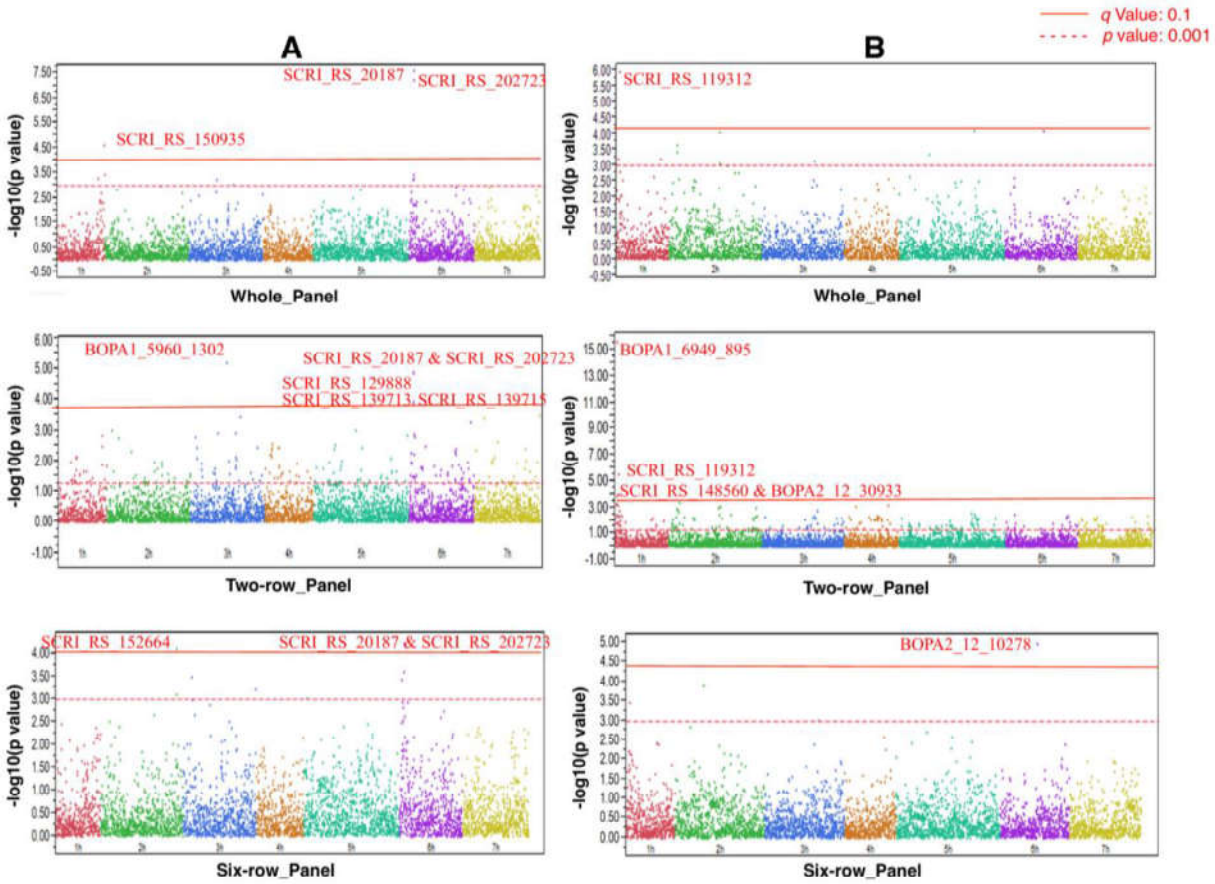

Fig. 3.3. Significantly associated SNP markers with resistance to two isolates in three panels. **A.** ND4008 and **B.** ND90Pr. The *p* values were adjusted using false discovery rate method to the *q* values. The criteria of significant SNP marker is indicated by the solid line at *q* value = 0.1. The dotted line indicates the *p* value at 0.001.

Table 3.3. Quantitative trait loci (QTL) and single nucleotide polymorphism (markers) significantly associated with resistance to *Cochliobolus sativus* isolates ND4008 (pathotype 3) and ND90Pr (pathotype 2)

For resistance to isolate ND4008								
QTL	**Marker**	**Position (cM)**	**Whole_Panel**		**Two-row_Panel**		**Six-row_Panel**	
			***q*/*p* value**	**R^2**	***q*/*p* value**	**R^2**	***q*/*p* value**	**R^2**
Rcs-qtl-1H-P3 (142.74~145.82 cM)	SCRI_RS_150935	142.74	3.94E-02/2.49E-05	0.018	--[a]	--	--	--
Rcs-qtl-2H-P3 (164.4 cM)	SCRI_RS_152664	164.4	--	--	--	--	7.88E-02/8.47E-05	0.018
Rcs-qtl-3H-P3 (66.15 cM)	BOPA1_5960_1302	66.15	--	--	2.14E-02/7.05E-06	0.038	--	--
Rcs-qtl-6H-P3 (16.16~16.66 cM)	SCRI_RS_129888	16.26	--	--	2.24E-02/1.48E-05	0.030	--	--
	SCRI_RS_202723	16.56	1.12E-05/4.74E-09	0.023	2.24E-02/1.34E-05	0.031	4.88E-02/4.25E-06	0.019
	SCRI_RS_20187	16.66	1.12E-05/4.74E-09	0.021	2.24E-02/1.36E-05	0.030	6.47E-02/2.28E-06	0.017
	SCRI_RS_139713	16.16	--	--	9.26E-02/1.26E-04	0.029	--	--
	SCRI_RS_139715	16.16	--	--	9.84E-02/1.22E-04	0.029	--	--
For resistance to isolate ND90Pr								
QTL	**Marker**	**Position (cM)**	**Whole_Panel**		**Two-row_Panel**		**Six-row_Panel**	
			***q*/*p* value**	**R^2**	***q*/*p* value**	**R^2**	***q*/*p* value**	**R^2**
Rcs-qtl-1H-P2 (6.68~14.2 cM)	BOPA1_6949_895	9.34	--	--	2.85E-12/3.13E-16	0.104	--	--
	SCRI_RS_119312	13.3	5.40E-03/1.14E-06	0.019	9.70E-03/2.13E-06	0.041	--	--
	BOPA2_12_30933	6.68	--	--	9.15E-02/1.23E-04	0.029	--	--
	SCRI_RS_148560	14.2	--	--	9.15E-02/1.03E-04	0.030	--	--
Rcs-qtl-6H-P2 (59.9 cM)	BOPA2_12_10278	59.9	--	--	--	--	5.05E-02/1.14E-05	0.023

[a] -- indicate the *q* values are greater than 0.1

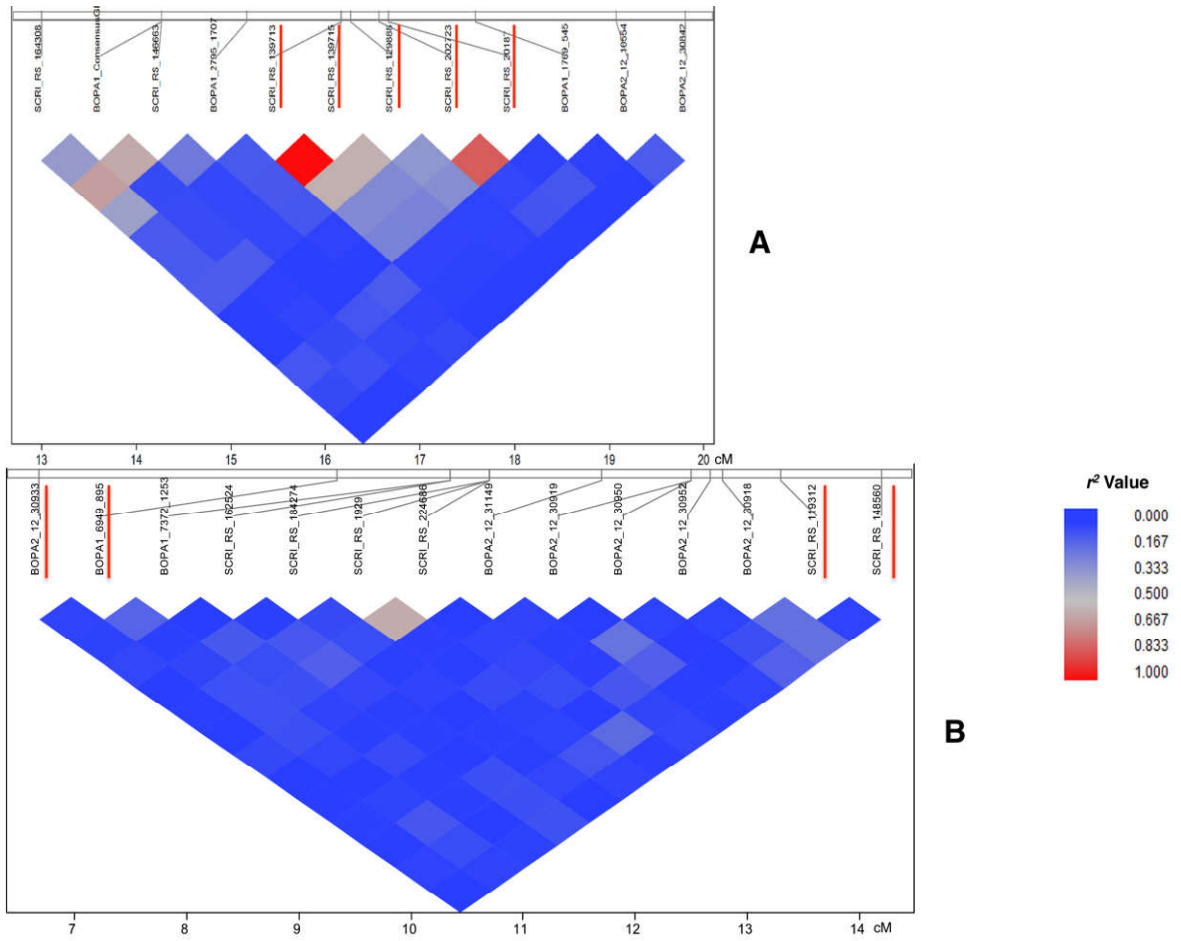

Fig. 3.4. LD analysis of the SNP markers linked to those markers significantly associated two QTL detected on chromosomes 6H and 1H. **A.** 6H and **B.** 1H. The blocks of colder colors show less LD between the two markers whereas the warmer colors show more LD between the two markers. The detected markers were under the red lines.

Discussion

Of the 1,480 barley accessions from the NSGC barley core collection, 87.4% and 24.9% of them were identified as resistant or moderate resistant at the seedling stage to pathotype 2 (ND90Pr) and pathotype 3 (ND4008) of *C*. *sativus*, respectively. This result indicates that sources of resistance to pathotype 2 are very common while the percentage of resistant accessions for pathotype 3 is relatively low in the germplasm. Fetch et al. (2008) screened over 5,000 barley accessions from USDA NSGC using the pathotype 1 isolate ND85F and found a

small percentage (5.8%) of them were resistant to ND85F in the field. More recently, Roy et al. (2010) evaluated 318 diverse wild barley accessions comprising the Wild Barley Diversity Collection (WBDC) for reaction to isolate ND85F at the seedling stage and showed 95% of them exhibited low infection responses. These studies suggest that sources of resistance to spot blotch exist in various germplasms but the percentage of resistant accessions depends on the germplasm screened and the pathotypes used.

Our AM analyses identified a major QTL (Rcs-qtl-6H-P3) conferring resistance to ND4008 on chromosome 6H in all the three panels. In the Two-row_Panel, five SNP markers are significantly associated with this QTL region and explained 14.9% phenotypic variation in total. Three QTL (Rcs-qtl-1H-P3, Rcs-qtl-2H-P3, and Rcs-qtl-3H-P3) located on 1H, 2H, and 3H were identified in the Whole_Panel, Six-row_Panel, and Two-row_Panel, respectively. For each of these three QTL, only one significantly associated SNP marker was identified, explaining 1.8%, 1.8%, 3.8% phenotypic variation, respectively. Based on the locations of SNP markers associated with the QTL, they are different from those identified in the previous studies for spot blotch resistance (Berger et al. 2013; Bilgic et al. 2005; Bilgic et al. 2006; Bovill et al. 2010; Grewal et al. 2012; Roy et al. 2010; Steffenson et al. 1996; Wilcoxson et al. 1990; Zhou and Steffenson 2013) and may represent novel loci for spot blotch resistance.

The QTL (Rcs-qtl-1H-P2) identified for resistance to isolate ND90Pr in Whole_Panel and Two-row_Panel may be the same as *Rcs6* mapped by Bilgic et al. (2006) because the SNP markers associated with the QTL mapped to the same region. However, the LD values among the four markers associated with Rcs-qtl-1H-P2 are extremely low. This could be due to multiple different QTL existing in this region. More interestingly, ten markers located at 10.35 to 12.67 cM (Fig. 3.4B) within this QTL region were found not associated with the resistance QTL. The

exact reason for this is not clear, but may be due to the very fast LD decay (LD is less than 0.1 even between the same location markers) and relatively low marker coverage (1.86 markers per centimorgan) in this region. More markers are needed to increase the resolution of this region and to fine map the Rcs-qtl-1H-P2 locus. The QTL (Rcs-qtl-6H-P2) located on 6H was identified only in the Six-row_Panel and only one SNP marker was significantly associated it, which explained 1.1% phenotypic variation. This may represent a novel QTL for spot blotch resistance since no other genes for spot blotch resistance have been mapped at the same region in previous studies (Berger et al. 2013; Bilgic et al. 2005; Bilgic et al. 2006; Bovill et al. 2010; Grewal et al. 2012; Roy et al. 2010; Steffenson et al. 1996; Wilcoxson et al. 1990; Zhou and Steffenson 2013).

The Q+K mixed model has been widely used in AM to detect marker-trait associations in plants because it can successfully control the relatedness as well as population structure and reduces inflation of *p* values. However, this model often masks true QTL, especially when the QTL are strongly correlated with population structure (Zhao et al. 2007; Zhao et al. 2011). For this reason, we divided the 1,480 barley accessions into two subpopulation panels (Two-row_Panel and Six-row_Panel) according to row type and conducted the association analysis for each panel. A major QTL for resistance to ND4008 on 6H was identified in the two sub panels as in the Whole_Panel, while two minor QTL located on 2H and 3H were only identified in the Six-row_Panel and Two-row_Panel, respectively. For isolate ND90Pr, a major QTL for spot blotch resistance was identified in Two-row_Panel as in the Whole_Panel, but it was not identified in the Six-row_Panel. Instead, another QTL located on 6H was detected in the Six-row_Panel. Our results further indicated that analyzing subpopulations independently may correct the false negative error caused by Q+K mixed model in AM analysis (Zhao et al. 2007; Zhao et al. 2011). A previous study indicated that expression of spot blotch resistance can be different in various

genetic backgrounds (Bilgic et al. 2005). For example, the spot blotch resistance QTL first identified in the Steptoe/Morex population by Steffenson et al (1996) was completely suppressed when introgressed into more diverse two- or six-row genetic backgrounds (e.g., Harrington/Morex and Dicktoo/Morex populations) (Bilgic et al. 2005). In addition, another QTL (Rcs-qtl-4H-10-11) conferring moderate seedling resistance to ND85F was identified in two-row barley Bowman but not in six-row barley cultivars (Bilgic et al. 2006). Therefore, different QTL conferring resistance to spot blotch may exist in two-row and six-row barleys and their full discovery requires AM analysis of subpopulations according to row types.

In summary, we identified novel QTL for seedling resistance to spot blotch caused by the new pathotype of *C*. *sativus* by genome-wide association in the barley core collection. We also detected QTL for resistance to the pathotype 2 isolate of the fungus. These QTL will be useful for developing new barley cultivars with seedling resistance to spot blotch. Further studies are needed to identify QTL in the same population for spot blotch resistance at the adult plant stage.

Acknowledgements

The authors thank Joseph Mullins, Zhongxing Sun, Qiang Li and Mingxia Zhao for assistance in phenotyping work. We also acknowledge Dr. María Muñoz-Amatriaín for her precious suggestions in the association analyses. This research was funded by the Triticeae-CAP project (2011-68002-30029) of the US Department of Agriculture National Institute of Food and Agriculture.

References

Berger, G. L., Liu, S., Hall, M. D., Brooks, W. S., Chao, S., Muehlbauer, G. J., Baik, B. K., Steffenson, B., and Griffey, C. A. 2013. Marker-trait associations in Virginia Tech winter barley identified using genome-wide mapping. Theor. Appl. Genet. 126:693-710.

Bilgic, H., Steffenson, B., and Hayes, P. 2005. Comprehensive genetic analyses reveal differential expression of spot blotch resistance in four populations of barley. Theor. Appl. Genet. 111:1238-1250.

Bilgic, H., Steffenson, B. J., and Hayes, P. M. 2006. Molecular mapping of loci conferring resistance to different pathotypes of the spot blotch pathogen in barley. Phytopathology 96:699-708.

Bovill, J., Lehmensiek, A., Sutherland, M. W., Platz, G. J., Usher, T., Franckowiak, J., and Mace, E. 2010. Mapping spot blotch resistance genes in four barley populations. Mol. Breed. 26:653-666.

Fetch, T. G., and Steffenson, B. J. 1994. Identification of *Cochliobolus-sativus* isolates expressing differential virulence on 2-row barley genotypes from North Dakota. Can. J. Plant Pathol. 16:202-206.

Fetch, T. G., and Steffenson, B. J. 1999. Rating scales for assessing infection responses of barley infected with *Cochliobolus sativus*. Plant Dis. 83:213-217.

Fetch, T. G., Steffenson, B. J., Bockelman, H. E., and Wesenberg, D. M. 2008. Spring barley accessions with dual spot blotch and net blotch resistance. Can. J. Plant Pathol. 30:534-542.

Ghazvini, H., and Tekauz, A. 2007. Virulence diversity in the population of *Bipolaris sorokiniana*. Plant Dis. 91:814-821.

Grewal, T. S., Rossnagel, B. G., and Scoles, G. J. 2012. Mapping quantitative trait loci associated with spot blotch and net blotch resistance in a doubled-haploid barley population. Mol. Breed. 30:267-279.

Gyawali, S. 2010. Association mapping of resistance to common root rot and spot blotch in barley, and population genetics of *Cochliobolus sativus*. Ph.D. Dissertation. North Dakota State University, Fargo, ND.

Laido, G., Marone, D., Russo, M. A., Colecchia, S. A., Mastrangelo, A. M., De Vita, P., and Papa, R. 2014. Linkage disequilibrium and genome-wide association mapping in tetraploid wheat (*Triticum turgidum* L.). PLoS One 9: e95211.

Mamidi, S., Chikara, S., Goos, R., Hyten, D., Annam, D., Moghaddam, S., Lee, R., Cregan, P., and McClean, P. 2011. Genome-wide association analysis identifies candidate genes associated with iron deficiency chlorosis in soybean. Plant Genome 4:154-164.

Munoz-Amatriain, M., Cuesta-Marcos, A., Endelman, J. B., Comadran, J., Bonman, J. M., Bockelman, H. E., Chao, S., Russell, J., Waugh, R., Hayes, P. M., and Muehlbauer, G. J. 2014. The USDA barley core collection: genetic diversity, population structure, and potential for genome-wide association studies. PLoS One 9: e94688.

Rafalski, A. 2002. Applications of single nucleotide polymorphisms in crop genetics. Curr. Opin. Plant Biol. 5:94-100.

Risch, N. J. 2000. Searching for genetic determinants in the new millennium. Nature 405:847-856.

Roy, J., Smith, K., Muehlbauer, G., Chao, S., Close, T., and Steffenson, B. J. 2010. Association mapping of spot blotch resistance in wild barley. Mol. Breed. 26:243-256.

Steffenson, B. J., Hayes, P. M., and Kleinhofs, A. 1996. Genetics of seedling and adult plant resistance to net blotch (*Pyrenophora teres* f. *teres*) and spot blotch (*Cochliobolus sativus*) in barley. Theor. Appl. Genet. 92:552-558.

Storey, J. D. 2002. A direct approach to false discovery rates. J Roy. Stat. Soc. B. 64:479-498.

Tamang, P., Neupane, A., Mamidi, S., Friesen, T., and Brueggeman, R. 2015. Association mapping of seedling resistance to spot form net blotch in a worldwide collection of barley. Phytopathology 105:500-508.

Valjavec-Gratian, M., and Steffenson, B. J. 1997a. Genetics of virulence in *Cochliobolus sativus* and resistance in barley. Phytopathology 87:1140-1143.

Valjavec-Gratian, M., and Steffenson, B. J. 1997b. Pathotypes of *Cochliobolus sativus* on barley in North Dakota. Plant Dis. 81:1275-1278.

Wilcoxson, R. D., Rasmusson, D. C., and Miles, M. R. 1990. Development of barley resistant to spot blotch and genetics of resistance. Plant Dis. 74:207-210.

Yu, J. M., Pressoir, G., Briggs, W. H., Bi, I. V., Yamasaki, M., Doebley, J. F., McMullen, M. D., Gaut, B. S., Nielsen, D. M., Holland, J. B., Kresovich, S., and Buckler, E. S. 2006. A unified mixed-model method for association mapping that accounts for multiple levels of relatedness. Nat. Genet. 38:203-208.

Zhao, K., Aranzana, M. J., Kim, S., Lister, C., Shindo, C., Tang, C., Toomajian, C., Zheng, H., Dean, C., Marjoram, P., and Nordborg, M. 2007. An Arabidopsis example of association mapping in structured samples. PLoS Genet 3:e4.

Zhao, K., Tung, C.-W., Eizenga, G. C., Wright, M. H., Ali, M. L., Price, A. H., Norton, G. J., Islam, M. R., Reynolds, A., Mezey, J., McClung, A. M., Bustamante, C. D., and McCouch, S. R. 2011. Genome-wide association mapping reveals a rich genetic architecture of complex traits in *Oryza sativa*. Nat. Commun. 2:467.

Zhong, S. B., Ali, S., Leng, Y. Q., Wang, R., and Garvin, D. F. 2015. *Brachypodium distachyon-Cochliobolus sativus* pathosystem is a new model for studying plant-fungal interactions in cereal Crops. Phytopathology 105:482-489.

Zhou, H., and Steffenson, B. J. 2013. Genome-wide association mapping reveals genetic architecture of durable spot blotch resistance in US barley breeding germplasm. Mol. Breed. 32:139-154.

CHAPTER 4: MOLECULAR MAPPING OF A SINGLE DOMINANT GENE FOR RESISTANCE TO A NEW PATHOTYPE OF *COCHLIOBOLUS SATIVUS* IN BARLEY

Abstract

Spot blotch, caused by *Cochliobolus sativus*, is an economically important disease on barley in Upper Midwest region of the USA and Prairie Provinces of Canada. A new pathotype (pathotype 3 isolate ND4008) of the causal pathogen was recently identified in this region, which can overcome the spot blotch resistance widely used in six-row barley cultivars. To identify and characterize genetic loci conferring resistance to this new pathotype, genetic analysis of spot blotch resistance was conducted using a cross between a highly resistant line (PI 235186) and a highly susceptible accession (PI 356741). Seven F_1 plants from the PI 235186/PI 356741 cross were resistant to isolate ND4008 and 212 F_2 individual plants derived from one of the F_1 plants segregated into a 3 (resistant) to 1 (susceptible) ratio ($\chi 2$ =0.23, p=0.63), suggesting a single dominant gene (*Rcsp3-1*) controls the resistance in PI 235186. The result was confirmed by genetic analysis of the $F_{2:3}$ families derived from individual F_2 plants of the cross. *Rcsp3-1* was mapped to the short arm of chromosome 6H based on bulk segregant analysis using 194 SSR markers and genotyping-by-sequencing using 20 SNP markers in the F_2 population. To saturate the genetic region containing *Rcsp3-1*, six co-dominant and two dominant markers were developed based on the genome sequences of barley cv. Morex in the Ensembl Plants database. The resistance gene was finally localized to a ~6.5 centimorgan (cM) region between markers *2548555* and *368749*, which spans 2.8 Mbp in the physical map. *Rcsp3-1* is localized at the same region with the QTL *Rcs-qtl-6H-P3* previously identified by genome-wide association analysis. The identified resistance gene and the associated molecular markers will be useful for developing spot blotch resistance varieties in barley breeding programs.

Introduction

Spot blotch caused by *Cochliobolus sativus* (Ito & Kurib.) Drechs. ex Dastur. [anamorph: *Bipolaris sorokiniana* (Sacc.) Shoem.] is one of the most common and economically important diseases on barley. This disease has been reported in many regions of the world, but is particularly severe in the Upper Midwest region of the USA and Prairie Provinces of Canada. It can cause up to 30% yield loss and negatively impact the malting quality (Wilcoxson et al. 1990; Tekauz and Mueller 2006). Previously, three pathotypes (0, 1, and 2) of *C*. *sativus* were identified based on virulence patterns on three barley differential lines (ND 5883, Bowman, and ND B112) in the Upper Midwest. Resistance from the barley line ND B112 has been effective against all these three pathotypes (Valjavec-Gratian and Steffenson 1997b) and duration of this resistance has lasted for over 50 years (Steffenson et al. 1996; Zhou et al. 2013). However, new pathotypes of *C*. *sativus* showing high virulence on all three barley differential lines were recently identified in Canada (Ghazvini and Tekauz 2007) and North Dakota (Gyawali 2010). This poses a potential threat to barley production in the region and there is an urgent need to identify new sources of resistance to the new pathotypes for developing new resistant barley cultivars.

To utilize the genetic resistance, it is important to determine the genetic loci and identify molecular markers for their quick introgression into cultivars. In the past, great efforts have been made on mapping the spot blotch resistance to pathotype 1 isolate ND85F. The resistance gene *Rcs5* was identified in barley cv. Morex and mapped on the short arm of chromosome 7H (Wilcoxson et al. 1990; Bilgic et al. 2005; Steffenson et al. 1996). Further fine mapping localized this gene to a physical interval of ~240 kb DNA sequence containing two expressed wall-associated kinase genes (Drader 2011). A QTL (Rcs-qtl-4H-10-11) on chromosome 4H

conferring moderate seedling resistance to isolate ND85F was identified in the two-row barley cultivar Bowman using a doubled haploid population derived from the Calicuchima-sib/Bowman-BC cross (Bilgic et al. 2006). In the same study, a resistance locus (*Rcs6*) conferring seedling resistance to pathotype 2 isolate ND90Pr was identified on the short arm of chromosome 1H (Bilgic et al. 2006). In addition, QTL for spot blotch resistance to isolate ND85F have been identified on chromosome 1H, 3H, and 7H through association analyses of various barley germplasms (Zhou and Steffenson 2013; Berger et al. 2013). However, genetic analysis of resistance to the newly emerged pathotype of *C*. *sativus* was not well studied.

Leng et al. (unpublished) screened 2,062 barley accessions from USDA barley core collection for spot blotch resistance to this new pathotype and found 24.5% of the barley accessions showed resistance or moderate resistance. To identify and characterize the genetic loci for spot blotch resistance in this germplasm, genome-wide association analysis was conducted and four QTLs located on chromosome 1H, 2H, 3H, and 6H were found to be associated with the seedling resistance to ND4008 (Wang et al. 2015b). The objective of this study was to localize and fine map the chromosomal location of the resistance gene in PI 235186, one of the highly resistant barley accessions.

Materials and methods

Plant materials

Seven F_1 plants, 212 F_2 individuals and their derived $F_{2:3}$ families from a cross between two parental barley accessions PI 235186 and PI 356741 were used to study the genetics of spot blotch resistance to the new pathotype of *C*. *sativus*. PI 235186 is a six-row spring barley and highly resistant to the new pathotype of *C*. *sativus*, and PI 356741 is a six-row spring barley but

highly susceptible to the new pathotype (Leng et al. unpublished). Both lines are landraces from Mediterranean countries (Libya and Morocco, respectively); they belong to the USDA barley core collection from the USDA-ARS National Small Grains Collection in Aberdeen, Idaho. Five barley lines (Bowman, ND 5883, ND B112, ND 23329, and ND 23345) were used as checks in the phenotyping experiments. Bowman, ND 5883 and ND B112 are three differential barley lines used to identify pathotypes of *C. sativus* (Valjavec-Gratian and Steffenson 1997a; Zhong and Steffenson 2001) while ND 23329 and ND 23345 are two barley lines showing moderately resistant to the isolate ND4008 (Gyawali 2010).

Inoculation and disease assessment

The pathotype 3 isolate ND4008 of *C. sativus* was used to evaluate the spot blotch resistance of barley plants at the seedling stage. Inoculum preparation and inoculation procedure were the same as described in Leng et al. (unpublished). Briefly, inoculum suspension was prepared and adjusted to 1,500 conidia per ml and then was sprayed on the twelve days old seedlings (when the second leaf fully expanded) at a rate of approximately 0.5 ml per plant. After inoculation, seedling plants were transferred into a moist chamber under dark for 18~24 hours before they were returned to the greenhouse under the same growth conditions as described in Leng et al. (unpublished).

Infection responses (IRs) were rated on the second leaves of seedling plants one week after inoculation based on the 1-9 rating scale developed by Fetch and Steffenson (1999), which was based on the lesion type and relative size of lesion observed on barley lines.

DNA extraction and quantification

The newest emerging barley leaves were harvested from four weeks old seedlings (one week after the disease assessment) of individual F_2 plants and their two parents. Genomic DNA was isolated from these leaf samples using the SDS DNA extraction method described in Dellaporta et al. (1983), except that the Elution Buffer (10 mM Tris-Cl, pH 8.0) was used as the dissolve reagent instead of 10 mM Tris-EDTA (pH 8.0). DNA concentration was determined using Qubit 2.0 Fluorometer (Life Technologies) and then was adjusted to 20 ng/μL by adding more Elution Buffer.

Bulked segregant analysis

DNA samples from 8 homozygous resistant F_2 plants (confirmed by $F_{2:3}$ family analyses) were equally combined to form the resistant bulk while DNA samples from 8 homozygous susceptible F_2 plants were equally combined to constitute the susceptible bulk. Then, each of the DNA samples from the two parents and the two bulks was diluted to the concentration of 4 ng/μL for the following SSR genotyping experiment. A total of 194 simple sequence repeat (SSR) markers were used to amplify DNA fragments from the two parents and the two bulks. These SSR markers are distributed on all 7 chromosomes (Appendix D). The markers showing the polymorphism between the two parents as well as between the two bulks were further used to screen the F_2 population.

SSR primers for the 193 SSR markers were obtained from Dr. Shiaoman Chao in USDA-ARS at Fargo, ND and the primers for Bmag0500 were synthesized by Eurofins MWG Operon (www.operon.com) based on the sequence information in GrainGenes Database (http://wheat.pw.usda.gov/GG3/) (Table 4.1). PCR amplifications were carried out in a 10-μl

reaction volume containing 4 ng genomic DNA, 200 nM forward primer with M13 tail, 200 nM reverse primer, 100 nM M13 primer labeled with infrared dyes (IRD-700), 200 μM dNTPs, 1 U *Taq* DNA Polymerase (New England Biolabs, Ipswich, MA, USA), and 1 X ThermoPol Buffer (New England Biolabs, Ipswich, MA, USA) with an Applied Biosystems 2720 Thermal Cycler (Life Technologies, USA) according to the conditions listed in the Appendix E. The amplicons were separated on 6 % acrylamide gel using LI-COR 4300 DNA Analyzer (LI-COR Biosciences, Lincoln, Nebraska USA).

Table 4.1. Primers used in this study

Primer	Sequence 5' to 3'	Purpose
Bmag0500-L	CACGACGTTGTAAAACGACGGG AACTTGCTAATGAAGAG	SSR markers used in BSA
Bmag0500-R	AATGTAAGGGAGTGTCCATAG	
BOPA1_10927_876_L	TTCCTCTGATGCTGCCTGAA	SNP markers used in Ion Torrent
BOPA1_10927_876_R	TTCATTTTCGGAAGGCACGG	
BOPA1_3178_1276_L	GGCCAGCCCATGTATCATTT	
BOPA1_3178_1276_R	AGAAACCGAGGTGAGGGAAG	
BOPA1_3378_619_L	GTCCCTGTTTAAGCGGTCCT	
BOPA1_3378_619_R	AGACATCAAGACACTCCCGT	
BOPA1_3580_331_L	CGGGAGTGTCTTGATGTCTTC	
BOPA1_3580_331_R	TTTCCTCTCCACCCTTGTCC	
BOPA1_4191_268_L	GGTGTTTTAAGTAGCGGGCT	
BOPA1_4191_268_R	AGTACATGCAACCAACGCTG	
BOPA1_4445_1911_L	GCGTGACTTTGTTGCACCAT	
BOPA1_4445_1911_R	TCAAGGGAAGGACTAAGGCC	
BOPA1_5159_579_L	GGATTGTCTTGTCCCGGTTG	
BOPA1_5159_579_R	AAAAGTAGCACCGCCAACAG	
BOPA1_6018_235_L	TGTCAAGAGCTAGAGTCCGC	
BOPA1_6018_235_R	CCCAACTCGCCAAACCAAAT	
BOPA2_12_30658_L	TGAGAGAGGAGGAGGAGGAC	
BOPA2_12_30658_R	CGTAACGGCCCTTCTTGAG	
SCRI_RS_121633_L	ATGCGTGCCAAACAGTGAAT	

Table 4.1. Primers used in this study (continued)

Primer	Sequence 5' to 3'	Purpose
SCRI_RS_129888_R	TGTCTTGGTCCTCATCGCTT	SNP markers used in Ion Torrent
SCRI_RS_138556_L	TGCACCTATCATACATGGCAA	
SCRI_RS_138556_R	TTCGTCTCCATACCACCCAC	
SCRI_RS_141429_L	AGCCTTCACCAACTCCTCTG	SNP markers used in Ion Torrent
SCRI_RS_141429_R	GCAACCAGTAGCCAGCAAAT	
SCRI_RS_142506_L	GCTAGTCCATACAGAGGAGCT	
SCRI_RS_142506_R	GACGTATTCAGCCTGGGACA	
SCRI_RS_147342_L	GACATGACATCGAACCCACG	
SCRI_RS_147342_R	GTTGCCCCTATTGAAAGCCC	
SCRI_RS_150028_L	TGCACTACACACACATTGCT	
SCRI_RS_150028_R	AATGGCTAGATCACCGCTCA	
SCRI_RS_171247_L	CCCCATGTGAACAGTAGCAAC	
SCRI_RS_171247_R	CCCAACCAACACCATATGCC	
SCRI_RS_228181_L	CCCTCAGATGGCAGGAATGA	
SCRI_RS_228181_R	TGCGGTTTCCAAATTGAGGG	
SCRI_RS_231003_L	TGGATGGAAGGAGTCGTGAG	
SCRI_RS_231003_R	GAAGCTGACGAGGAAGAGGA	
SCRI_RS_238639_L	CCATGACCAAGAGCCGAAAG	
SCRI_RS_238639_R	AGAACTTGATGCAGATGGGC	
96_1-F	CCCTCCAGGTGCTTCGTATT	Genome sequence-based markers used in fine mapping of the resistance gene
96_1-R	GATCGACGTCAACAGCCTC	
137_1-F	TTCTCCAGCACTGTCGGAAT	
137_1-R	GAATACGTCGGTGAGGATCG	
107_1-F	TTGCTTCTACGGTCAAGGGT	
107_1-R	GGCTTCTTCCCACAGATGAC	
103_1-F	ATGCATAACTCAAGCAGCCG	
103_1-R	GATCAACGTCACCTTGGCC	
368749-2-F	GCTCGGAAAACTGGCTAACC	
368749-2-R	GAACAGGAGTGCTCTTCCC	
2548555-1-F	GAGCAGCATCTCTTCCCTGA	
2548555-1-R	CGAGCAGCCATCCGTTAT	
56795-1-F	GAGCCTCATCATCGGGTACA	
56795-1-R	CCAGCTAAGCACATTCCCAA	
6354-2-F	TGAAAACCGGCTTGTCCTTG	
6354-2-R	ATTACCTTTGTCACGCGAGC	

Genotyping-by-sequencing

Based on the genotyping data developed by the Triticeae Coordinated Agricultural Project (TCAP) for USDA barley core collection, twenty single nucleotide polymorphism (SNP) markers located on the short arm of barely chromosome 6H (Table 4.2) were selected for genotyping-by-sequencing the 212 F_2 individuals using the Ion Torrent technology. The primers were designed using Primer3web (http://bioinfo.ut.ee/ primer3/) and listed in Table 4.1.

Table 4.2. Information for SNP makers used in the genotyping-by-sequencing

SNP name	Chromosome	Position (cM)	PI356741	PI235186	SNP source
BOPA1_3178_1276	6H	0.5	AA	BB	[A/C]
BOPA1_5159_579	6H	1.4	AA	BB	[A/G]
SCRI_RS_231003	6H	11.1	AA	BB	[A/C]
SCRI_RS_129888	6H	15.7	AA	BB	[A/G]
SCRI_RS_138556	6H	24.5	AA	BB	[T/C]
BOPA1_10927_876	6H	43.6	BB	AA	[A/G]
SCRI_RS_141429	6H	43.6	BB	AA	[T/C]
BOPA1_3580_331	6H	44.1	BB	AA	[A/C]
SCRI_RS_150028	6H	44.1	BB	AA	[T/C]
SCRI_RS_171247	6H	47.5	AA	BB	[T/C]
BOPA1_4445_1911	6H	48.8	AA	BB	[A/G]
SCRI_RS_228181	6H	48.8	BB	AA	[A/G]
SCRI_RS_238639	6H	48.8	AA	BB	[T/C]
SCRI_RS_147342	6H	48.9	AA	BB	[A/G]
BOPA1_6018_235	6H	49.1	BB	AA	[A/C]
BOPA1_4191_268	6H	49.1	BB	AA	[A/G]
BOPA2_12_30658	6H	49.1	BB	AA	[A/G]
SCRI_RS_121633	6H	49.1	AA	BB	[T/C]
SCRI_RS_142506	6H	49.1	BB	AA	[C/G]
BOPA1_3378_619	6H	49.8	AA	BB	[A/G]

Marker development based on barley genome sequences

Based on the genome sequence and physical map of barley cv. Morex in the Ensembl Plants database developed by European Bioinformatics Institute (EBI) (http://plants.ensembl.org/Hordeum_vulgare/Location/Genome), DNA contigs around the genomic region containing the resistance gene on the short arm of chromosome 6H were selected for primer design and PCR amplification (The designed primers for each contig were listed in Table 4.1). For each contig, about 1 kb length of DNA sequence was amplified from the two parental barley lines used in this study. PCR amplifications were carried out in a 20-µl reaction volume containing 20 ng genomic DNA, 200 nM forward primer with M13 tail, 200 nM reverse primer, 200 µM dNTPs, 2 U *Taq* DNA Polymerase (New England Biolabs, Ipswich, MA, USA), and 1 X ThermoPol Buffer (New England Biolabs, Ipswich, MA, USA) with an Applied Biosystems 2720 Thermal Cycler (Life Technologies, USA) according to the conditions as following: 1 cycle of 1 min at 95ºC, 40 cycles of 1 min at 94ºC, 30s at 58ºC or 60ºC, 1.5 min at 72ºC, and 1 cycle of 5 mins at 72ºC. The amplified PCR products were loaded and separated on 1.2 % agarose gel stained with ethidium bromide and scanned using UV gel photograph system. 1 kb ladder (New England Biolabs, Ipswich, MA) was used to determine the size of DNA fragment. If the amplified fragment was only present in one parent but absent in the other parent, it was used as the dominant marker. If the amplified fragments were present in both parents with similar size, the two amplified PCR products were purified and then sent to GenScript (http://www.genscript.com/) for sequencing. By aligning the two sequences from the parents, SNPs were identified and then detected using restriction enzyme digestion. Finally, different sized DNA fragments resulting from the enzyme digested PCR products of the two parents and

the F_2 population were separated in 1.2% agarose gel and photographed using a UV gel photograph system.

Data analyses and genetic map construction

To determine the goodness-of-fit of the observed segregation ratios with the expected genetic ratios in F_2 population and $F_{2:3}$ families, chi-square analyses were performed in RStudio v0.98.1091 (RStudio, Inc. Boston, MA). The markers with the percentage of missing calls > 10% were removed for the further genetic linkage analysis. The genetic linkage map was constructed and drawn in MapDisto (Lorieux 2012) with the setting of minimum LOD at 3.0 and Kosambi mapping function.

Results

Inheritance of spot blotch resistance in PI 235186

The two parental barley accessions PI 235186 and PI 356741 exhibited mean IR of 2.7 and 8.2, respectively (Table 4.3). The two moderately resistant checks ND 23329 and ND 23345 exhibited the expected infection responses with mean IRs of 4.7 and 4.3, respectively, whereas the susceptible checks, Bowman, ND B112 and ND 5883, exhibited high infection response with mean IRs of 6.0, 6.7, and 7.0, respectively (Table 4.3). The seven F_1 plants from the cross between PI 235186 and PI 356741 had IRs from 2 to 3, similar to the resistant parent PI 235186, indicating a dominance relationship of resistance/susceptibility. The 212 F_2 individuals derived from one of the F_1 plants segregated into a 3 (resistant) to 1 (susceptible) ratio with $\chi 2$ of 0.23 and *p* value of 0.63 (Table 4.4). The $F_{2:3}$ families derived from these 212 F_2 plants segregated

into a 1 (homozygous resistant) : 2 (segregating) : 1 (homozygous susceptible) ratio with $\chi 2$ of 1.43 and *p* value of 0.49 (Table 4.4). These results suggest the involvement of one dominant gene for resistance in PI 235186 as reported in Leng et al. (unpublished). The resistance gene was designated as *Rcsp3-1*.

Table 4.3. Infection responses for two parents and checks

Lines	Country of origin	Row type	IR to ND4008
PI 235186	Libya	6	2.7±0.8
PI 356741	Morocco	6	8.2±0.6
ND 23345	United States	6	4.3±0.6
ND 23329	United States	6	4.7±0.7
Bowman	United States	2	6.0±0.7
ND B112	United States	6	6.7±0.7
ND 5883	United States	2	7.0±0.9

Table 4.4. Frequency distribution of the F_2 population and corresponding $F_{2:3}$ family when tested against pathotype 3 of *C*. *sativus* at the seedling stage

Ratio of F2 plants	Expected ratio	$\chi 2$	*p* value
156:56 (R:S)[a]	3:1	0.226	0.6342
Ratio of F2:3 families	**Expected ratio**	**$\chi 2$**	***p* value**
46:108:58 (HR:SEG:HS)[b]	1:2:1	1.434	0.4882

[a] R = resistant plants exhibiting low infection responses (ranges 1 to 4), similar to those of the resistant parent PI 235186
S = susceptible plants exhibiting high infection responses (range 6 to 9, with an occasional 5), similar to the susceptible parent PI356741.
[b] HR = homozygous resistant
SEG = segregating
HS = homozygous susceptible

Chromosomal location of *Rcsp3-1*

Among the 194 SSR markers screened, only two markers (*Bmac0316* and *Bmag0500*) located on the short arm of chromosome 6H showed polymorphism between the resistant and

susceptible bulks as well as the two parents. Genotyping of the 212 F_2 barley individual plants with these two markers indicated that they are linked with *Rcsp3-1* (Fig. 4.1). Further genotyping-by-sequencing of the F_2 population with 20 SNP markers located on the short arm of chromosome 6H identified two SNP markers (*BOPA1_5159_579* and *SCRI_RS_129888*). With the two SSR markers, two SNP markers and the resistance gene *Rcsp3-1*, a genetic linkage map was constructed, which spanned over a total genetic distance of 29.3 cM (Fig. 4.1). The two markers (SSR marker *Bmac0316* and SNP marker *SCRI_RS_129888*) flanking *Rcsp3-1* were at distances of 10.9 cM distal and 5.0 cM proximal, respectively (Fig. 4.1).

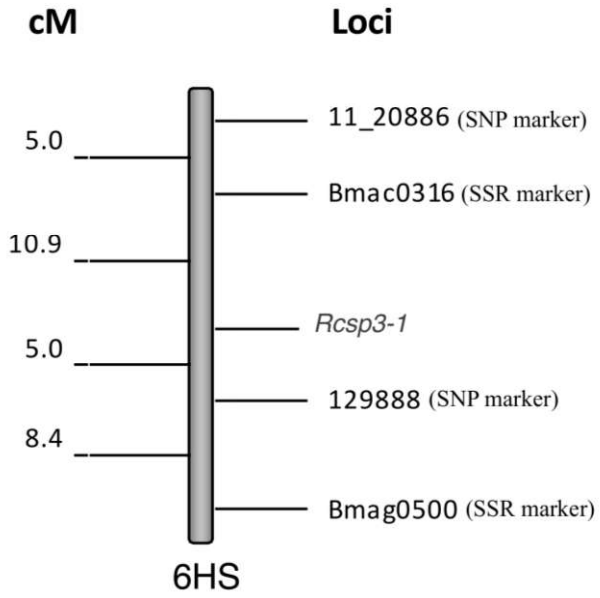

Fig. 4.1. Genetic linkage map of chromosome 6H showing location of spot blotch resistance gene *Rcsp3-1* based on SSR and SNP markers.

Fine mapping of *Rcsp3-1*

To fine map *Rcsp3-1*, genome sequences of barley cv. Morex were used to develop additional markers to saturate the *Rcsp3-1* carrying region. From the contigs located between 9

Mbp to 15 Mbp on short arm of chromosome 6H in the Morex physical map, eight markers, including two dominant and six co-dominant markers, were identified and mapped to the linkage map (Fig. 4.2). The primer sequences of these markers and their corresponding contigs as well as the physical positions of the contigs were listed in Table 4.5. As illustrated in Fig. 4.2, the linkage map spanned over a total genetic distance of 16.8 cM with two closely linked markers (*2548555* and *368749*) flanking *Rcsp3-1*. The marker *2548555* was mapped 2.0 cM distal to *Rcsp3-1*, and the marker *368749* was mapped at 4.5 cM proximal to *Rcsp3-1* (Fig. 4.2). This 6.5 cM genetic region spans a 2.8 Mbp distance from 12 Mbp to 13.8 Mbp based on the Morex physical map. The genetic map developed by the F_2 population of the cross PI 235186/PI 356741 showed a very good colinearity with the physical map of barley cv. Morex, because the positions of molecular markers in genetic map are highly consistent with the positions of the markers' corresponding contigs in the physical map (Fig. 4.2).

Table 4.5. List of markers developed based on barley genome sequences and their physical position

Marker Name[a]	Contig	Chromosome	Genetic position (cM)[b]	Physical position[c]
1588985	Morex_contig_1588985	6HS	-[d]	unordered
41676	Morex_contig_41676	6HS	13.67	6:10609473-10622470
40985	Morex_contig_40985	6HS	13.53	6:10265560-10275542
6354	Morex_contig_6354	6HS	13.67	6:10787934-10792922
2548555	Morex_contig_2548555	6HS	15.16	6:11006445-11016693
368749	Morex_contig_368749	6HS	16.01	6:13806160-13814889
56795	Morex_contig_56795	6HS	17.71	6:14976307-14990427
1561906	Morex_contig_1561906	6HS	17.71	6:15035784-15044711

[a] The marker names indicate the Morex contig names in Ensembl Plants database.
[b] The genetic position is based on Barley WGS Morex Assembly version3 (International Barley Genome Sequencing).
[c] This physical position is based on Ensembl Plants database.
[d] - indicates no data is available.

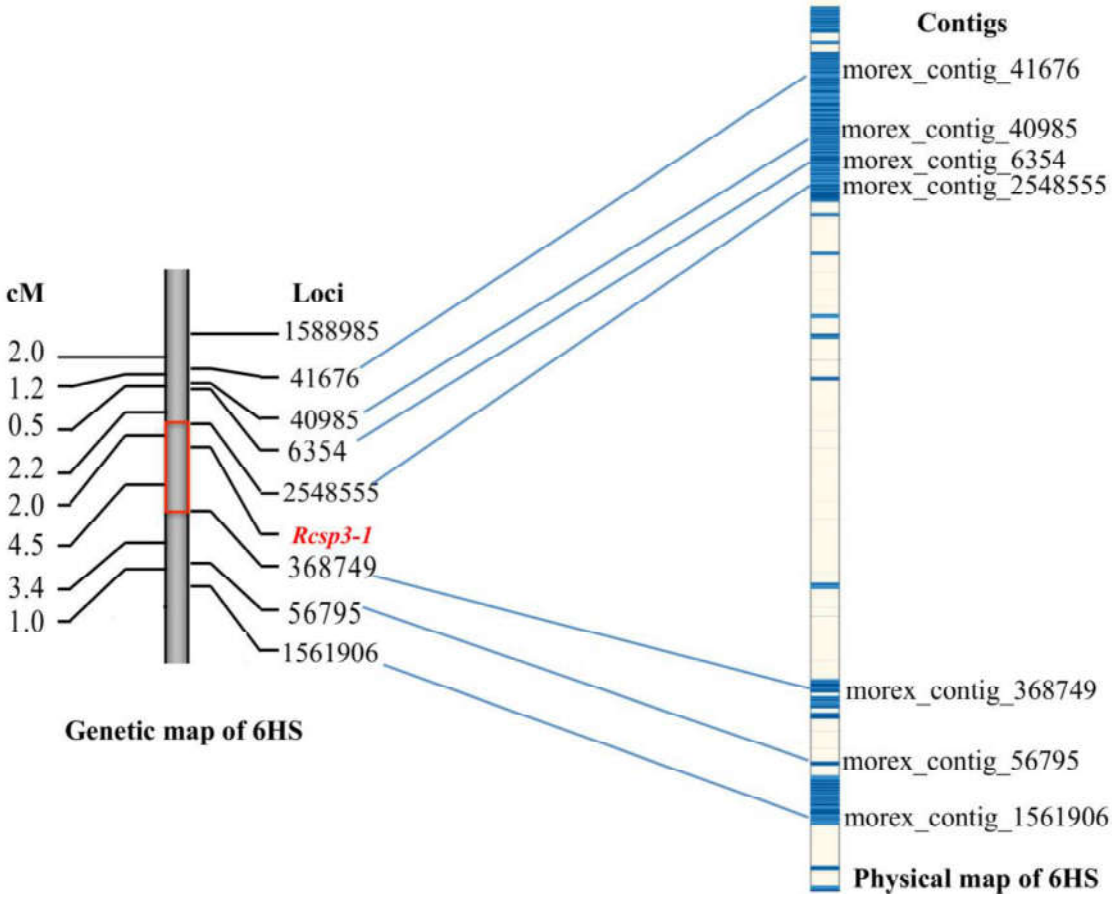

Fig. 4.2. Saturated genetic linkage map of chromosome 6H showing location of spot blotch resistance gene *Rcsp3-1* based on genome sequence-derived markers. The resistance gene region was flanked by two markers (*2548555* and *368749*) that define a 6.5 cM region in the genetic map and span 2.8 Mbp in physical map. The blue lines indicated the colinearity between the genetic map and the physical map.

Discussion

Although the spot blotch resistance derived from ND B112 has been effective for over 50 years and almost all the six-row malting barley cultivars in the Upper Midwest region contain this resistance, the emergence of the new pathotype that can overcome this resistance is alarming and may cause widespread disease epidemic considering the uniformity of the barley genetic background in this region. By screening of 2,062 barley accessions from the USDA barley core collection, 44 accessions were identified as resistant to the new pathotype (Leng et al.

unpublished). However, genetic analysis and molecular mapping of the resistance in these resistant barley accessions were not well studied. Association analysis identified four QTL associated with the resistance to isolate ND4008 (Wang et al. 2015). In this study, we studied the genetics of the resistance in one of the resistant accessions using a bi-parental cross and showed that a single dominant gene confers the resistance in PI 235186. This result is consistent with those of Leng et al. (unpublished), who investigated the inheritance of resistance to ND4008 in three barley accessions and indicated that a single dominant gene is responsible for resistance in each of the three resistant barley lines.

Using bulk segregant analysis and genotyping-by-sequencing technology, we mapped the resistance gene *Rcsp3-1*on the short arm of chromosome 6H. Based on the genome sequence of barley cv. Morex, the resistance gene was further localized to a ~6.5 cM region which spans 2.8 Mbp in the physical map. The same region contains the resistance QTL *Rcs-qtl-6H-P3*, which was previously detected by association analysis of the USDA barley collection (Wang et al. 2015b). Based on positions of the markers identified in genome-wide association analysis and the genome-based markers developed in this study, *Rcsp3-1* and *Rcs-qtl-6H-P3* may be the same gene or localized at the same locus. However, further fine mapping is needed to reveal the relationship of *Rcsp3-1* and *Rcs-qtl-6H-P3* since the genome sequence for the detected QTL region is missing in the database.

The QTL conferring resistance to spot blotch have been identified in several mapping populations and germplasms using different pathotypes of *C*. *sativus*. These QTL are located on all barley chromosomes except for 6H (Berger et al. 2013; Bilgic et al. 2005; Bilgic et al. 2006; Bovill et al. 2010; Grewal et al. 2012; Roy et al. 2010; Steffenson et al. 1996; Wang et al. 2005;

Wilcoxson et al. 1990; Zhou and Steffenson 2013). Therefore, *Rcs-qtl-6H-P3* and *Rcsp3-1* on the short arm of 6H may represent a novel gene for spot blotch resistance.

Genetic analysis of F_1 plants and F_2 as well as F_3 progenies from the cross between PI 235186 and PI 356741 indicated that a single dominant gene (*Rcsp3-1*) controls the resistance to ND4008 in PI 235186. This resistance gene may function differently from the two genes (*Rcs5* and *Rcs6*) previous identified to confer resistance/susceptibility to other two pathotypes (ND85F and ND90Pr) of *C*. *sativus*. The resistance gene *Rcs5* identified in Morex was fine mapped to a physical interval of ~240 kb DNA sequence containing two expressed wall-associated kinase (WAK) genes on chromosome 7H (Drader et al. 2011). However, further allele analysis of the WAK gene *ctg37* suggested that the gene allele at the *Rcs5* locus in Morex might function as a recessive gene (Drader et al. 2011). Similarly, Valjavec-Gratian (1996) showed that the F_1 plants of the Bowman (resistant to ND85F) / ND 5883 (susceptible to ND85F) cross were susceptible to the isolate ND85F, indicating that the susceptibility to isolate ND85F is dominant. For the pathosystem involving pathotype 2 of *C*. *sativus* (ND90Pr) and the barley cv. Bowman, a single gene (*Rcs6*) on chromosome 1H was identified conferring resistance to pathotype 2 using a doubled haploid (DH) population derived from the cross Calicuchima-sib/ Bowman-BC (Bilgic et al. 2006). *Rcs6* is a recessive resistance gene allele contributed by the resistant parent Calicuchima-sib because the other parent Bowman-BC is highly susceptible to isolate ND90Pr. This result is further confirmed by genetic analysis of the cross between Bowman and ND 5883 (resistant to ND90Pr), which showed that the F_1 plants exhibited susceptible reactions to ND90Pr (Vejevec and Steffenson 1997b; Leng et al. unpublished). Using a F_2 population derived from the cross between ND 5883 and Bowman, a single dominant gene allele (*Scs1*) conferring susceptibility in Bowman to ND90Pr was mapped to the same locus as *Rcs6* (Leng et al.

unpublished). The virulence factor of isolate ND90Pr inducing susceptibility of Bowman was identified as a secondary metabolite peptide synthesized by two nonribosomal peptide synthetases (NRPSs) based on the fact that deletion of either of the genes encoding the NRPSs abolished the virulence of the pathogen (Condon et al. 2013; Leng and Zhong, unpublsihed data). Further studies of global regulators *velvet*-complex, containing CsLaeA, CsVeA, CsVelB, and CsVelC (Wang et al. unpublished) as well as CsVosA (Wang et al. 2015a), supported the hypothesis that the secondary metabolite, presumably synthesized by the NRPSs, is the main virulence factor in ND90Pr. All these results led to a hypothesis that molecular interactions between the isolates ND85F and ND90Pr and their corresponding barley hosts follow the reverse gene for gene interactions, in which the virulence effector produced by the pathogen interacts with the receptor in the host to trigger the susceptibility response, as has been found in other related species in Dothidemycete*, including C. heterostrophus*, *C. victoriae* , *Pyrenophora tritici-repentis* and *Stagonospora nodorum* (Ciuffetti et al. 2010; Friesen et al. 2008; Hooker et al. 1970; Lorang et al. 2004; Lorang et al. 2007). In all these cases, the fungal effector interacts with host targets to cause disease and so the susceptibility of the host is dominant while resistance is recessive.

For the new pathotype 3 isolate ND4008, deletion of *PPT1*, a gene required for activation of NRPSs, significantly reduced the virulence on susceptible barley lines (Leng et al. unpublished), suggesting the virulence factor in this pathotype isolate may require NRPSs for biosynthesis just like as found for the pathotype 2 isolate ND90Pr (Condon et al. 2013; Leng and Zhong 2012). However, the interaction between isolate ND4008 and barley is different from the pathosystems involving isolates ND85F and ND90Pr. The gene *Rcsp3-1* conferring resistance to ND4008 is dominant while the genes *Rcs5* and *Rcs6* conferring resistance to ND85F and ND90Pr,

respectively, are recessive. One possible mechanism of *Rcsp3-1* may be through producing an enzyme to detoxify the virulence factor, just like the gene *Hm1* for resistance to the north corn leaf blight fungus *C*. *carbonum* (Johal and Briggs 1992). In this mechanism, *Hm1* encodes a carbonyl reductase that inactivates the HC toxin produced by *C*. *carbonum* (Johal and Briggs 1992). Another possible mechanism of *Rcsp3-1* may by encoding a protein that can enhance cellular processes that are important for restricting toxin-induced cell death (Mengiste 2012). In this situation, although the virulence factor can interact with the susceptibility target in the host to induce cell death, the host can restrict this process by some defense reaction. For example, *Asc-1* gene in resistant tomatoes rescues hairy roots from SAM (sphinganine-analog mycotoxins)-induced cell death by the production of alternative ceramides whereas in sensitive plants, EGGAP (ER-to-Golgi transport of glycosylphosphatidylinositol anchored proteins) transport could be halted by SAM because of a lack of alternative ceramide production by the dysfunctional ASC1 protein, leading to apoptosis (Brandwagt et al. 2000). Further cloning and functional characterization of the resistance genes in host and the virulence genes in different pathotypes will facilitate a better understanding of the molecular interactions between barley and *C*. *sativus*.

Acknowledgements

The authors thank Joseph Mullins, Qiang Li and Mingxia Zhao for assistance in phenotyping work. We also acknowledge Dr. Shiaoman Chao in USDA-ARS at Fargo, ND for providing the primers for SSR markers and the corresponding information. This research was funded by the Triticeae-CAP project (2011-68002-30029) of the US Department of Agriculture National Institute of Food and Agriculture.

References

Berger, G. L., Liu, S., Hall, M. D., Brooks, W. S., Chao, S., Muehlbauer, G. J., Baik, B. K., Steffenson, B., and Griffey, C. A. 2013. Marker-trait associations in Virginia Tech winter barley identified using genome-wide mapping. Theor. Appl. Genet. 126:693-710.

Bilgic, H., Steffenson, B., and Hayes, P. 2005. Comprehensive genetic analyses reveal differential expression of spot blotch resistance in four populations of barley. Theor. Appl. Genet. 111:1238-1250.

Bilgic, H., Steffenson, B. J., and Hayes, P. M. 2006. Molecular mapping of loci conferring resistance to different pathotypes of the spot blotch pathogen in barley. Phytopathology 96:699-708.

Bovill, J., Lehmensiek, A., Sutherland, M. W., Platz, G. J., Usher, T., Franckowiak, J., and Mace, E. 2010. Mapping spot blotch resistance genes in four barley populations. Mol. Breed. 26:653-666.

Brandwagt B. F., Mesbah L. A., Takken F. L., Laurent P. L., Kneppers T. J., Hille J., Nijkamp H. J. 2000. A longevity assurance gene homolog of tomato mediates resistance to *Alternaria alternata* f. sp. *lycopersici* toxins and fumonisin B1. Proc. Natl. Acad. Sci. USA 97:4961–4966.

Castro, A. J., Gamba, F., German, S., Gonzalez, S., Hayes, P. M., Pereyra, S., and Perez, C. 2012. Quantitative trait locus analysis of spot blotch and leaf rust resistance in the BCD47 Baronesse barley mapping population. Plant Breeding 131:258-266.

Ciuffetti, L. M., Manning, V. A., Pandelova, I., Betts, M. F., Martinez, J. P. 2010. Host-selective toxins, Ptr ToxA and Ptr ToxB, as necrotrophic effectors in the *Pyrenophora tritici-repentis*-wheat interaction. New Phytol. 187: 911-919.

Condon, B., Leng, Y. Q., Wu, D., Bushley, K., Ohm, R., Otillar, R., Martin, J., Schackwitz, W., Grimwood, J., MohdZainudin, N., Xue, C., Wang, R., Manning, V., Dhillon, B., Tu, Z., Steffenson, B., Salamov, A., Sun, H., Lowry, S., LaButti, K., Han, J., Copeland, A., Lindquist, E., Barry, K., Schmutz, J., Baker, S., Ciuffetti, L., Grigoriev, I., Zhong, S. B., and Turgeon, B. 2013. Comparative genome structure, secondary metabolite, and effector coding capacity across *Cochliobolus* pathogens. PLoS Genet. 9:e1003233.

Dellaporta, S. L., Wood, J., Hicks, J. B. 1983. A plant DNA minipreparation: version II. Plant Mol. Biol. Rep. 1:19-21.

Drader, T. B. 2011. Cloning of the seedling spot blotch resistance gene Rcs5. Ph.D. Thesis. Washington State University, Pullman, WA.

Fetch, T. G., and Steffenson, B. J. 1994. Identification of *Cochliobolus-sativus* isolates expressing differential virulence on 2-row barley genotypes from North-Dakota. Can. J. Plant Pathol. 16:202-206.

Fetch, T. G., and Steffenson, B. J. 1999. Rating scales for assessing infection responses of barley infected with *Cochliobolus sativus*. Plant Dis. 83:213-217.

Friesen, T. L., Faris, J. D., Solomon, P. S., Oliver, R. P. 2008. Host-specific toxins: effectors of necrotrophic pathogenicity. Cell Microbiol. 10:1421-1428.

Ghazvini, H., and Tekauz, A. 2007. Virulence diversity in the population of *Cochliobolus sativus*. Ph.D. Dissertation. Plant Dis. 91:814-821.

Grewal, T. S., Rossnagel, B. G., and Scoles, G. J. 2012. Mapping quantitative trait loci associated with spot blotch and net blotch resistance in a doubled-haploid barley population. Mol. Breed. 30:267-279.

Gyawali, S. 2010. Association mapping of resistance to common root rot and spot blotch in barley, and population genetics of *Cochliobolus sativus*. Ph.D. Dissertation. North Dakota State University, Fargo, ND.

Hooker, A., Smith, D., Lim, S., Beckett, J. 1970. Reaction of corn seedlings with male-sterile cytoplasm to *Helminthosporium maydis*. Plant Dis. Reptr. 54:708-712.

Johal, G. S., and Briggs, S. P. 1992. Reductase activity encoded by the *HM1* disease resistance gene in maize. Science 258:985-987.

Leng, Y. Q., and Zhong, S. B. 2012. Sfp-type 4 '-phosphopantetheinyl transferase is required for lysine synthesis, tolerance to oxidative stress and virulence in the plant pathogenic fungus *Cochliobolus sativus*. Mol. Plant Pathol. 13:375-387.

Liu, Z. W., Biyashev, R. M., Saghai Maroof, M. A. 1996. Development of simple sequence repeat DNA markers and their integration into a barley linkage map. Theor. Appl. Genet. 93:869–876.

Lorang, J. M., Carkaci-Salli, N., Wolpert, T. J. 2004. Identification and characterization of victorin sensitivity in *Arabidopsis thaliana*. Mol. Plant Microbe In. 17:577-582.

Lorang, J. M., Sweat, T. A., Wolpert, T. J. 2007. Plant disease susceptibility conferred by a "resistance" gene. P. Natl. Acad. Sci. USA 104:14861-14866.

Lorieux, M. 2012. MapDisto: fast and efficient computation of genetic linkage maps. Mol. Breed. 30:1231-1235.

Mengiste, T. 2012. Plant immunity to necrotrophs. Annu. Rev. Phytopathol. 50:267-294.

Röder, M. S., Korzun, V., Wendehake, K., Plaschke, J., Tixier, M. H., Leroy, P., Ganal, M. W. 1998. A microsatellite map of wheat. Genetics 149:2007–2023

Roy, J., Smith, K., Muehlbauer, G., Chao, S., Close, T., and Steffenson, B. J. 2010. Association mapping of spot blotch resistance in wild barley. Mol. Breed. 26:243-256.

Sreenivasulu, N., Graner, A., and Wobus, U. 2008. Barley genomics: An overview. Int. J. Plant Genomics 2008:486258.

Steffenson, B. J., Hayes, P. M., and Kleinhofs, A. 1996. Genetics of seedling and adult plant resistance to net blotch (*Pyrenophora teres* f *teres*) and spot blotch (*Cochliobolus sativus*) in barley. Theor. Appl. Genet. 92:552-558.

Tekauz, A., and Mueller, E. 2006. The leaf spot complex of barley in Manitoba, Canada: a 10-year perspective. In: Proceedings of the 3rd international workshop on barley leaf blights. Edmonton, Alberta, Canada, pp. 63–66.

Tinline, R. D., Strauffer, J. F., and Dickson, J. G. 1960. *Cochliobolus sativus* III. Effects of ultraviolet radiation. Can. J. Bot. 38:275–282.

Valjavec-Gratian, M. 1996. Genetics of resistance and virulence in the *Hordeum vulgare*:*Cochliobolus sativus* pathosystem. Ph.D. Dissertation. North Dakota State University, Fargo.

Valjavec-Gratian, M., and Steffenson, B. J. 1997a. Genetics of virulence in *Cochliobolus sativus* and resistance in barley. Phytopathology 87:1140-1143.

Valjavec-Gratian, M., and Steffenson, B. J. 1997b. Pathotypes of *Cochliobolus sativus* on barley in North Dakota. Plant Dis. 81:1275-1278.

Van Esbroeck, G. A., Bowman, D. T., May, O. L., and Calhoun, D. S. 1999. Genetic similarity indices for ancestral cotton cultivars and their impact on genetic diversity estimates of modern cultivars. Crop Sci. 39:323-328.

Wang, R., Leng, Y. Q., and Zhong, S. B. 2015a. The regulatory gene *VosA* affects conidiogenesis and is involved in virulence of the fungal cereal pathogen *Cochliobolus sativus*.

Wang, R., Leng, Y. Q., Wang, M., and Zhong, S. B. 2015b. Genome-wide association mapping of seedling resistance to two different pathotypes of *Cochliobolus sativus* in a USDA barley core collection. Phytopathology.

Wilcoxson, R. D., Rasmusson, D. C., and Miles, M. R. 1990. Development of barley resistant to spot blotch and genetics of resistance. Plant Dis. 74:207-210.

Zhong, S. B., and Steffenson, B. J. 2001. Genetic and molecular characterization of mating type genes in *Cochliobolus sativus*. Mycologia 93:852-863.

Zhou, H., and Steffenson, B. J. 2013. Genome-wide association mapping reveals genetic architecture of durable spot blotch resistance in US barley breeding germplasm. Mol. Breed. 32:139-154.

APPENDIX A: GENERATION AS WELL AS SOUTHERN BLOT CONFIRMATION OF *VELVET*-COMPLEX GENE MUTANTS AND COMPLEMENTED STRAINS IN *COCHLIOBOLUS SATIVUS*

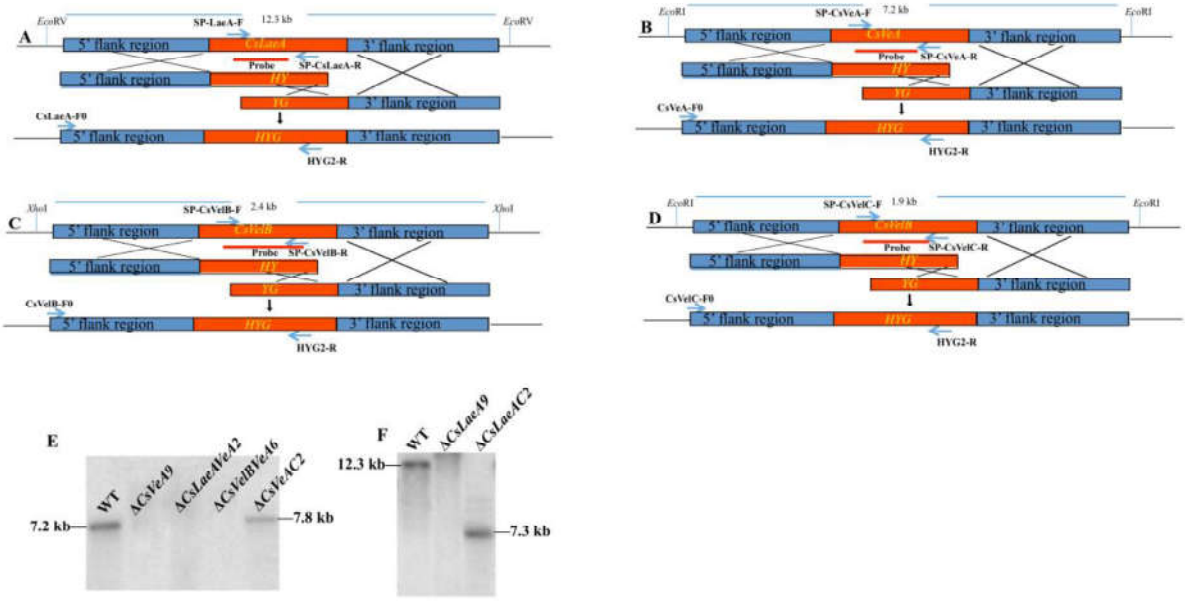

A-D. Schematic representation of the replacement of the *Csvelvet* genes by a 2.6-kb fragment carrying the *Escherichia coli* hygromycin phosphotransferase gene (*hph*) using the split-marker system. **E-F.** Southern blot of digested genomic DNA from the wild type, knockout mutants, and complemented strains using the probes from the Cs*velvet* gene encoding sequences using primer pair SP-Cs*velvet*-F and SP-Cs*velvet*-R and labeled by ^{32}P. The fragments in the wild type strain and complemented strain were indicated while no hybridization signal were observed in the knockout mutants strain.

APPENDIX B: POLYMERASE CHAIN REACTION (PCR) AMPLIFICATION ANALYSIS OF THE WILD TYPE (ND90PR), KNOCKOUT MUTANTS AND COMPLEMENTED STRAINS USING PRIMER PAIRS

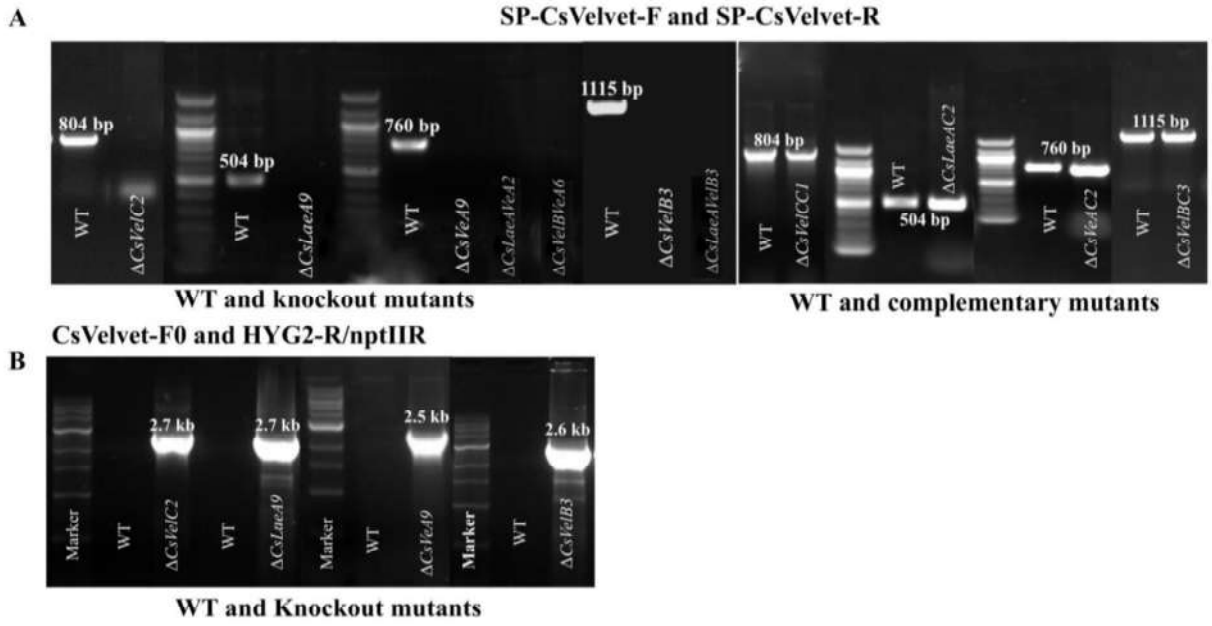

A. SP-Cs*velvet*-F/SP-Cs*velvet*-R and **B.** Cs*velvet*-F0/HYG2-R or nptIIR.

APPENDIX C: *VELVET*-COMPLEX GENES INFLUENCE THE CONIDIAL AND CULTURAL MORPHOLOGY AS WELL AS AERIAL MYCELIUM GROWTH

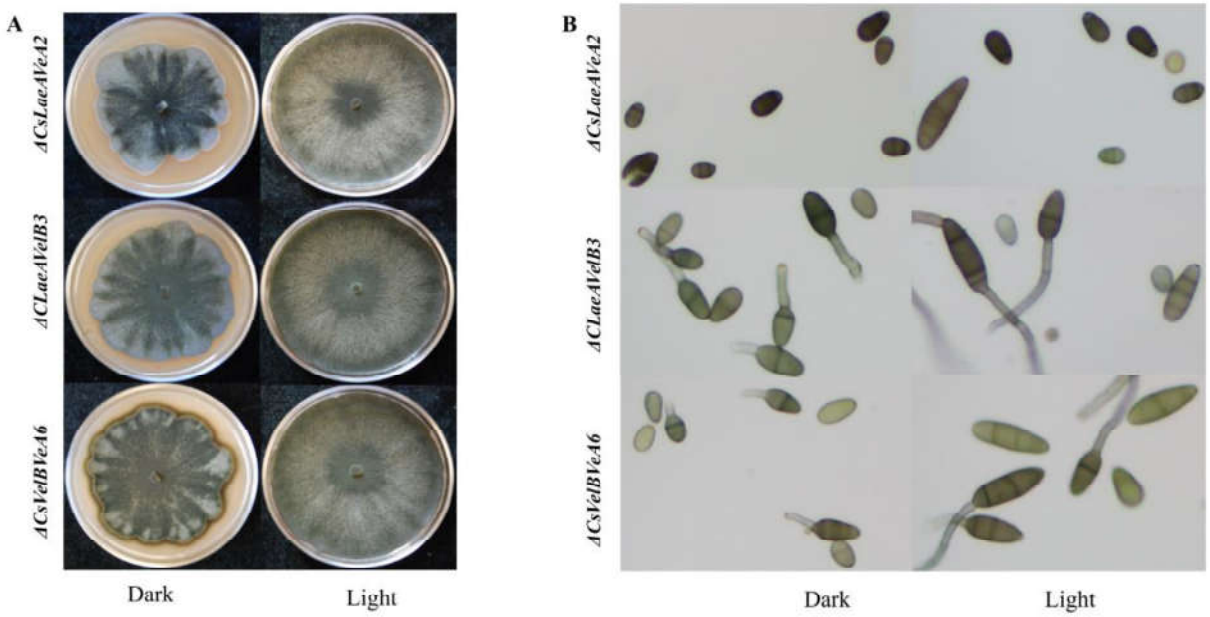

A. Cultural morphology and aerial mycelium growth of three double knockout mutants grown on V8 PDA under constant dark and constant light conditions. **B.** Conidial morphology of three double knockout mutants. The strains were grown on V8 PDA plates at 25 °C under constant dark and light conditions for 7 days, and then the conidia were harvested and photographed using Olympus BX51 microscope (Olympus, Center Valley, PA, USA) with the CCD camera digital imaging system (Diagnostic Instruments, Inc., Sterling Heights, MI, USA) under 20X magnification.

APPENDIX D: SIMPLE SEQUENCE REPEAT (SSR) MARKERS USED IN THE BULK SEGREGANT ANALYSIS

SSR name	Chr. [a]	Location (cM)	Repeat	Size (bp)	PCR condition
Bmac0213	1H	27.7	(AC)23	168	F
Bmac0063	1H	52.9	(AC)14	125	E
Bmac0032	1H	55.5	(AC)7T(CA)15(AT)9	215	D
Bmag0105	1H	56.2	(AG)10	108	E
Bmac0090	1H	57.6	(AC)20	221	F
EBmac0501	1H	57.6	(AC)13	151	F
HVM20	1H	58.4	(GA)19	151	A
HVM64	1H	58.4	(GA)4(GT)7(CT)2(GT)4 (GA)8	253	A
Bmag0211	1H	61.6	(CT)16	174	F
Bmag0345	1H	65.3	(CT)6AA(CT)9AA(CT)6 AA(CT)7AA(CT)7	140	F
Bmag0347	1H	69	(CT)28	107	E
Bmag0382	1H	97.3	(AG)7AA(AG)7	109	F
HvHVA1	1H	112.4	(ACC)5	136	E
WMC1E8	1H	159.3	(AC)24	197	E
HVM43	1H	-[b]	(CA)9	239	A
Bmag0579	1H	-	(AC)6(AG)15	126	E
EBmac0783	1H	-	(CA)5	200	E
Bmag0504	1H	-	(AG)6,(GAGG)4,(GA)7	157	F
Bmag0718	1H	-	(GA)18,(AG)6	169	I
Bmag0770	1H	-	(GT)13,(AG)19	158	I
Bmac0134	2H	15.1	(AC)28	148	E
HVM36	2H	25.8	(GA)13	114	A
Bmac0222	2H	47	(AC)23	165	E
EBmac0737	2H	62.1	(TG)17	160	K
Bmag0381	2H	66.3	(CT)7(ATCT)6(CT)14	141	D
HvXan	2H	67.6	(CCT)6	140	F
Bmag0140	2H	68.6	(AG)15	157	F
Bmag0378	2H	68.6	(AG)14	147	F
EBmac0850	2H	72	-	132	D
EBmac0640	2H	74	-	176	F
EBmac0785	7H	-	(TA)9(GT)22	105	K

SSR name	Chr.	Location (cM)	Repeat	Size (bp)	PCR condition
HVM23	2H	75.1	(GA)9	246	B
EBmac0557	2H	75.1	(AC)8	154	D
Bmac0093	2H	75.1	(AC)24	151	E
HvTUB	2H	75.1	(AGC)8	149	E
EBmac0558	2H	75.1	(AC)7	160	F
EBmac0607	2H	75.1	-		F
EBmac0623	2H	75.1	-	154	F
EBmac0521	2H	77.3	(AC)18	163	E
Bmac0216	2H	87.7	(AC)5	190	E
Hv5s	2H	87.7	(AGT)5	238	F
Bmag0125	2H	89.9	(AG)19	134	E
HVM54	2H	132.8	(GA)14	159	A
EBmac0615	2H	-	(TG)5CG(TG)3,(TG)10	173	E
Bmag0692	2H	-	(CT)19	182	E
HVHOTR1	2H	-	(CAA)6	165	E
EBmag0793	2H	-	(GT)13,(AG)36	177	E
Bmag0518	2H	-	(TC)23	168	F
EBmatc0039	2H	-	(ATC)5	139	F
Bmag0720	2H	-	(GT)6,(AG)49	171	I
Bmag0742	2H	-	(TC)29	148	I
Bmag0749	2H	-	(AG)11	166	I
Bmag0813	2H	-	(CT)6,(CT)7,(TATC)17	197	I
Bmag0829	2H	-	(GA)28	189	I
HvLTPPB	3H	23.4	(AC)10(AT)5	221	E
Bmag0023	3H	49.1	(AG)18	137	E
Bmac0067	3H	51	(AC)18	171	E
Bmag0006	3H	51	(AG)17	174	F
HVM27	3H	52	(GA)14	192	A
HVM44	3H	52	(GA)8	114	A
Bmac0043	3H	52	(AC)11	159	D
Bmag0131	3H	52	(AG)16G(AG)15	149	E
Bmac0209	3H	52	(AC)13	176	F
Bmag0136	3H	58	(AG)6-(AG)10-(AG)6	197	F
HVM33	3H	63.9	(CA)7	157	A
Bmag0112	3H	63.9	(AG)18	196	F

SSR name	Chr.	Location (cM)	Repeat	Size (bp)	PCR condition
HVM60	3H	67.6	(AG)11,(GA)14	115	A
Bmag0225	3H	69.4	(AG)26	162	F
Bmag0013	3H	134.1	(CT)21	155	F
HVM62	3H	151.9	(GA)11	251	A
EBmac0541	3H	153.8	(AC)9	106	F
HVM15	3H	-	(GA)8	166	A
Bmag0606	3H	-	(CT)22	140	E
EBmac0708	3H	-	(AT)5(GT)16CT(GT)5(GC)6	138	E
EBmac0871	3H	-	(TG)13	180	E
EBmag0705	3H	-	(TC)31	155	E
Bmag0603	3H	-	(AG)24	120	E
Bmag0508A	3H	-	(AG)14	175	E
Bmag0841	3H	-	(TC)8(CCTC)4,(CT)11	125	I
Bmag0828	3H	-	(TC)39	124	I
Bmag0877	3H	-	(GA)15	153	I
Bmag0905	3H	-	(TC)14	177	I
EBmac0705	3H	-	(AC)16	150	K
HVM40	4H	13.8	(GA)6(GT)4(GA)7	160	A
HvOle	4H	21.2	(GCCT)4	198	H
Bmag0384	4H	42.1	(AG)18	116	F
Bmag0375	4H	42.9	(AG)19	135	F
EBmac0669	4H	42.9	-	168	F
HVM13	4H	45.1	(GA)6,(GA)6,(GA)6	173	A
Bmac0181	4H	45.1	(AC)20	177	E
HVM03	4H	45.1	(AT)29	188	E
EBmac0540	4H	46.1	(AC)8	114	D
HVM68	4H	47.5	(GA)22	204	A
Bmag0353	4H	47.5	(AG)21	119	F
Bmac0310	4H	48.3	(CT)11(AC)20	176	E
EBmac0906	4H	53.7	-	153	D
EBmac0691	4H	59.6	(CA)3CG(CA)7	111	K
EBmac0658	4H	60.8	-	198	F
Bmag0914	7H	-	(CT)16	170	I
EBmac0603	7H	-	(CA)10	149	F

SSR name	Chr.	Location (cM)	Repeat	Size (bp)	PCR condition
EBmac0701	4H	79.5	(AC)23	149	E
EBmac0635	4H	83.7	-	116	F
EBmac0788	4H	87	-	168	D
HVM67	4H	116.8	(GA)11	116	A
HVM77	4H	-	(CA)7	199	A
EBmag0781	4H	-	(CT)21	149	E
EBmac0775	4H	-	(TG)4TT(TG)17(AG)10	149	E
EBmacc0009	4H	-	(CAA)14(CAC)7(CAA)4	240	F
Bmag0740	4H	-	(CT)28	150	I
Bmag0808	4H	-	(GA)16	177	I
Bmag0357	5H	32.1	(AG)8G(AG)9	146	F
Bmag0387	5H	34	(AG)16	123	F
Bmag0337	5H	34.9	(AG)22	145	E
Bmag0394	5H	34.9	(AG)9CG(AG)4CG(AG)4	171	F
Bmag0323	5H	35.5	(CT)24	158	E
Bmac0306	5H	35.5	(AC)10-(AC)5	127	F
Bmac0303	5H	37.1	(AG)13(AC)21	138	F
HVM30	5H	40.8	(CA)8	150	B
Bmac0163	5H	40.8	(AC)6(GC)3(AC)17	146	E
EBmac0518	5H	40.8	(AC)5/(AC)5	150	E
Bmac0096	5H	40.8	(AT)6(AC)16	173	F
Bmac0113	5H	40.8	(AT)7(AC)18	187	F
Bmag0005	5H	40.8	(AG)15	173	F
EBmac0684	5H	51.8	(TA)7(TG)11,(TG)11(TTTG)5	172	E
Bmag0223	5H	65.6	(AG)16	127	F
Bmag0222	5H	92.3	(AC)9(AG)17	179	F
EBmac0824	5H	115	(TG)4,(TG)4,(TG)4,(GT)4,(GT)4	308	K
HvLOX	5H	120.1	(AG)9	150	F
HVM06	5H	-	(GA)9	175	A
HVLEU	5H	-	(ATTT)4	166	D
EBmatc0040	5H	-	(ATC)6N3(ATC)3	179	D
EBmatc0054	5H	-	(GGA)3,(ATC)4	128	D
EBmac0970	5H	-	(AC)8	112	E
Bmag0507	7H	-	(AG)23	147	F

SSR name	Chr.	Location (cM)	Repeat	Size (bp)	PCR condition
EBmatc0003	5H	-	(ATC)4N3(ATC)3	111	F
Bmag0751	5H	-	(GA)20,(AGAT)10,(AG)5	189	I
Bmag0760	5H	-	(GA)24	110	I
Bmag0812	5H	-	(CT)26	157	I
Bmac0316	6H	5.5	(AC)19	135	E
Bmac0218	6H	78	(AC)14	135	F
Bmag0219	6H	81	(AG)5GG(AG)14	181	F
Bmac0251	6H	89.5	(AC)12A(AC)13	185	F
HVM65	6H	100.4	(GA)10	129	A
HVM31	6H	100.4	(AC)9	163	A
HVM14	6H	100.4	(CA)11	158	A
Bmac0018	6H	100.4	(AC)11	138	D
Bmag0009	6H	100.4	(AG)13	172	F
Bmgtttttt0001	6H	101.5	(GTTTTT)5	215	G
EBmac0806	6H	114.1	(CA)4GA(CA)8,(CA)5	168	E
Bmac0040	6H	143	(AC)20	236	F
HVM22	6H	66.3[c]	(AC)13	167	A
HVM34	6H	62.4[c]	(GA)10	222	B
HVM74	6H	62.7[c]	(GA)13	163	C
Bmag0613	6H	69.8[c]	(GA)17	171	E
Bmag0496	6H	63.8[c]	(CT)20	189	E
Bmag0500	6H	31.65	(AG)6CG(AG)29 (AGAGGG)3(AG)6		E
EBmac0874	6H	62.0[c]	(CA)8AA(CA)4CG(CA)8AA (CA)7AA(CA)9(TA)8	185	F
Bmag0867	6H	63.5[c]	(TC)20	131	I
Bmag0870	6H	-	(TC)33	125	I
Bmag0021	7H	0	(CA)10AA(GA)28	143	F
Bmag0206	7H	10.5	(GT)5(AG)14	239	F
HVM04	7H	17.9	(AT)9	198	E
Bmag0007	7H	17.9	(AG)16(AC)16	185	F
EBmac0713	7H	33.6	-	168	D
HVCMA	7H	73.3	(AT)9	141	D
Bmac0031	7H	80.3	(AC)28	175	D
Bmac0224	7H	80.3	(AC)5/(AC)5	166	E
Bmag0516	7H	-	(TC)8(TATC)7(TC)19	147	F

SSR name	Chr.	Location (cM)	Repeat	Size (bp)	PCR condition
Bmac0273	7H	80.3	(AC)20(AG)20	186	E
Bmag0011	7H	80.3	(AG)25	147	F
Bmac0579	7H	80.9	(AC)8	244	A
Bmac0162	7H	80.9	(AC)15(CT)16	187	F
Bmac0582	7H	82.3	(AC)12	170	D
Bmac0187	7H	83.9	(AC)13(AT)9	177	F
Bmag0217	7H	87.8	(AG)19	196	F
Bmag0321	7H	87.8	(AG)17(AC)16	218	F
Bmag0359	7H	87.8	(AG)25	150	F
Bmag0369	7H	87.8	(CT)16	191	F
Bmag0189	7H	88.8	(CT)21	151	E
Bmag0341	7H	88.8	(AG)14	215	E
Bmag0385	7H	94.5	(AG)18(TG)10	226	F
Bmag0120	7H	101.1	(AG)15	230	F
HvAMY2	7H	118.4	(GCT)5	134	F
Bmac0156	7H	149.5	(AC)22(AT)5	139	E
HVM49	7H	152.7	(CA)12	105	A
HVPRP1B	7H	160.7	(AC)6(AT)16	167	D
Bmag0135	7H	160.7	(AG)10GG(AG)12	161	F
HvID	7H	161.7	(AC)16(AT)10	182	F
HVM51	7H	-	(GA)3(GGGA)3(GA)8	151	A
EBmatc016	7H	-	(ATC)4N9(ATC)12	143	D
EBmac0755	7H	-	(AC)16	143	E
EBmag0757	7H	-	(AG)31	116	E

The information for 193 SSR markers were obtained from Dr. Shiaoman Chao in USDA-ARS at Fargo, ND and the information for marker Bmag0500 was obtained from GrainGenes Database (http://wheat.pw.usda.gov/cgi-bin/GG3/report.cgi?class=marker&name=Bmag0500).

[a] Chr. means chromosome

[b] - indicates no data is available.

[c] These positions are added based on the map of Hordeum-Consensus2007-SSR-6H in GrainGenes Database (http://wheat.pw.usda.gov/GG3/).

APPENDIX E: PCR CONDITIONS USED FOR THE BARLEY SSRS

A	Identical to the PCR conditions 1 of Liu et al. (1996).
B	Identical to the PCR conditions 2 of Liu et al. (1996).
C	Identical to the PCR conditions 3 of Liu et al. (1996).
D	1 cycle of 3 mins at 94ºC, 1 min at 66ºC, 1 min at 72ºC, 5 cycles of 30 secs at 94ºC, 30 secs at 65ºC (decreasing 1ºC per cycle), 30 secs at 72ºC, 24 cycles of 30 secs at 94ºC, 30 secs at 60ºC, 30 secs at 72ºC, 1 cycle of 5 mins at 72ºC.
E	1 cycle of 1 min at 94ºC, 1 min at 55ºC, 1 min at 72ºC, 30 cycles of 1 min at 94ºC, 1 min at 55ºC, 1 min at 72ºC, 1 cycle of 5 mins at 72ºC.
F	1 cycle of 3 min at 94ºC, 1 min at 58ºC, 1 min at 72ºC, 30 cycles of 30 secs at 94ºC, 30 secs at 58ºC, 30 secs at 72ºC, 1 cycle of 5 mins at 72ºC.
G	1 cycle of 3 min at 94ºC, 1 min at 69ºC, 1 min at 72ºC, 5 cycles of 30 secs at 94ºC, 30 secs at 68ºC (decreasing 1ºC per cycle), 30 secs at 72ºC, 24 cycles of 30 secs at 94ºC, 30 secs at 63ºC, 30 secs at 72ºC, 1 cycle of 5 mins at 72ºC.
H	1 cycle of 3 min at 94ºC, 1 min at 53ºC, 1 min at 72ºC, 30 cycles of 30 secs at 94ºC, 30 secs at 53ºC, 30 secs at 72ºC, 1 cycle of 5 mins at 72ºC.
I	Identical to that described by Röder et al. (1998) with an annealing except temperature of 55ºC, that the 25 microlitre reactions contained 125 nM of each primer.
J	Identical to that described by Röder et al. (1998) with an annealing temperature of 60ºC, except that the 25 microlitre reactions contained 125 nM of each primer.
K	Identical to programme E, except that an annealing temperature of 53ºC was used in the presence of 2.5 nM of $MgCl_2$.

This information was obtained from Dr. Shiaoman Chao in USDA-ARS at Fargo, ND.